The Dissertation Committee for Gopika Geetha Jayadev
certifies that this is the approved version of the following dissertation:

Optimization Approaches for Energy Infrastructure Network Design

Committee:

Benjamin D. Leibowicz, Supervisor

Jonathan F. Bard, Co-Supervisor

Erhan Kutanoglu

Varun Rai

Optimization Approaches for Energy Infrastructure Network Design

by

Gopika Geetha Jayadev

DISSERTATION

Presented to the Faculty of the Graduate School of

The University of Texas at Austin

in Partial Fulfillment

of the Requirements

for the Degree of

DOCTOR OF PHILOSOPHY

THE UNIVERSITY OF TEXAS AT AUSTIN

May 2021

Dedicated to the memory of my father, Jayadev K. Nair,
who always inspired me to believe in myself and to never give up.
You are gone but your faith in me has made this journey possible.

Acknowledgments

I would like to gratefully acknowledge the guidance and support of my doctoral advisors, Dr. Benjamin D. Leibowicz and Dr. Jonathan F. Bard, throughout my time at the University of Texas (UT) at Austin. Their expertise was invaluable in identifying and framing the research questions and also in developing the solution methodologies. Their insightful feedback pushed me to sharpen my thinking and enhanced my ability to think critically about research problems and develop novel techniques to tackle them.

I would like to sincerely thank Dr. Erhan Kutanoglu for his continued mentorship and collaboration on the projects I worked on during my Ph.D. and agreeing to be part of my dissertation committee. I would also like to extend my deepest gratitude to Dr. Varun Rai for being a part of my dissertation committee and for the references, advice, and insightful suggestions, which have helped make my dissertation more refined.

I would like to thank the Operations Research and Industrial Engineering (ORIE) faculty for their guidance and support. The courses that I took during my studies at UT Austin have provided me with a strong background, technical expertise, and tools needed to choose the right direction for my research and successfully complete my dissertation. At UT, I have learned a great deal about statistics, operations research, and machine learning from classes, research group meetings, and seminars.

I want to acknowledge my colleagues in the ORIE program for their incredible collaboration and participation. I would like to particularly thank Baturay Çalcı for being a wonderful research collaborator and a good friend. He provided the data utilized for the two case studies and he was always available to answer any data-related questions I had. I would also like to thank Prateek Srivastava for his unwavering support, many hours of insightful

discussions, and advice regarding references and tools that made the successful completing of this dissertation much smoother. I would also like to thank Qianru Zhu, Lilian Ding, and the many other friends I made at UT for their continued support and for making UT a home away from home.

I extend my deepest gratitude to the Energy Institute at UT Austin and Exxon Mobil for the funding provided for the work done in this dissertation. I greatly appreciate the financial support provide by the Energy Institute, which receives funding from a diverse mix of internal, industry, foundation, and government sponsors. I also thank Exxon Mobil and the team at Exxon Mobil for their mentorship, guidance, and their continued support in pursuing new avenues of research areas. I want to thank Dr. Xiang Ma for his continued feedback, support in identifying exciting research areas, and for providing me the opportunity to pursue the research areas I found to be the most interesting. I also want to extend my most heartfelt thanks to Dr. Yuanyuan Guo for her invaluable suggestions, insightful questions, and guidance. She helped me recognize relevant references and ideas for developing algorithms to solve challenging problems with her stochastic optimization expertise.

I would like to thank my family and friends for always being there for me and providing happy distractions when I needed to take a break. I want to thank my uncle Chandran and aunt Sangita for all the love and care they gave me and for being my family away from family. Finally, I want to especially thank the one person that made this all possible, my mother, Geetha Jayadev, for her unconditional love and unwavering support throughout my life. She has made an uncountable number of sacrifices for the family and for me to be able to follow my dreams. I also want to thank my siblings Govind and Gouthami for their support and encouragement and for always lending an ear whenever I needed it.

Optimization Approaches for Energy Infrastructure Network Design

Publication No. _____

Gopika Geetha Jayadev, Ph.D.
The University of Texas at Austin, 2021

Supervisors: Benjamin D. Leibowicz
Jonathan F. Bard

This dissertation focuses on applying operations research techniques to problems arising in the energy sector. The work presented attempts to push the existing frontiers in energy optimization by adding to an existing open-source framework in electricity infrastructure optimization and applying bilevel programming to relatively unexplored applications in natural gas market modeling. This dissertation consists of five chapters. Chapter 1 provides an introduction encompassing a brief description and motivation for the dissertation's work.

The future development of the U.S. electricity sector will be shaped by technological, economic, and policy drivers whose trajectories are highly uncertain. Chapter 2 describes an optimization model for the integrated generation and transmission system in the continental U.S., which is used to explore electricity infrastructure pathways from the present through 2050. By comparing and contrasting results from numerous scenarios and sensitivity settings, we ultimately affirm five key policy-relevant insights. (1) U.S. electricity can be substantially decarbonized at a modest cost, but complete decarbonization is very costly. (2)Significant expansion of solar PV and wind to combine for at least 40% of the generation mix by 2050 is fairly certain. However, solar PV and battery storage are more affected by

economic and policy assumptions than wind. (3) Investments in long-distance transmission are minimal, while investments in battery storage are much more significant under a wide range of assumptions. (4) Optimal solutions include large investments in natural gas capacity, but gas capacity utilization rates decline steadily and significantly. (5) Cost structures shift away from operating expenditures and toward capital expenditures, especially under climate policy. We conclude our article by discussing the policy implications of these findings.

Chapter 3 presents a bilevel programming model to aid decision-making in natural gas markets where multiple autonomous agents interact strategically, possibly with conflicting interests. In the proposed model, a liquefied natural gas (LNG) operator is the leader, and a natural gas (NG) producer is the follower. The LNG operator attempts to optimally locate LNG export terminals, purchase gas from the NG producer, and export it as LNG. The NG producer aims to optimize production, pipeline investments, and sales to domestic consumers and the LNG operator. To solve the bilevel problem, we first reformulate it as a single-level problem by exploiting the lower-level problem's convexity. Then, we use disjunctive reformulations of complementarity constraints and piecewise linear approximations of objective function terms to convert the problem into a convex quadratic mixed-integer program (QMIP). Computational experiments confirm that the QMIP is tractable and can be solved efficiently. We apply our bilevel framework to a case study of the Gulf-Southwest region of the United States and evaluate several decision-making scenarios. The scenario results emphasize the importance of using the bilevel methodology to anticipate the effects of new LNG export facilities on NG prices across the domestic gas network. Adding these large gas-consuming facilities at specific locations puts upward pressure on domestic gas prices, although this is somewhat mitigated by the NG producer's optimal production response to the increased demand.

Chapter 4 presents a risk-based integer bilevel programming model that considers two players in a leader-follower setting, where each tries to maximize their individual profits.

The leader or manufacturer makes decisions pertaining to facility location and the amount of raw material to buy from the supplier. The supplier or follower decides how much raw material to produce. Both players face demand uncertainty in their respective markets while making investment, production, and sales decisions. We develop models for optimal decision-making under risk-neutral and risk-averse objectives and explore the effects of different risk attitudes on the problem and its optimal solution. These problems are hard to solve as the number of scenarios increase, and solving them generally involves developing customized algorithms. To find feasible solutions to the resulting stochastic bilevel problem, an algorithm is developed that iteratively solves a restricted version of the problem to obtain feasible solutions to the original problem. Extensive computational experiments are performed to evaluate algorithmic tractability and solution quality. The proposed algorithm is able to find high-quality feasible solutions to the bilevel problem in very reasonable amount of time, and the attained solutions are found to be close to the optimal solution. The methodology is demonstrated with an example that addresses strategic issues in the natural gas market. The model considers two players, the liquefied natural gas (LNG) operator or leader and the natural gas (NG) producer or follower acting in a leader-follower setting. The LNG operator makes decisions pertaining to the locations of LNG facilities and the amount of gas to buy from the producer. The follower decides how much gas to produce. Both players face demand uncertainty in their respective markets and make investments, production, and sales decisions. The case study explores the Gulf-Southwest region of the United States and demonstrates the impact of the risk-averse decision-making approach on investment and operational decisions.

Chapter 5 concludes this dissertation by summarizing the most important findings from each study and outlining valuable directions for future research.

Table of Contents

List of Tables

List of Figures

Chapter 1

Introduction

Two of the most prominent features of the ongoing energy transition are the substitution of coal by natural gas and the rise of cost-effective renewable technologies. The degree to which the United States (U.S.) electricity system would transform to incorporate more renewable-based generation and the pace at which it is expected to happen is often debated. It is of deep interest to see how the U.S. electricity system would evolve in the years to come and the extent to which renewables would penetrate the generation fleet. This question is further explored in detail in this dissertation and how the future of the U.S. electricity system would be shaped.

The abundance of supply and affordable prices for natural gas driven by the shale revolution, along with its lower carbon footprint compared to coal, has brought on much significance to natural gas in the past decade. Moreover, the future transition to renewable generation is often accompanied by the opinion of natural gas power plants as a complementary generation to renewable generation sources. The ability of natural gas power plant capacity to be ramped up or down with relative ease compared to other conventional sources of generation coupled with low fuel prices could make them a perfect transition fuel. The natural gas market involves multiple players and many moving parts. Natural gas prices are impacted by various factors, including events and trends happening globally and domestically. The increase in global natural gas demand and the shale gas revolution in the U.S. has paved the way for the emergence of the LNG export industry in the U.S. In this dissertation, we attempt to study how the LNG export industry's emergence would impact domestic gas

markets in terms of prices and natural gas availability.

Optimization in energy can lower energy costs while improving operational performance and has gained significant importance over the years. It can aid in making high-cost and high-risk investments efficiently while mitigating risks and maximizing profits. In this dissertation, we develop optimization models to aid decision-making in the energy sector. The methodologies proposed in this dissertation have various applications. While it can be used as a business strategy tool wherein a firm attempts to maximize profits or choose an optimal investment portfolio, these models also find applications in developing policies and regulations for a given objective like achieving environmental objectives.

The electricity sector in the U.S. has undergone multiple changes in terms of technologies and policies. The changes in the past decade have significantly shifted focus to the diversification of the electricity sector. The falling cost of renewable technologies, including solar photovoltaic (PV) panels, wind turbines, and battery storage, have brought the discussion of renewable energy sources and their integration into the generation mix in the U.S. to the forefront. Conventional generation technologies like coal have been declining in usage over the past decade, with natural gas surpassing coal as the primary fuel in electricity generation, and this trend is expected to continue. Hence, it becomes pertinent to study how the electricity generation landscape in the U.S. would change in response to the penetration of renewable technologies, clean energy initiatives, government regulations, and policies that will impact the generation fleet in the years to come.

The U.S. is expected to transition from being an importer of natural gas to an exporter in the near future, caused due to the low natural gas prices owing to the shale gas revolution. Natural gas is a major energy source in the U.S. and has multiple applications, including but not limited to electricity generation, residential and commercial heating, and transportation. Natural gas production in the U.S. has been growing steadily in the past decade and is projected to continue well into the next decade, with the U.S. expected to become a net

exporter by 2022 (Conti et al., 2018). The increase in the global natural gas demand has resulted in the liquefied natural gas (LNG) trade's rapid growth. The LNG operators work by procuring natural gas locally and using large liquefaction facilities to liquefy the natural gas. The liquefied gas is then transported globally to regasification centers using specially designed tankers. The regasification centers convert the LNG into natural gas, which is then sold in the regional markets. The U.S. was the third-largest exporter of LNG in 2019, and the export volume is expected to increase with multiple LNG facilities in the U.S. expected to become operational in subsequent years. We can anticipate that an increasing fraction of domestically produced gas in the U.S. will be sold to LNG operators for export to foreign markets. The LNG operators significantly increase demand for gas supplies in the regions where they operate, and the presence of these large demands will exert influence on the local market players in the region. The high gas demand can influence the natural gas production in the region and the local spot market dynamics, influencing the gas consumption and prices in the spot market. Therefore it is imperative to study the strategic interactions between the LNG operator and the natural gas producer under a non-cooperative setting and how they make decisions in response to each other's presence.

The dissertation comprises work that primarily focuses on developing decision-making tools pertaining to infrastructure investment and operational decisions for the energy sector. The case studies used to demonstrate the methodologies focus on the electricity sector and natural gas markets in the United States. The work presented in this dissertation attempts to push the existing frontiers in energy optimization by adding to an existing open-source framework in electricity infrastructure optimization and using bilevel programming to study natural gas markets, which has not been done before to the best of my knowledge. The dissertation is broadly divided into the following components:

1.1 U.S. electricity infrastructure of the future: Generation and transmission pathways through 2050

The first part of the dissertation focuses on designing an electricity infrastructure planning model for the continental U.S. and exploring how the electricity infrastructure will evolve over the next several decades. We develop a least-cost optimization model of the integrated generation and transmission system in the continental U.S., which includes 13 regions, representative 24-hour profiles for every season, with investment and capacity decisions made every five years. We apply this model to the U.S. electricity network for a time frame of 35 years, from 2016-2050, to identify generation and transmission expansion pathways under multiple scenarios. The future development of the U.S. electricity sector will be shaped by technological, economic, and policy drivers whose trajectories are highly uncertain. We consider four scenarios representing various parametric assumptions and policy interventions in the model to analyze these effects. The results obtained from these scenarios reveal several policy-relevant insights, which are summarized below.

1. U.S. electricity can be substantially decarbonized at modest cost, but complete decarbonization is very costly.

2. Significant expansion of solar PV and wind to combine for at least 40% of the generation mix by 2050 is fairly certain, although solar PV and battery storage are more affected by economic and policy assumptions than wind.

3. Investments in long-distance transmission are very limited, while investments in battery storage are much greater, under a wide range of assumptions.

4. Optimal solutions include large investments in natural gas capacity, but gas capacity utilization rates decline steadily and significantly.

5. Cost structures shift away from operating expenditures and toward capital expenditures, especially under climate policy.

The scenario-specific results and their policy implications are further discussed in detail in this chapter.

1.2 Strategic interactions between liquefied natural gas and domestic gas markets: A bilevel model

In the second part of the dissertation, we develop a bilevel model to aid decision-making in natural gas markets where multiple autonomous agents interact strategically, possibly with conflicting interests. The proposed model consists of two players, a liquefied natural gas (LNG) operator and natural gas (NG) producer operating under a leader-follower setting. The LNG operator purchases gas from the NG producer, liquefies it at the LNG terminals, and ships it to the overseas LNG market. The LNG operator makes high fixed cost and lumpy decisions and hence is considered the leader. The LNG operator's decisions include optimally locating the LNG terminals, the amount of gas to purchase from the NG producer, and the sales quantities and prices in LNG markets. The NG producer is the follower and attempts to optimize the production, pipeline investments, and sales to domestic consumers and the LNG operator.

The bilevel problem is solved by reformulating it into a single-level problem by exploiting the lower-level problem's convexity. The resulting mathematical program with complementarity constraints is then reformulated into a set of linear constraints using disjunctive formulations and binary variables. We further linearize the non-convex quadratic terms in the objective function using piecewise linear approximations to convert the problem into a convex quadratic mixed-integer program (QMIP). The computational experiments run on multiple random instances of the problem confirm that the QMIP is tractable and can ef-

ficiently solve problems of reasonable size. Then, we apply our bilevel framework to a case study of the Gulf-Southwest region of the United States. We evaluate the model results under several decision-making scenarios to study the impact of both players' non-cooperative interactions on each other's decisions. The scenario results further emphasize the importance of using the bilevel methodology to anticipate the effects of new LNG export facilities on NG prices across the domestic gas network. We also analyze the effects of adding these large gas-consuming facilities at specific locations on domestic gas prices and the NG producer's production.

1.3 Risk-averse stochastic bilevel programming: An application to natural gas markets

The third part of the dissertation focuses on extending the bilevel model developed in the previous section to incorporate demand uncertainty and risk aversion. The players' decisions can be significantly impacted when the markets they operate in have uncertain future demands. We analyze this setting using a multi-stage stochastic modeling framework that captures the strategic interactions between two players, a leader or manufacturer and a follower or supplier, under demand uncertainty. Both players make investment, operational, sales, and pricing decisions. The leader makes large-scaled, high fixed cost investment decisions and hence we analyse how his decisions change when he follows risk-neutral and risk-averse approaches for decision-making. The production, sales, and prices for both players are directly impacted by the market conditions, which are uncertain. Hence, we capture the stochastic behavior in these models by introducing uncertainty in demand for each player's respective markets. We capture the demand uncertainty using scenarios that correspond to various demand conditions in the market.

We propose an algorithm to efficiently find high quality feasible solutions to the stochastic bilevel problem. We first reformulate the bilevel problem into a single-level problem using

the KKT conditions of the lower-level problem and strong duality. The non-linear complementarity constraints in the resulting single-level problem are linearized using disjunctive formulations with binary variables and big M. The non-convex terms in the objective function are further approximated using piecewise linear functions resulting in a QMIP. The QMIP is intractable for larger numbers of scenarios, and we propose an iterative algorithm that finds a feasible solution to the QMIP relatively fast. The computational studies conducted on random instances show that even larger instances of the the stochastic bilevel problem can be solved within a very reasonable amount of time. The analysis also addresses the "quality" of the solution attained using the algorithm, where the feasible solutions are found to be consistently very close to the optimal solution.

We apply the stochastic bilevel modeling framework to study the strategic issues arising in the natural gas market. The model considers two players, an LNG operator or leader and a NG producer or follower acting in a leader-follower setting. The LNG operator makes investment, gas procurement, LNG export, and pricing decisions. The NG producer produces gas and sells it in the spot market and to the LNG operator. The natural gas spot market and LNG market behavior can be far from deterministic and can be significantly impacted by events worldwide. Hence, it becomes crucial to analyze how the LNG operator's and NG producer's decisions change when the markets they operate in have uncertain future demands. The LNG operator's large investment decisions would impact his risk, and his optimal strategy could be quite different depending on whether he is risk-averse or risk-neutral. The case study explores the Gulf-Southwest region of the United States and demonstrates the impact of the the LNG player's risk behavior on investment and operational decisions.

1.4 Organization of the dissertation

In this chapter, we have provided a brief introduction to the problems considered in this dissertation. More detailed problem descriptions and reviews of related literature are given

in the respective chapters. The rest of this dissertation is organized as follows. In Chapter 2, we develop an optimization model for the integrated generation and transmission system in the continental U.S. and use it to explore electricity infrastructure pathways from the present through 2050. In Chapter 3, we develop a bilevel model to aid decision-making in natural gas markets for an LNG operator and an NG producer who act as autonomous agents interacting strategically with conflicting interests. In Chapter 4, we develop a stochastic risk-based bilevel model to study an LNG operator's behavior and an NG producer who faces demand uncertainty in the respective markets they operate in. We also attempt to study the LNG player's behavior and how his decisions change under various risk behaviors. Chapter 5 presents the concluding remarks on the work presented in this dissertation.

Chapter 2

U.S. electricity infrastructure of the future: Generation and transmission pathways through 2050

2.1 Introduction

The electricity sector in the United States (U.S.) is in the midst of a dynamic period in its long-run evolution, driven by profound technological, economic, and policy changes. The shale gas revolution has resulted in lower natural gas prices that caused natural gas to surpass coal as the leading fuel used to generate electricity, and continue to drive substitution of gas for coal (Feijoo et al., 2018). Costs of intermittent renewable technologies such as wind turbines and solar photovoltaic (PV) panels, as well as battery electricity storage, have decreased sharply in recent years and continue to decline (Sivaram et al., 2018). Electricity market restructuring has instituted competitive markets in many regions of the U.S., a shift which is causing generation utilities to be cautious about investing in large, capital-intensive generation facilities, and instead favor smaller, more flexible projects (Rhodes, 2018). Growing awareness of the dangers associated with climate change has led to a complex and constantly evolving patchwork of regulations governing greenhouse gas (GHG) emissions at local, state, and federal levels. These include renewable portfolio standards in a majority of the 50 states (Barbose et al., 2016), the Clean Power Plan setting carbon dioxide (CO_2) emissions reduction targets for individual states, subsidies and tax

This chapter has been published in the *Applied Energy* journal. Jayadev, Gopika, Benjamin D. Leibowicz, and Erhan Kutanoglu. "US electricity infrastructure of the future: Generation and transmission pathways through 2050." Applied energy 260 (2020): 114267. Gopika Jayadev is the lead author and Dr. Leibowicz and Dr. Kutanoglu supervised the work.

incentives for clean technologies like solar PV (Hagerman et al., 2016), and cap-and-trade programs in California and the Regional Greenhouse Gas Initiative states on the East Coast (Chan and Morrow, 2019).

Considerable uncertainty about the trajectories of technological, economic, and policy drivers has led to a wide range of projections for how the U.S. electricity sector will – or ought to – evolve over the coming decades. For instance, there is a general consensus that the power sector will have to play a crucial role in climate change mitigation, as most analyses suggest that a highly decarbonized electricity system is required for climate stabilization (de Sisternes et al., 2016). Nevertheless, researchers disagree about the costs of reducing CO_2 emissions from electricity, the ideal extent of decarbonization, and the optimal mix of technologies to deploy. Some argue that the U.S. electricity system can achieve complete decarbonization (zero CO_2 emissions) at no additional cost, based on a combination of wind, water, and solar energy together with various storage technologies (Jacobson et al., 2015). Other scholars propose relying on a broader portfolio of technology options to transition to a low-carbon electricity future (Clack et al., 2017). For example, MacDonald et al. MacDonald et al. (2016) contend that U.S. electricity CO_2 emissions can be reduced substantially at no additional cost by deploying renewables in concert with nuclear and natural gas generation, and investing in long-distance transmission lines to balance variability in intermittent renewable power supplies. On the other hand, based on the very long and gradual energy transitions typically observed in the historical record, some researchers claim that any large-scale transition from fossil fuel electricity to intermittent renewables will necessarily take many decades (Smil, 2016).

In this dissertation, we investigate the future development of U.S. electricity infrastructure through 2050 by developing a least-cost optimization model of the integrated generation and transmission system in the continental U.S. Our model is a customized and expanded version of the core Open Source Energy Modeling System (OSeMOSYS) framework. We

represent 13 regions distinguished by their electricity demand profiles, wind and solar PV capacity factors, hydro and geothermal resources, and existing generation capacities. Compared to existing tools, our model incorporates greater temporal resolution using a multi-level representation of time. Generation and transmission capacity investment decisions are made every five years, inter-seasonal variability in loads and resources is captured, and 24-hour dispatch solutions in each season allow us to faithfully project the operation of future electricity systems featuring significant intermittent renewables and battery storage. We apply this model to compare and contrast results from four main scenarios (No Policy, No New Transmission, Pessimistic Costs, Carbon Tax) and additional sensitivity analyses in order to obtain policy-relevant insights into future pathways for the U.S. electricity sector. Based on our results, we affirm five key takeaways regarding the optimal development of the electricity system, and discuss their policy implications in Section 2.6.

1. The U.S. electricity sector can be substantially decarbonized at modest cost, but complete decarbonization is very costly.

2. Significant expansion of solar PV and wind to combine for at least 40% of the generation mix by 2050 is fairly certain, although solar PV and battery storage are more affected by economic and policy assumptions than wind.

3. Investments in long-distance transmission are very limited, while investments in battery storage are much greater, under a wide range of assumptions.

4. Natural gas capacity growth is strong and robust, but utilization of gas capacity declines steadily and significantly.

5. Electricity system costs shift away from operating expenditures and toward capital expenditures over time, especially in the presence of climate policy.

The remainder of this chapter is organized as follows. In Section 2.2, we review the literature on energy system modeling and its application to the U.S. electricity sector. We describe our model in Section 2.3 and document our data sources. Scenario results are presented and compared in Section 2.4. We discuss the five key takeaways in Section 2.5, then conclude in Section 2.6 with a brief summary of our most important contributions.

2.2 Literature review

Researchers have developed a multitude of energy system models to explore how energy system pathways are shaped by technological, economic, and policy drivers. In this section, we review the literature on two modeling paradigms that are commonly applied to electricity generation and transmission expansion: optimization and market equilibrium. We devote most of this section to the former class of models because the framework we develop for this study adopts an optimization structure. Afterward, we briefly summarize what equilibrium models tend to reveal about the future of the electricity sector.

2.2.1 Energy system optimization models

Energy system optimization models aim to identify the ideal transformations of energy systems over time, including decisions on capacity investments and operations (Pfenninger et al., 2014). The objective is typically to minimize the total present discounted cost while satisfying all demands and respecting a host of technological, economic, and policy constraints. Energy system optimization is often considered a bottom-up modeling approach since it represents energy technologies and competition among them in great detail, but handles macroeconomic drivers of energy demand via broad, exogenous assumptions. This modeling paradigm inherently assumes that a single, rational decision maker controls all investment and operational decisions throughout the system, effectively acting as a benevolent system planner. The energy system pathways that optimization models produce should

therefore be viewed as normative results describing how a system *should* evolve (conditional on the sets of structural and parametric assumptions encoded in the model) rather than as predictions for how the system *will* in fact evolve.

A few examples of energy system optimization frameworks appearing in the literature are the Open Source Energy Modeling System (OSeMOSYS) (Howells et al., 2011), Regional Energy Deployment System (ReEDS) (Short et al., 2011), Market Allocation (MARKAL)/The Integrated MARKAL-EFOM System (TIMES) (Loulou et al., 2004; Loulou and Labriet, 2007), Solar and Wind Energy Integrated with Transmission and Conventional Sources (SWITCH) (Nelson et al., 2012), National Electricity with Weather System (NEWS) (MacDonald et al., 2016), SimWIND (Phillips and Middleton, 2012), and SimCCS (Middleton and Bielicki, 2009). Some of these tools are designed to examine a specific energy system (e.g., NEWS for the U.S. power sector) while others are essentially *model generators* that can be used to define a wide range of models tailored to particular applications (e.g., OSeMOSYS). The models differ in many respects such as geographical scope, regional disaggregation, temporal resolution, sets of technologies, and whether they represent spatial infrastructure networks (e.g., transmission). Which features are represented in detail, and which are treated in a simple manner or omitted entirely, depend on the modeler's perspective and the goals of the analysis (Wilkerson et al., 2015).

2.2.1.1 Open Source Energy Modeling System (OSeMOSYS)

The model we develop in this study to explore the future development of the U.S. electricity system is a customized and expanded version of OSeMOSYS. We describe the standard version of OSeMOSYS here, then delineate our modified implementation in Section 2.3. OSeMOSYS is a highly flexible and modular energy system optimization framework structured as a linear program that minimizes cost by determining optimal technology capacity investments and dispatch schedules (Howells et al., 2011). Unlike many other energy modeling

platforms, the standard version of OSeMOSYS is available open source to encourage dissemination and improve research transparency (DeCarolis et al., 2012). An OSeMOSYS implementation consists of different "blocks" of functionality that represent various components of the overall system being modeled. These blocks can be selectively enabled or disabled depending on the scope of the analysis, and integrated together to form a coherent model architecture that captures the interactions among them. For a comprehensive description of the standard OSeMOSYS framework, see the original documentation (Howells et al., 2011).

The literature based on OSeMOSYS showcases a diverse range of applications. (Welsch et al., 2014) uses OSeMOSYS to analyze scenarios with high renewable electricity penetration in Ireland. Cervigni et al. (2015) employs OSeMOSYS as one tool to study strategies for enhancing the climate resilience of African infrastructure. (Groissböck and Pickl, 2016) applies the model to the Saudi Arabian power sector to study the tradeoff between cost and environmental objectives. Brozynski and Leibowicz (2018) builds a version of OSeMOSYS with integrated electricity generation and transportation sectors to evaluate urban-scale decarbonization strategies in Austin, Texas. de Moura et al. (2018) incorporates endogenous transmission investments into OSeMOSYS to study cross-border electricity trade in South America. By reformulating OSeMOSYS as a stochastic (rather than deterministic) optimization program, Leibowicz (2018) investigates optimal hedging strategies for expanding electricity generation under climate policy uncertainty. The review article (Gardumi et al., 2018) describes the evolution of the OSeMOSYS developer and user communities since their inception, as well as a number of customized extensions that researchers have created.

The standard OSeMOSYS model and more information about it can be found at the website www.osemosys.org.

2.2.1.2 Other energy system optimization models

Among other energy system optimization platforms, ReEDS (Short et al., 2011) is perhaps the model most similar to the one we develop in this chapter. ReEDS also depicts the regionally disaggregated U.S. electricity sector, integrates generation and transmission, and simultaneously solves for capacity investments and dispatch. ReEDS uses geographic information system (GIS) databases to achieve impressive spatial resolution, but this focus on spatial detail comes at the expense of temporal resolution. Specifically, ReEDS includes 134 load balancing areas and 356 regions for establishing renewable capacity factor profiles, but only 17 representative timeslices to capture the annual electricity demand and dispatch solution (Eurek et al., 2016). These timeslices correspond to four six-hour blocks on four representative seasonal days, plus one additional timeslice to reflect peak load conditions. Relative to ReEDS, our model developed in Section 2.3 features less spatial disaggregation, but more granularity in the time dimension to capture temporal variations in demands and renewable capacity factors, and to more faithfully analyze generation dispatch and electricity storage operations.

Cole and Frazier (2018) employs the ReEDS model to study 38 scenarios for the evolution of the U.S. electricity system. It finds that wind and solar PV capacities grow significantly in almost all scenarios, and that their expansions raise the demand for flexibility within the rest of the generation fleet. The number of low-cost electricity hours increases over time, and substantial solar PV deployment shifts the most costly hours from the afternoon to the evening. Zhou et al. (2018) uses ReEDS to evaluate the impacts of misestimating renewable capacity credits on the U.S. power sector. It finds that the system is robust to small underestimates of renewable capacity credits, but large underestimates ($> 50\%$) can adversely affect the relative costs and values of variable renewable energy technologies enough to reduce their deployment. Using ReEDS, Reimers et al. (2019) demonstrates that the optimal capacity expansion pathway is sensitive to the way that regional planning reserve

margins are formulated. Energy modelers often assume the reserve margins recommended by the North American Electric Reliability Council (NERC), but regional reserve margins have historically exceeded these in many cases. Therefore, using NERC reserve margins typically leads to lower near-term capacity investments.

Mignone et al. (2017) uses the National Energy Modeling System (NEMS) developed by the U.S. Energy Information Administration (EIA) to study how carbon prices after 2030 affect investment in natural gas combined cycle (NGCC) plants prior to 2030. They assess various scenarios from 2010–2050 and find that investment in NGCC prior to 2030 is robust to a wide range of carbon price trajectories. Cole et al. (2016) uses the ReEDS model in tandem with the Rice World Gas Trade Model (RWGTM) to investigate how the electricity and natural gas sectors co-evolve from 2010–2050, and how the results respond to different input price assumptions for natural gas. They find that the generation mix in the future predominantly consists of natural gas, wind, and solar PV generation. Due to their assumption of no re-licensing of nuclear power plants, nuclear generation declines steadily and nearly reaches zero in 2050.

Nelson et al. (2012) uses the SWITCH mixed-integer linear programming model to analyze least-cost generation and transmission expansion in the western U.S. and Canada. The authors find that stronger carbon policy can achieve a 54% reduction in power sector emissions below the 1990 level by 2030, using a mix of existing generation technologies. Intermittent renewables contribute 17–29% of total generation in 2030, depending on cost assumptions. Furthermore, while the carbon prices needed to achieve this emissions reduction can be high, the increase in overall electricity system cost does not exceed 20%. MacDonald et al. (2016) obtains even more optimistic results using the NEWS model, which co-optimizes generation investments, transmission expansion, and dispatch across the U.S. The model incorporates very detailed weather data and captures cost savings stemming from geographic diversity, load smoothing, reserve pooling, and reduced energy density requirements. Its

results claim that emissions can be reduced 80% below the 1990 level using existing technologies and their current cost projections, and without electricity storage, at no increase in levelized electricity cost.

Additional energy system optimization models focus on one particular energy technology and its associated spatial infrastructure networks. SimCCS (Middleton and Bielicki, 2009) optimizes the spatial configuration of an infrastructure network for capturing, transporting, and storing CO_2. The model represents candidate facilities where CO_2 can be captured and candidate sites where CO_2 can be injected into geological storage as nodes in a network whose arcs serve as candidate CO_2 pipeline segments. SimCCS minimizes the cost of storing a target quantity of CO_2 by constructing and operating capture facilities, pipelines, and storage facilities. The closely related SimWIND tool (Phillips and Middleton, 2012) applies this same general modeling principle to identify optimal wind farm locations and transmission capacity investments, considering the existing transmission network. It represents the electric grid in great detail, including transmission losses and investment costs based on topography, population density, land availability, and other factors. Krishnan et al. (2016) discusses the general benefits of co-optimizing resources, transmission, and fuel supply on an underlying network structure, in contrast to traditional planning methods. The authors present several existing and emerging co-optimization approaches, along with challenges encountered in their implementation. One principal challenge is that the broader scopes of these models entail higher computational and data requirements that can necessitate cruder representations of time.

2.2.2 Energy system equilibrium models

While the model we develop in this dissertation follows the optimization paradigm, it is helpful to briefly introduce a few equilibrium-based energy-economy models to gain more insights into future electricity sector pathways, and to clarify the relative strengths and limi-

tations of the two modeling approaches. Equilibrium models endogenously determine prices that balance supply and demand in a set of represented markets. Models that endogenously solve for equilibria only in selected energy markets (e.g., electricity, natural gas) are known as *partial* equilibrium models, whereas *general* equilibrium models balance supply and demand across all markets that comprise an economy. This top-down approach is valuable for studying the macroeconomic forces that drive energy demand, as well as demand-side mitigation levers such as energy efficiency investments and price-induced demand reductions. It is also useful for analyzing interactions among multiple decision makers (e.g., firms, consumers, different countries), unlike optimization models which adopt the point of view of a single agent. Computable general equilibrium (CGE) models capture the ripple effects of energy and climate policies throughout the economy, beyond just the energy sectors. Relative to optimization-based platforms, equilibrium models typically feature much less technological, temporal, and spatial detail. However, researchers have experimented with hybrid modeling approaches that couple a bottom-up optimization model with a top-down equilibrium model, and solve them iteratively (Messner and Schrattenholzer, 2000; Young et al., 2017).

The U.S. Regional Economy, Greenhouse Gas, and Energy (US-REGEN) model is one such hybrid framework that couples a capacity expansion and dispatch model of the power sector with a CGE model of the U.S. economy (Young et al., 2017). Blanford et al. (2014) employs US-REGEN to analyze the effects of a clean energy standard under scenarios with varying technology assumptions. Results show that the future capacity and generation mixes are very sensitive to constraints on technology deployment; for example, constraints on inter-regional transmission expansion limit the growth of wind and allow nuclear to take on a larger role. It also finds that the clean energy standard can induce extreme electricity system transformations at the regional level even when the national transformation is relatively moderate. Bistline (2017) uses US-REGEN to quantify the decline in the marginal value of wind and solar PV capacity as deployment levels increase. The analysis reveals that the

correlations in capacity factors across space are critical determinants of this relationship, and that electricity storage helps mitigate the drop in value. Greater availability of inter-regional transmission and electricity trade also bolster the value of intermittent renewables by connecting locations with complementary resource profiles.

The Energy Modeling Forum (EMF) 32 study assesses GHG emissions reduction strategies in the U.S. power sector using a collection of 15 different models (Creason et al., 2018; Murray et al., 2018), 11 of which are based on a partial or general equilibrium structure. These include US-REGEN and ReEDS-USREP, which links the ReEDS model described in the previous subsection to a CGE formulation. For the most part, all models agree that the largest emissions reductions are achieved under scenarios with low natural gas prices, low renewable technology costs, and low energy efficiency costs. Gas prices and renewable costs exert the most significant effects on projected capacity investments, generation mixes, and emissions. Mai et al. (2018) evaluates the effects of model structure and input assumptions on renewable energy penetration. It finds that inter-model differences in the structural representations of storage, transmission, and intermittency of renewables can cause significant variations in model outcomes even if input parameter values are harmonized as much as possible.

2.3 Methods

2.3.1 Model scope

The model we develop for this analysis is a customized and expanded version of OSeMOSYS implemented in Python as a linear program, and solved using CPLEX. We described the standard OSeMOSYS framework (Howells et al., 2011) in Section 2.2.1.1, and in this section we document our structural extensions and original input database. For more detailed information, please note that the complete model formulation can be found in the appendix.

Our model determines the least-cost transformation of the integrated electricity gener-

ation and transmission system in the continental U.S., including capacity investments and operational dispatch. The timeframe of the analysis is 2016–2050, with each model period corresponding to a five-year decision making time step for capacity investments. Within each model period, a total of 96 timeslices representing 24-hour profiles for four average seasonal days allow for a simplified computation of dispatch. Our inclusion of a full day of hourly dispatch in each season is crucial for capturing temporally varying solar and wind capacity factors, loads, and the endogenous dynamics of battery storage operations. Since the analysis spans several decades, we apply a 5% discount rate to convert all costs to present values.

We divide the continental U.S. into the 13 regions outlined in Table 2.1, which are defined according to state boundaries. The regional definitions are based on the regions that the EIA uses to report electricity system operating data, which are themselves based on the territories of load balancing authorities and independent system operators (ISOs). However, we make several modifications to the regions to ensure that states grouped together have roughly similar energy resources and demand profiles. Regions are linked in the model by the inter-regional transmission network, which we add on top of the standard OSeMOSYS structure. We do not represent the transmission and distribution grids within each region, so the network in our model should be interpreted as capturing long-distance transmission that serves to balance electricity supply and demand on a broad spatial scale by leveraging each region's unique generation resources.

Each region in the model has its own electricity demand growth projection, load profile,

Most long-term energy modeling studies use real discount rates in the 3–7% range (Brozynski and Leibowicz, 2018; Blanford et al., 2014; Eurek et al., 2016; Jacobson et al., 2015; Nelson et al., 2012), so our 5% discount rate reflects the middle of the typical range. The sensitivity analysis results for the discount rate presented in Table A.1 show that it does not strongly affect optimal capacity additions.

For example, we divide the Northwest region used by the EIA into a Northwest region consisting of Washington and Oregon, and a separate Mountain North region including states in the interior West. We consider this important because Washington and Oregon feature significant hydroelectric resources and less extreme seasonal load variations than the Mountain North states.

Table 2.1. Model region definitions.

Model region	Abbreviation	States included
Northwest	NW	WA, OR
California	CA	CA
Mountain North	MN	MT, ID, WY, NV, UT, CO
Southwest	SW	AZ, NM
Central	CE	ND, SD, NE, KS, OK
Texas	TX	TX
Midwest	MW	MN, WI, IA, IL, IN, MI, MO
Arkansas-Louisiana	AL	AR, LA
Mid-Atlantic	MA	OH, PA, WV, KY, VA, NJ, DE, MD
Southeast	SE	TN, NC, SC, MS, AL, GA
Florida	FL	FL
New York	NY	NY
New England	NE	VT, NH, ME, MA, CT, RI

hydroelectric and geothermal resources, and solar and wind capacity factor profiles. A model run begins in the 2016 base year with the existing regional generator fleets and transmission network, and can endogenously invest in additional generation and transmission capacity over the model timeframe. The annual retirement schedule for existing generation assets included in the EIA-860 data (EIA, 2017d) is exogenously incorporated into the model. The set of included generation technologies is delineated in Table 2.2. In addition to these generation technologies, the model can invest in transmission and battery electricity storage.

Table 2.2. Electricity generation technologies.

Electricity generation technology	Abbreviation
Coal integrated gasification combined cycle	COALPP
Natural gas fired combined cycle	NGCC
Natural gas fired combustion turbine	NGCT
Nuclear	NUC
Hydroelectric	HYDROPP
Wind turbine	WINDPP
Solar photovoltaic	PV
Biomass	BIOPP
NGCC with carbon capture and storage	NGCCCCS
IGCC with carbon capture and storage	COALCCS
Geothermal	GEOPP

2.3.2 Structural extensions

In this subsection, we describe structural extensions that we add to the equations of the standard OSeMOSYS framework (Howells et al., 2011) to incorporate new capabilities into our model. For the full model formulation, please refer to the SI available online.

2.3.2.1 Flow balance constraints

Incorporating an inter-regional transmission network into the model requires us to impose the flow balance constraints

$$Production(r,l,y) + \sum_{s \in R} Import(s,r,l,y) \geq Demand(r,l,y) + Use(r,l,y) + \sum_{s \in R} Import(r,s,l,y) \qquad \forall\ r \in R, l \in L, y \in Y. \tag{2.1}$$

These constraints mandate that for every region r, dispatch timeslice l, and year y, the sum of local electricity production plus electricity imports from all adjacent regions must satisfy the sum of local electricity demand, endogenous local use (e.g., for battery storage charging), and exports to all adjacent regions. The *Import* decision variables are added to standard OSeMOSYS to depict the operation of the transmission segments.

2.3.2.2 Capacity growth constraints

Ample historical evidence suggests that energy transitions are long affairs that unfold gradually over time, due to system inertia and lags in deploying large-scale, capital-intensive, infrastructure-dependent technologies (Fouquet, 2010; Grubler, 2012). Therefore, we introduce capacity growth constraints that limit the annual scale-up rates of technologies to avoid unrealistic "bang-bang" solutions where the optimization scheme could respond to a small change in the relative costs of technologies by rapidly altering the capacity mix. The formulation we use, adapted from (Leibowicz et al., 2016) and (Brozynski and Leibowicz, 2018), is

Eq. (2.1) will hold with equality in most ordinary circumstances, but it does allow for excess generation relative to demand. In our model, this would only occur in an electricity system where zero-variable-cost renewable generation exceeds load in certain timeslices. We treat this as feasible to avoid ruling out such a system, which may well be optimal depending on the parameter setting. In reality, excess supply would have to be handled through interventions such as voltage regulation, turning off wind turbines, reorienting solar PV units, introducing artificial loads to dissipate excess energy as heat, and so on. These are important grid management challenges that our multi-decadal capacity expansion model is not well suited to explicitly represent.

$$NewCapacity(r,t,y) \leq TotalCapacityAnnual(r,t,y-\tau) \cdot MaxCapacityGrowthRate(r,t) + StartUpValue(t) \qquad \forall\, r \in R, t \in T, y \in Y. \tag{2.2}$$

In these constraints, the parameter $MaxCapacityGrowthRate$ is the maximum annual percentage growth in the total installed capacity of technology t and τ represents the time step used in the model (i.e., $\tau = 5$). The value of $MaxCapacityGrowthRate$ varies by technology to reflect the fact that granular technologies like solar PV, wind turbines, and battery storage typically diffuse faster than large-scale, capital-intensive options like thermal power plants (Grubler et al., 1999). The model thus allows large, centralized technology capacities to grow up to 10% annually, solar PV and wind capacities to grow up to 15%, and geothermal and battery capacities (which start at very low levels) to grow up to 25%. The $StartUpValue$ parameter is added to allow for some small initial deployment of new technologies with essentially no existing capacity (and is set to 100 MW).

2.3.2.3 Reserve margin constraints and capacity adequacy

Since our 96 dispatch timeslices represent average 24-hour profiles for the four seasons, they do not include the true peak load in each region. We account for this difference between the true peak load and the highest load featured in the 96 timeslices by adding to the reserve margin that drives total generation capacity. We assume that the reserve margin requires adequate capacity to satisfy demand 15% higher than the true peak load to accommodate unforeseen circumstances. Then, this reserve margin is raised to reflect the difference between the true peak load in the full 8760-hour profile and the maximum load included in the representative seasonal days. The reserve margin constraints are

$$TotalCapacityAnnual(r,t,y) \cdot CapacityFactor(r,t,l,y)$$
$$+\xi \sum_{s \in R} TotalTransmissionCapacityAnnual(s,r,y)$$
$$\geq TotalCapacityInReserveMargin(r,t,y) \qquad \forall\, r \in R, t \in T, l \in L, y \in Y. \tag{2.3}$$

In this formulation, the coefficient $\xi \in [0,1]$ determines the fractional contribution of import transmission capacity toward the regional reserve margin. Following de Moura et al. (2018), we credit import transmission links at 50% of their capacities (i.e., $\xi = 0.5$) for satisfying the regional reserve margin.

2.3.3 Input database

The input database includes values of numerous parameters such as existing generation and transmission capacities, capital costs, fixed and variable operation and maintenance (O&M) costs, fuel costs, conversion efficiencies, load profiles, demand growth projections, hydroelectric and geothermal resources, and solar and wind capacity factors. Table 2.3 documents our data sources. All input data used for the model come from publicly available sources. For wind and solar capacity factors, since empirical data in some parts of the country are lacking, we estimate regional capacity factor profiles by simulating generation time series at myriad locations using the National Renewable Energy Laboratory (NREL) System Advisor Model (SAM) software.

We provide a file with all model input data, which can be found at Jayadev (2019). By making the input data available, we aim to enhance the transparency of our modeling assumptions and provide other researchers with a set of U.S. electricity input data from publicly available sources that have been compiled according to standardized region definitions.

The sensitivity analysis results for ξ presented in Table A.2 show that results are not particularly sensitive to its assumed value.

Table 2.3. Documentation of data sources.

Parameter	Source
Annual demand forecast	ERCOT (2017a), NERC (2017), MISO (2017a) NYISO (2017a), PJM (2017a), ISO-NE (2017)
Hourly demand profile	ERCOT (2017b), MISO (2017b), NYISO (2017b), PJM (2017b), ISO-NE (2017)
Average hourly wind capacity factor	NREL (2017b)
Average hourly solar PV capacity factor	NREL (2017b)
Existing power plant capacity	EIA (2017d)
Existing transmission capacity	FERC (2017), EIA (2017c)
Power plant conversion efficiency	EIA (2017b)
Input activity ratio	EIA (2017a)
Capital cost	NREL (2017a)
Variable cost	NREL (2017a)
Fixed cost	NREL (2017a)
CO_2 emission factors	IPCC (2017)

The plots in Fig. 2.1 illustrate selected, key input parameters in the database. Fig. 2.1a shows how the annual electricity demand in each region is projected to evolve from the present through 2050. The projected trends vary considerably across regions, from strong growth in Texas (TX) to declining electricity demand in New York (NY). Projected capital costs for a sample of technologies are depicted in Fig. 2.1b. According to the NREL Annual

Technology Baseline data source, capital costs of most technologies will decline slightly over time, while solar PV and batteries will experience larger cost reductions. Meanwhile, the average cost for natural gas increases from $2.21/MMBtu in 2016 to $3.62/MMBtu in 2050, but it is worth noting that we capture regional variation in fuel costs. Fig. 2.1c visualizes the representative seasonal load profiles for two regions, TX and Northwest (NW). The TX load peaks sharply in summer due to strong space cooling demand, while the NW load varies less from season to season and actually peaks in the winter. The diurnal profiles within each season are also apparent, as loads tend to be highest in the late afternoon or early evening, and lowest in the early morning. Fig. 2.1d plots the 24-hour load profile for the entire U.S. in each season, demonstrating the same trends. The winter profile has two distinct peaks, one in the morning and one in the evening, reflecting when people are at home and the outdoor temperature is lower than it is in the afternoon. Altogether, the input data plotted in Fig. 2.1 confirm the importance of spatial and temporal disaggregation for capturing system operating conditions that vary across space and time (daily, seasonally, and annually).

We specify limits on the total regional installed capacities of the hydroelectric and geothermal technologies because they can only be sited in specific locations where these resources are available. Regional upper bounds on hydroelectric and geothermal deployment are based on US DOE (2014) and EERE (2014), respectively.

2.3.4 Scenario analysis

The optimal future development of the U.S. electricity system is dependent on a variety of technological, economic, and policy drivers. In this scenario analysis, we compare and contrast results from four scenarios to obtain insights into how the ideal evolution of generation and transmission varies with important parameters and uncertainties. The four scenarios we investigate are (1) No Policy, (2) No New Transmission, (3) Pessimistic Costs, and (4) Carbon Tax. They are summarized in Table 2.4 and described in the paragraphs

(a) Annual demand projection by region.

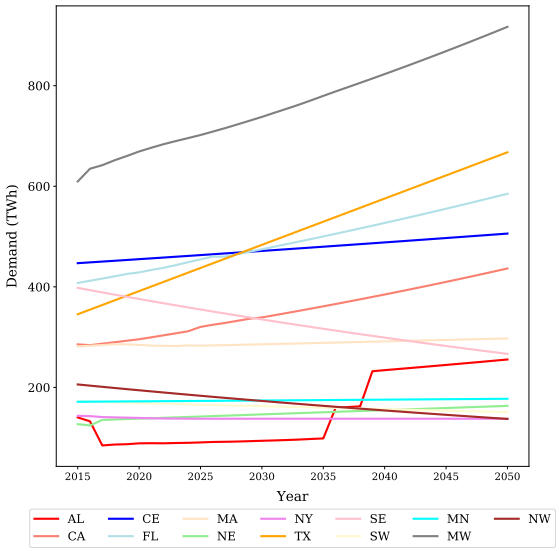

(b) Capital cost projection by technology.

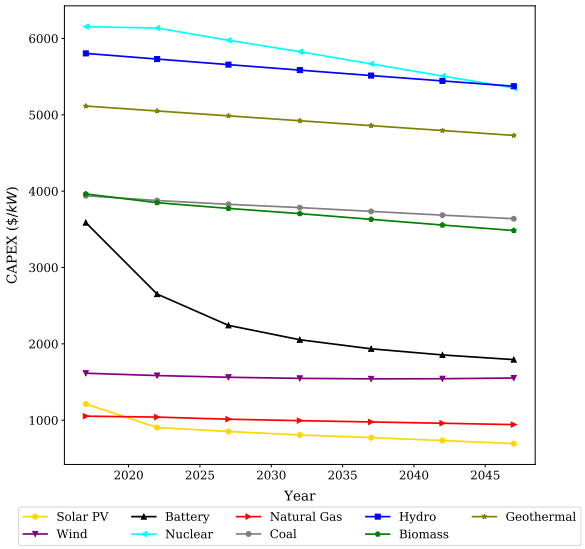

(c) Hourly demand profiles for TX and NW.

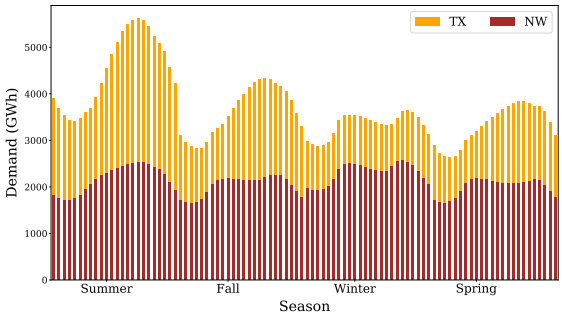

(d) Aggregate U.S. demand profile by season.

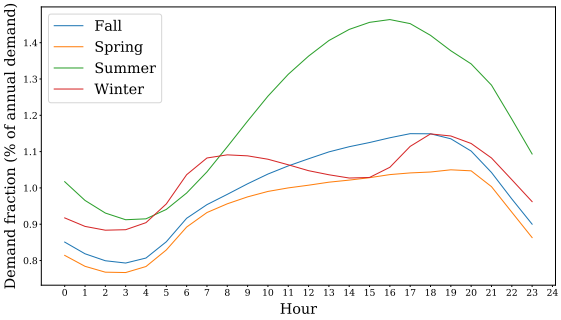

Fig. 2.1. Visualizations of selected parameters in the input database.

below.

The No Policy scenario is interpreted as a baseline development of the electricity system used to assess the effects of the particular factors that distinguish the other scenarios from it. It assumes that no policy constraints, incentives, or penalties are imposed to guide the electricity sector toward or away from particular technologies or environmental outcomes.

The No New Transmission scenario constrains the transmission capacity investment de-

cision variables to be zero, thus prohibiting expansion of the transmission network. By comparing the minimum cost objective value achieved under this scenario to that realized in the No Policy case, we are able to quantify the value of new transmission in the continental U.S. over the next several decades. This result helps put into perspective the potential economic losses stemming from regulatory constraints on new transmission lines, such as inadequate permitting processes and inability to obtain the right of way.

The declining costs of renewables and battery storage are assumed to have a strong influence on the future of electricity. However, there is considerable uncertainty about future costs, and the assumptions in the NREL Annual Technology Baseline could be viewed as optimistic. To test the sensitivity of optimal capacity investments and generation mixes to these costs, we consider the Pessimistic Costs scenario in which the capital costs of solar PV, batteries, and wind turbines decline over time at only 20% of the rate assumed in the other scenarios. Therefore, the increase in objective value from the No Policy scenario to the Pessimistic Costs scenario quantifies the value of realizing the full capital cost reductions assumed in the NREL Annual Technology Baseline as opposed to just 20% of those reductions.

The Carbon Tax scenario is used to explore how a tax on CO_2 would affect future investments and dispatch in the integrated electricity generation and transmission system. This scenario reflects the persistent uncertainty about the future of climate policy in the U.S. The sample tax trajectory we consider is introduced at the moderate level of \$20 per tonne of CO_2 (tCO_2) in the base period, then rises linearly over time to reach \$200/tCO_2 by the 2050 time horizon. The Carbon Tax scenario should shift investment toward less carbon-intensive generation technologies, reduce CO_2 emissions from the U.S. electricity sector, and increase total cost compared to the No Policy case.

In addition to thoroughly exploring these four scenarios, we also conduct wider sensitivity analyses over more parameter settings to establish how the capital cost of new transmission

Table 2.4. Summary of the four main scenarios we investigate.

Scenario name	Description
No Policy	• A scenario with no policy constraints, incentives, or penalties in effect. • Interpreted as a baseline development of the U.S. electricity system, against which the other scenarios are compared.
No New Transmission	• Prohibits new investments in the inter-regional transmission network. • Used to quantify the value of new, long-distance transmission investments in the U.S. electricity sector.
Pessimistic Costs	• Assumes that only 20% of the reductions in solar PV, battery, and wind turbine capital costs projected by the NREL Annual Technology Baseline will actually materialize. • Used to test the sensitivity of capacity investments, generation mixes, and total cost to uncertain future cost assumptions.
Carbon Tax	• Imposes a carbon tax initialized at \$20/tCO_2 in the base year that rises linearly over time to \$200/tCO_2 in 2050. • Used to assess how climate policy would affect capacity investments, generation mixes, CO_2 emissions, and total cost.

influences total transmission investments, and how the percentage reduction in total CO_2 emissions causes the total system cost to increase above the No Policy objective value.

2.4 Results

The base year model calibration is demonstrated in Section 2.4.1. Sections 2.4.2–2.4.5 present and discuss the results of each scenario individually and in detail. We begin with the No Policy case, which is interpreted as a baseline development of the U.S. electricity system

against which the other scenarios are compared. Then, in Section 2.4.6, we present and analyze summary figures that compare the developments of key electricity sector outcomes and metrics across the four scenarios, and emphasize policy-relevant insights.

2.4.1 Model calibration

Before we evaluate our forward-looking scenarios, we ensure that the model is properly calibrated to produce a base year (2016) dispatch solution that roughly matches the actual generation mixes from that year. The model results should not be expected to exactly match reality due to temporal, spatial, and technological aggregation in the model, as well as the fact that the real U.S. electricity sector is not operated by a single optimizing agent to achieve cost minimization. However, it is comforting to confirm that the model-based dispatch and the true generation mixes are quite similar. Fig. 2.2 shows the empirical, regional generation mixes from 2016, and then the regional generation mixes produced by our model using the existing generation capacities.

2.4.2 No Policy scenario

Fig. 2.3a illustrates the evolution of the national cumulative new capacity (top) and generation (bottom) mixes through 2050 in the No Policy scenario. Even without a policy stimulus, the generation mix shifts significantly toward renewable technologies like wind and solar PV. Combined, these two technologies contribute 57% of total generation in 2050. Coal and natural gas generation both decline, by 18% and 25%, respectively, from 2016 to 2050. Most of the reductions in coal and gas generation occur during the later years of the No Policy case, as the rates of wind and solar PV expansion increase due to falling costs, including the cost of battery storage, and retirements of conventional generation facilities. Natural gas generation is more affected than coal generation because gas complements intermittent renewables by serving as the marginal production technology, ramping up production when

(a) Actual generation mixes

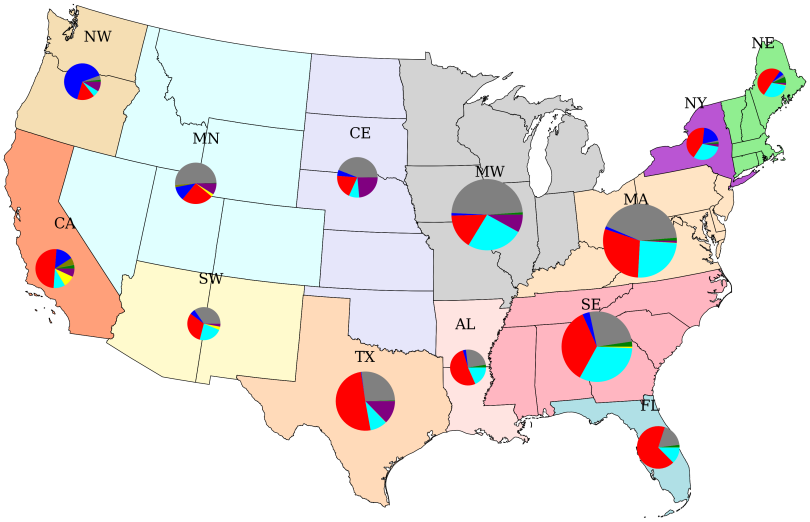

(b) Model output generation mixes

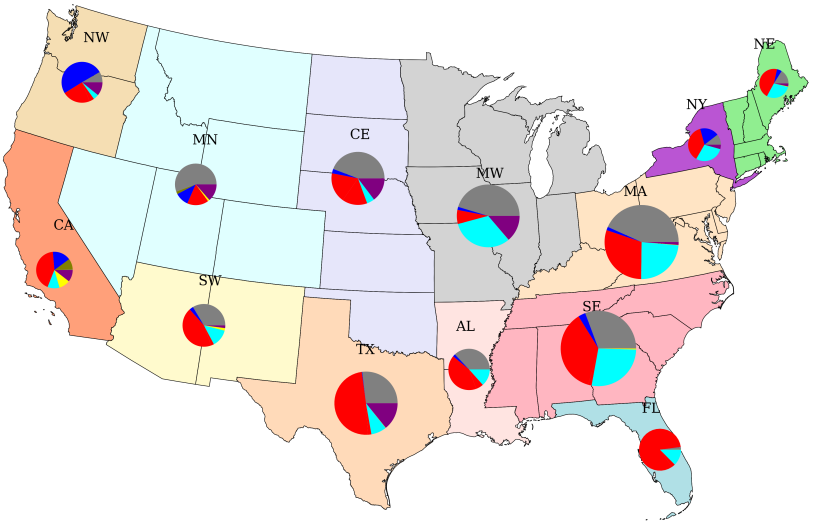

Fig. 2.2. Model calibration for the base year 2016. (a) illustrates the empirical, regional generation mixes from that year, and (b) plots the optimal dispatch solution computed by the optimization model.

renewable output drops or load is high. The story for capacity additions shown in the top plot of Fig. 2.3a is quite different, as far more gas power plant capacity is added through 2050 than coal capacity. Therefore, considerable investments in natural gas capacity are warranted in the No Policy case, but the utilization rate of gas capacity falls over time. This is an important theme that consistently emerges from our scenario results, with notable policy implications discussed in Section 2.5.

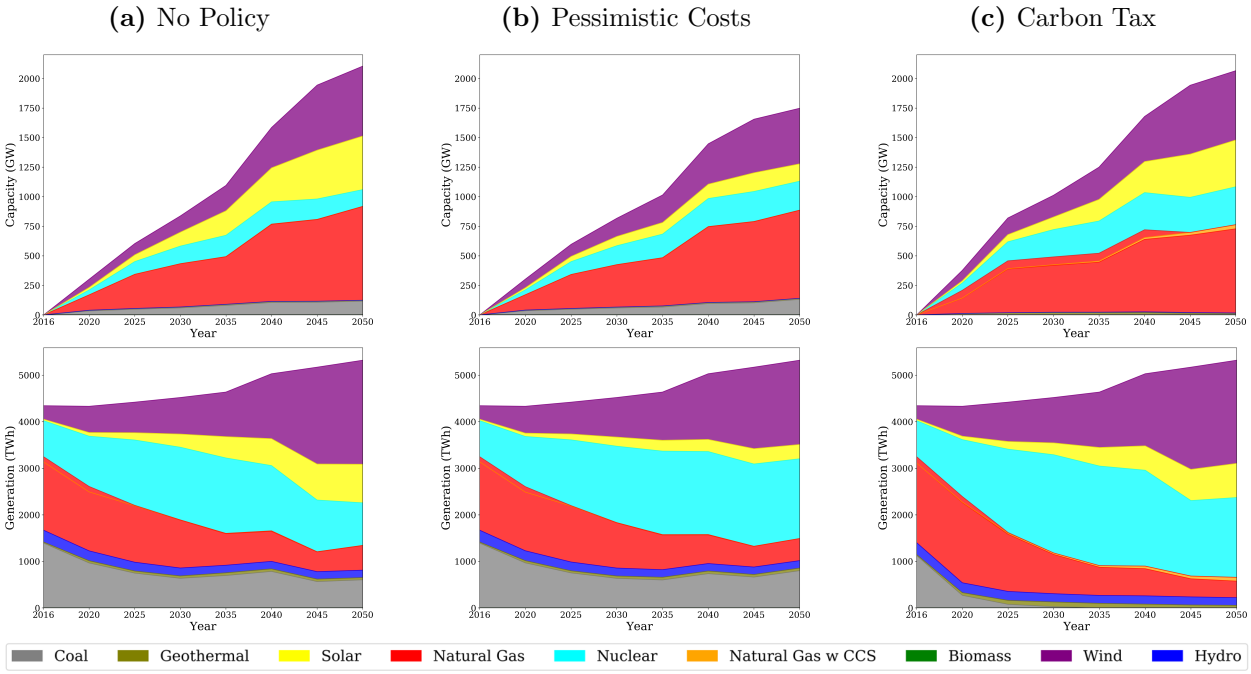

Fig. 2.3. Annual cumulative new installed capacity (top row) and generation mix (bottom row) for the whole continental U.S., by scenario.

Figs. 2.4a and 2.5a are map-based snapshots of the regional generation and cumulative installed capacity (new capacity only) mixes, respectively, in 2050 in the No Policy scenario. Wind still plays a larger role in generation than solar PV, despite solar PV having a lower capital cost than wind, an advantage that widens over the next few decades. Wind is valued for its higher average capacity factors and less extreme diurnal variability, which mean that less dispatchable generation or storage capacity is required to balance intermittency. Nuclear

capacity is added mainly in the southeastern regions of the U.S., where existing generation and transmission capacities must be supplemented, and alternatives like gas face higher fuel prices. Nuclear investment takes place during the early years of the No Policy scenario. Once installed, nuclear plants run essentially all the time for the full duration of the analysis, driven by low variable cost and a maximum capacity factor of 98%.

As shown by the arrows in Fig. 2.4a representing electricity imports, the model makes extensive use of the existing inter-regional transmission network. The optimal solution includes 6162 GW-miles of new long-distance transmission capacity added to the system by 2050. To put the scale of this investment in perspective, though, the existing network in the 2016 base year comprises a total of 190,395 GW-miles. Therefore, expanding the transmission network does not constitute a major component of the electricity system transformation in the No Policy scenario. The transmission that is added serves more to address existing imbalances between regional generation resources and demands in the base year than to take advantage of renewable resources in regions with superior availability and capacity factors.

Expansion of intermittent, renewable electricity induces complementary growth of battery storage capacity, illustrated by the black, vertical bars in Fig. 2.5a. Storage investment helps improve the utilization of wind and solar resources. As a result of significant growth in renewable generation and storage, CO_2 emissions decline substantially in the No Policy scenario. By 2050, annual CO_2 emissions from the U.S. electricity sector fall to 53% below their level in the 2016 base year. This reinforces the suggestion made by MacDonald et al. (2016) and others that emissions associated with electricity in the U.S. can be significantly reduced using existing technologies, assuming that costs decline as projected. This is true even without a clear policy stimulus, which reflects the impacts of recent and continuing reductions in the costs of renewable generation options and electricity storage. However, it should be noted that a 53% decline in power sector CO_2 emissions by 2050, while substantial, is almost surely insufficient to be in alignment with climate policy goals such as constraining

global warming to 2°C (Audoly et al., 2018).

2.4.3 No New Transmission scenario

Given the fairly limited role that transmission capacity additions play in the No Policy scenario, prohibiting the model from investing in the transmission network in the No New Transmission scenario has only minor effects on the electricity system. Power plant capacity investments and generation mixes are not noticeably affected by the inability to build new long-distance transmission, so we omit this scenario from a number of the figures in this section. Certain regions are forced to be slightly more self-sufficient in the No New Transmission case, so they add dispatchable capacity mainly in the form of coal to provide electricity when intermittent renewable output is low or demand peaks. The decline of CO_2 emissions by 2050 is 0.5% lower in this case than in the No Policy scenario, due to minor transmission constraints on the utilization of renewable electricity and greater investment in fossil-based generation capacity.

2.4.4 Pessimistic Costs scenario

The continued reductions in capital cost that the NREL Annual Technology Baseline projects for wind, solar PV, and battery technologies clearly underlie the significant expansions of these technologies in the No Policy results. While these decreases in cost might materialize, they are far from certain, so it is helpful to understand how sensitive the development of the U.S. electricity sector is to these cost projections. Therefore, we consider the Pessimistic Costs scenario in which the costs of wind, solar PV, and battery storage fall only 20% as much as the NREL data project them to decline.

Fig. 2.3b shows how the generation mix and cumulative capacity additions evolve in the Pessimistic Costs scenario. As expected, the conservative cost assumptions dampen the growth of wind and solar PV compared to the No Policy scenario, and have a larger effect

(a) No Policy

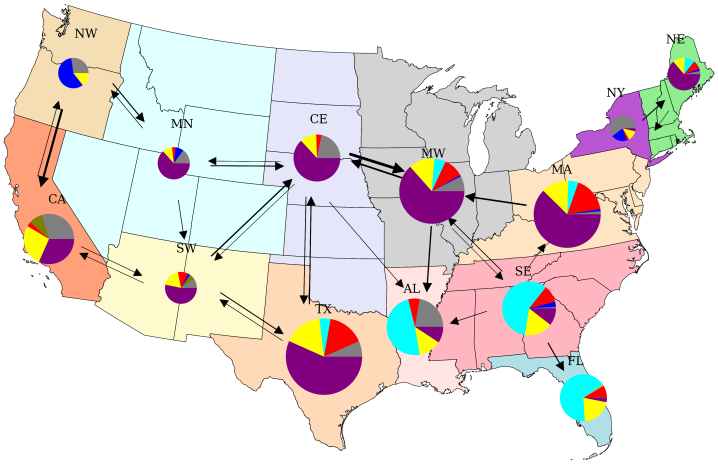

(b) Pessimistic Costs

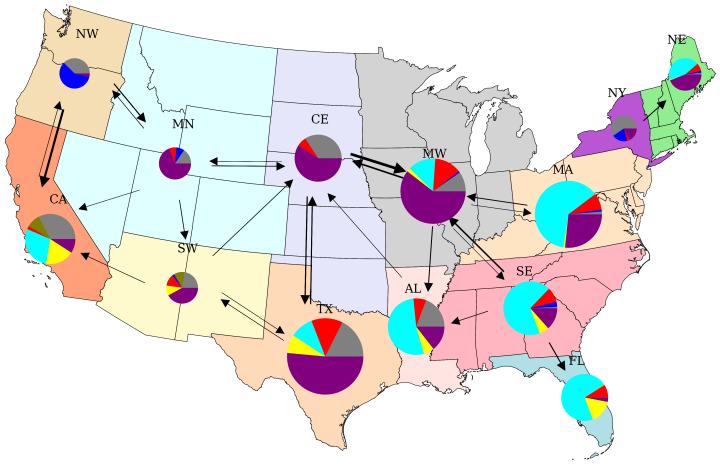

(c) Carbon Tax

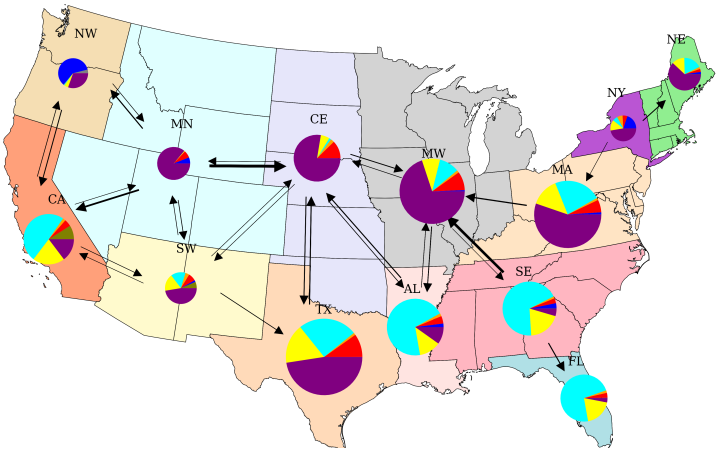

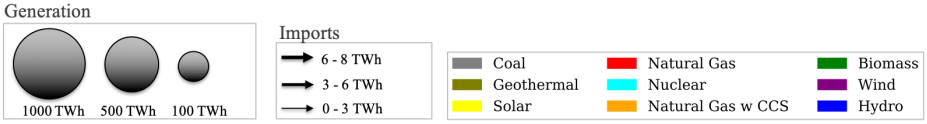

Fig. 2.4. Regional generation mixes and electricity imports in 2050, by scenario.

(a) No Policy

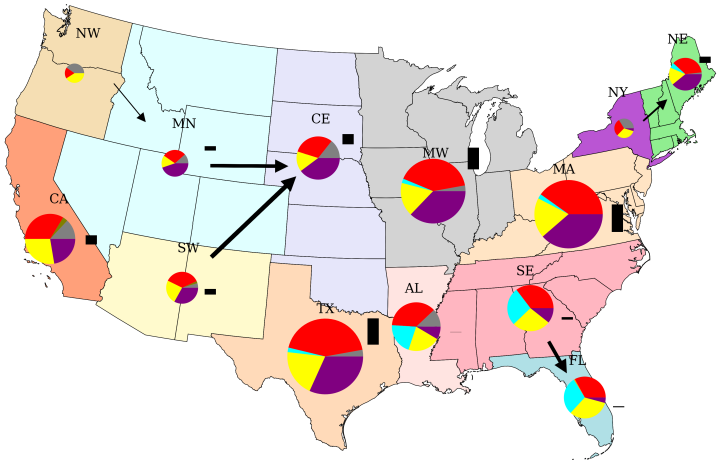

(b) Pessimistic Costs

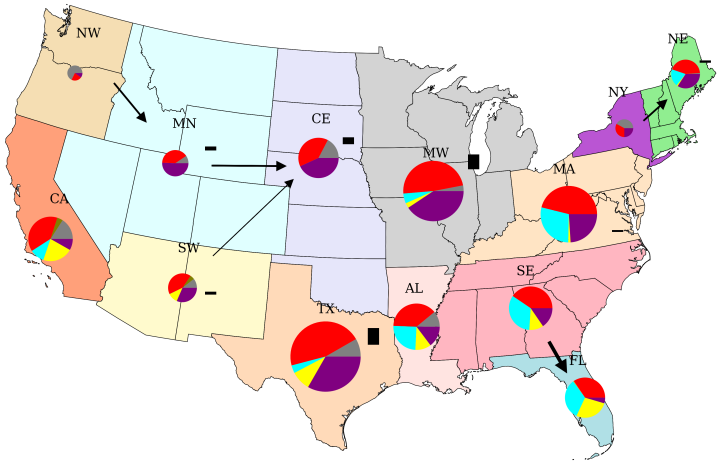

(c) Carbon Tax

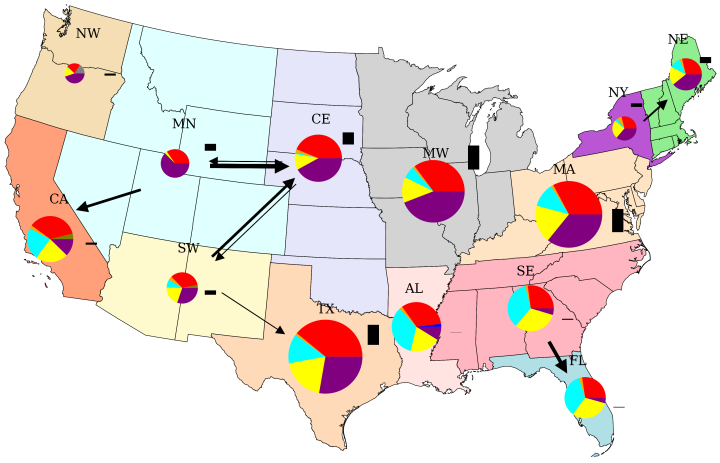

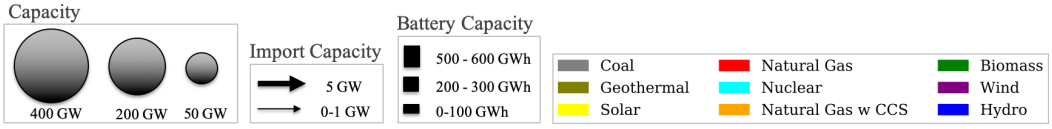

Fig. 2.5. Regional cumulative new installed capacity mixes in 2050, by scenario.

on the latter. Solar PV is more strongly affected because the baseline assumptions project its capital cost to fall more than that of wind, and also because solar PV is more reliant on cost-effective battery storage due to its more extreme diurnal variability. Interestingly, nuclear power benefits from the less favorable economics of wind, solar PV, and battery storage in the Pessimistic Costs setting. In this case, installed nuclear capacity doubles by 2050, when it provides 33% of the total generation. As seen in Fig. 2.4b, nuclear generation takes on a sizable share of the mix in more regions than in the No Policy scenario, including regions like MA and CA where it was a negligible contributor under the baseline technology cost assumptions. The substitution of nuclear electricity for intermittent renewables in the Pessimistic Costs scenario helps limit the increase in CO_2 emissions relative to the No Policy scenario.

On the other hand, while the Pessimistic Costs setting does not induce greater investment in fossil-based generation capacity, it does increase the utilization rates of coal and natural gas power plants. With lower deployment of wind and solar PV, the net load profiles are higher and more stable, allowing dispatchable fossil capacity to satisfy more demand during more hours. As a result, coal generation in Fig. 2.4b expands in regions like TX and CE. Since the capacity additions in the Pessimistic Costs scenario (e.g., nuclear) tend to have higher capacity factors than those in the No Policy scenario (e.g., wind, solar PV), cumulative capacity additions of all technologies combined are lower under Pessimistic Costs.

The smaller capacities of wind and solar PV added in the Pessimistic Costs case mean that investments in battery storage and transmission are lower than in the No Policy setting. The existing transmission network is still used extensively, but the new transmission added drops to 3266 GW-miles, relative to 6162 GW-miles under No Policy. The black, vertical bars representing battery storage capacity are lower in Fig. 2.4b than in Fig. 2.4a, and disappear completely from some regions where No Policy storage investment was substantial (e.g., MA). Battery storage capital cost has a long way still to decline in the Annual Technology Baseline

assumptions, and its deployment is also predicated on significant expansion of wind or solar PV. In consequence, its growth is very sensitive to cost assumptions for these technologies.

Total CO_2 emissions in the Pessimistic Costs case decline to 51% below their 2016 base year level by 2050. This is a slightly smaller reduction than in the No Policy scenario (53%), but overall, the results suggest that U.S. electricity sector emissions will fall substantially even if wind, solar PV, and battery costs do not decline nearly as much as the Annual Technology Baseline projects. Of course, this is also based on its assumptions about future nuclear costs, which are also highly uncertain. If nuclear were assumed to be more expensive, or were constrained by non-economic factors, then higher costs for intermittent renewables and storage would lead to more fossil-based generation and higher CO_2 emissions.

2.4.5 Carbon Tax scenario

Fig. 2.3c charts the growth of new capacity and the evolving generation mix in the Carbon Tax scenario. In the early years of this scenario, the penalty on CO_2 emissions causes the system to phase out coal generation faster than in the other scenarios, with natural gas use increasing to compensate for diminished coal output. Wind, solar PV, and other low- or zero-carbon technology options are still relatively expensive during these early years, and their up-scaling is limited by the capacity growth rate constraints. Furthermore, existing gas capacity can be dispatched at higher utilization rates to offset the drop in coal generation while reducing emissions. The near-term substitution of gas for coal is a familiar, ongoing trend in the U.S. electricity sector, partially due to relative fuel prices, and partially driven by policy goals. As seen in Fig. 2.4c, regional generation mixes increasingly consist of wind, solar PV, and nuclear electricity by 2050, with natural gas shares still sizeable but nevertheless decreasing. With a high carbon price in place at the end of the timeframe, gas-fired power plants with CCS account for small shares of generation in many regions, while geothermal capacity is added in the western NW, CA, and SW regions.

The Carbon Tax scenario is a boon for nuclear capacity investment, which is 2.3 times higher in this setting than in the No Policy case. Wind capacity additions are 7% higher in the Carbon Tax scenario, but solar PV capacity additions are interestingly 9% lower. The latter outcome reflects the ability of increased nuclear capacity to provide substantial carbon-free baseload generation, as continuing to expand solar PV would require significantly higher investments in battery electricity storage. On the whole, the optimal solution in the Carbon Tax case includes more investment in battery storage and in the transmission network compared to that in the No Policy case. Total storage additions are 4% higher under the Carbon Tax, and these investments are logically concentrated in regions where wind and solar PV contribute more than 55% of electricity in 2050 (see Figs. 2.4c and 2.5c). Cumulative transmission investments sum to 8231 GW-miles, which represents a one-third increase over the No Policy result. Additional transmission capacity helps maximize the utilization of carbon-free, intermittent, renewable electricity output by allowing it to satisfy demands in multiple regions. Fig. 2.5c reveals that the transmission links which are augmented in the Carbon Tax scenario are largely in the western U.S., used to import more renewable electricity into the high-demand regions CA and TX.

The implemented carbon price successfully reduces CO_2 emissions far below the level reached in the No Policy case. Under the Carbon Tax, total annual CO_2 emissions are 91% lower in 2050 than in the 2016 base year, a much larger decline than we observed in the No Policy scenario (53% reduction). Looking at the full timeframe from the base year through 2050, the Carbon Tax scenario leads to 48% lower cumulative CO_2 emissions than the No Policy case. The deeper GHG reductions achieved under the Carbon Tax do come at a cost, but the cost appears to be fairly moderate given the magnitude of the additional decarbonization. The total cost objective value is 13.5% higher than in the No Policy scenario.

2.4.6 Scenario comparisons

2.4.6.1 Capacity investments

Fig. 2.6a compares the cumulative capacity additions installed by the model over the full analysis timeframe across the four scenarios. Wind and solar PV capacities are expanded in all cases, though solar PV investment is more sensitive to the particular scenario than wind investment. Continued deployment of solar PV will rely more heavily on further cost reductions, so its growth is noticeably dampened in the Pessimistic Costs scenario. Some nuclear capacity is added in every scenario, but nuclear growth is much stronger if either wind, solar PV, and battery costs decline less over time (Pessimistic Costs), or a carbon price penalizes fossil generation (Carbon Tax). New coal investments are relatively small in all cases, and nearly extinguished under the Carbon Tax. At least in terms of new capacity added, natural gas growth is significant and evidently robust to the particular scenario parameterization assumed. Gas capacity has a relatively low capital cost, and can serve versatile roles ranging from providing affordable bulk generation with lower CO_2 emissions than coal, to backing up intermittent renewables when required to satisfy net load. Generation facilities incorporating CCS are only deployed in the Carbon Tax case, as expected. The scale of total CCS investment, however, is not large. Total cumulative capacity additions are lower in the Pessimistic Costs scenario than in the other settings, because it features less solar PV capacity (lower capacity factors) and more nuclear capacity (higher capacity factor).

2.4.6.2 Costs

The total discounted present costs in each scenario are broken down into capital costs, O&M costs, and fuel costs in Fig. 2.6b. Capital costs are further decomposed into generation, storage, and transmission assets. As previously described, long-distance transmission expansion plays a minor role in all scenarios, and the associated capital costs are barely no-

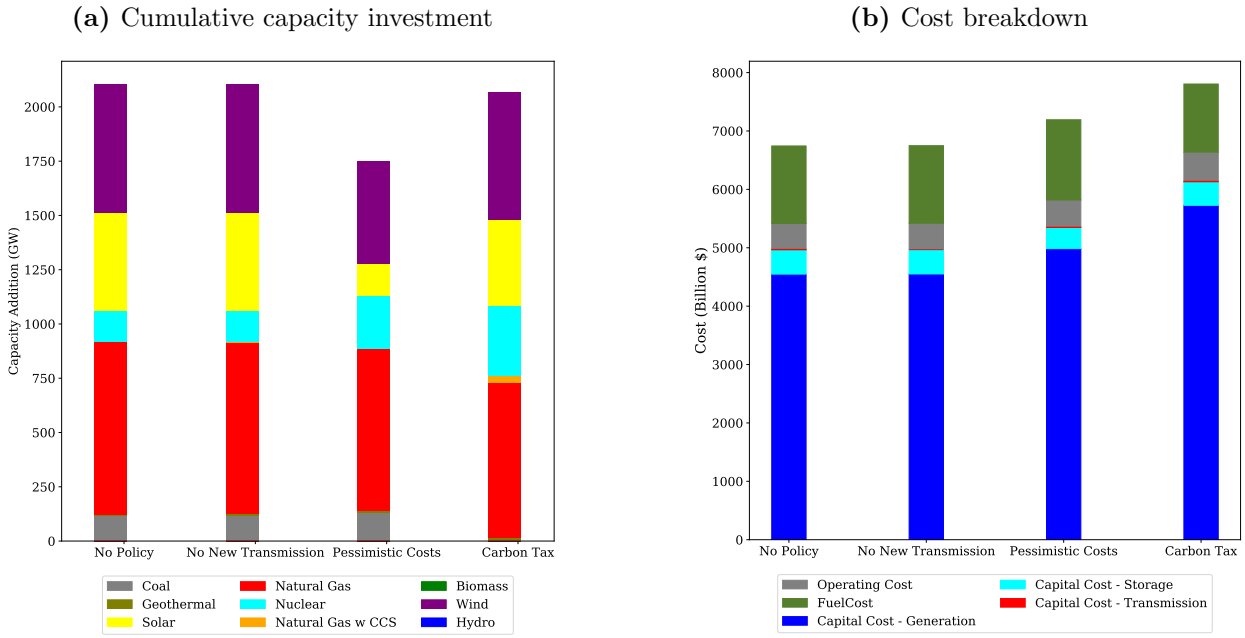

Fig. 2.6. Comparison of cumulative capacity investments (a) and cost breakdowns (b) across the scenarios.

ticeable in the bar chart. The existing transmission network continues to be heavily utilized, but only limited transmission capacity additions can be economically justified, a finding similar to what (Phillips and Middleton, 2012) observed. Battery storage investments are larger, signaling an interesting trend in the electricity sector as less investment is allocated to transmission and more resources are invested in storage. However, capital costs for storage are still small compared to the total investment in the generation system. Capital costs for new generation capacity are greater in the Pessimistic Costs scenario, where intermittent renewable and battery costs decline less, and in the Carbon Tax scenario, which induces a swifter and more extensive electricity system transformation toward low- and zero-carbon technologies. In general, the results in Fig. 2.6b reveal that electricity sector expenditures over the next three decades will slant heavily toward capital costs, with fuels accounting for a smaller fraction of overall costs than in the past. This is particularly pronounced under the

(a) Annual average gas capacity utilization

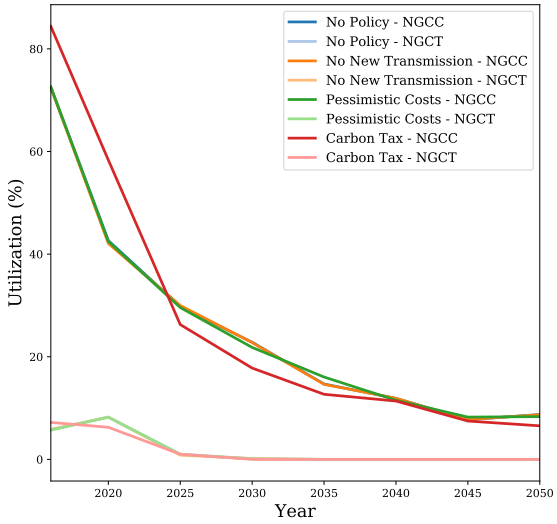

(b) Cumulative additions of gas capacity

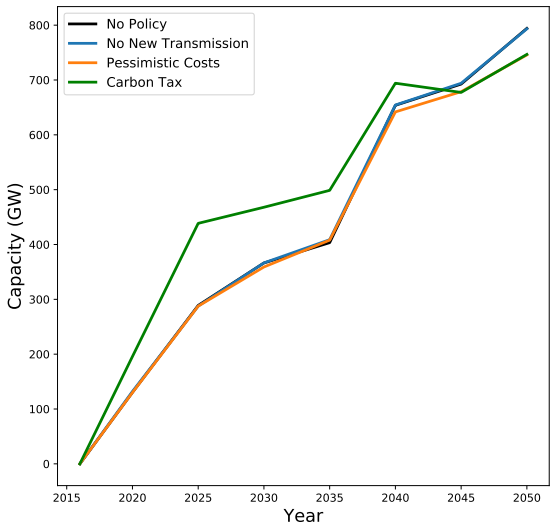

Fig. 2.7. Annual average utilization rates of natural gas capacity (a) and cumulative additions of gas capacity (b) in the whole continental U.S., by scenario.

Carbon Tax, which leads to more deployment of capital-intensive technologies like nuclear, wind, gas plants equipped with CCS, geothermal, and battery storage.

2.4.6.3 Gas capacity utilization

Fig. 2.7b shows that natural gas capacity growth is significant and robust across the four scenarios, with 700-800 GW added from 2016–2050 in all cases. For much of the model timeframe, the Carbon Tax scenario actually induces the strongest expansion of gas capacity, due to its ability to substitute for coal in the short run and to complement intermittent renewables in the long run. Additional gas capacity helps a system with significant intermittent renewables cope with fluctuations in their output to satisfy net load plus the reserve margin in all hours of the year. However, as the 2050 time horizon is approached, the Carbon Tax case ceases to feature the most cumulative gas investment because the carbon price reaches very high levels and the costs of renewables and storage become increasingly competitive.

While gas capacity continues to be added, the average utilization rate of this capacity declines steadily through 2050, another outcome which holds across all four scenarios. This is clearly visible in Fig. 2.7a. The average utilization rate falls from roughly 40–45% in 2016 down into the 5–10% range by 2050. The decline in utilization rate is much steeper for NGCC plants than for NGCT plants, as the former are utilized 70–80% of the time in the base year but are relegated to more of a peaking role as intermittent renewables expand over time. Early on, gas capacity utilization is highest in the Carbon Tax scenario, reflecting coal-to-gas switching due to the effect of the carbon price on economic dispatch. Pretty soon, however, the Carbon Tax case exhibits the lowest gas utilization rate as gas plants assume more of a backup generation role due to the growth of nuclear, wind, and solar PV generation, as well as battery storage that offers an alternative strategy for balancing intermittency. The availability of gas capacity is still imperative for satisfying peak net loads plus reserve margins, but increasing variable renewable power output with essentially zero marginal cost will continue to erode gas capacity utilization. The fact that gas-fired generation capacity still has considerable system value, but produces electricity during fewer hours of the year, has important policy implications that we discuss in Section 2.5.

2.4.6.4 Growth of transmission and battery storage

Fig. 2.8a illustrates the relative timing of transmission and storage investments in the four scenarios. In all parameter settings, the model expands the transmission network early on, and finishes investing in transmission capacity by 2035. Battery storage capacity, on the other hand, grows steeply later in the analysis timeframe once the costs of intermittent renewables and batteries have been reduced from their base year values. The Carbon Tax case induces the largest capacity additions in both transmission and storage, both of which help maximize the utilization of intermittent, carbon-free renewables. Interestingly, storage investments are nearly as high in the No New Transmission scenario. The inability to add

(a) Cumulative additions of battery and transmission capacities, by year

(b) Cumulative additions of battery and transmission capacities, with respect to renewables

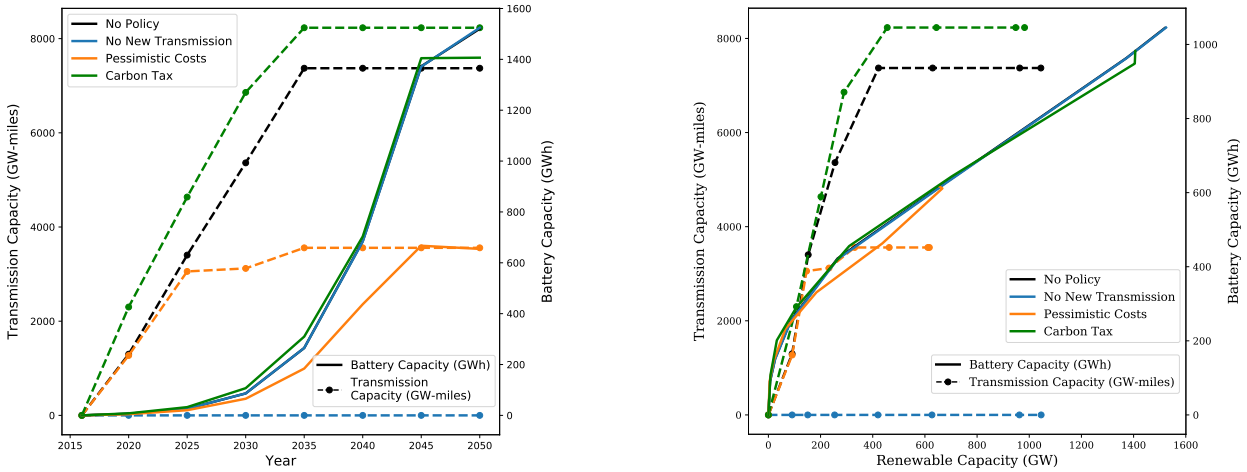

Fig. 2.8. Cumulative additions of battery storage and transmission capacities in the whole continental U.S. with respect to time (a) and cumulative growth in intermittent renewable generation capacity (b).

transmission capacity makes storage more valuable as a way of addressing the intermittency issue locally within a region, and also because storage allows for more complete utilization of transmission capacity by spreading electricity imports over time.

Fig. 2.8b also plots cumulative transmission and storage capacity additions, but does so relative to the endogenous growth of wind and solar PV capacity on the x-axis. The results show that all scenarios produce similar transmission and storage expansion trajectories with respect to their growth in intermittent renewables. As renewable capacity increases, the transmission network initially grows quite fast, but this relationship does not continue indefinitely and the growth of transmission capacity saturates. Battery storage, by contrast, continues to grow roughly linearly with the increase in intermittent renewable capacity even as the latter reaches progressively higher levels of penetration. In general, our scenario analysis suggests that the contributions of long-distance transmission expansion to balancing intermittent renewable electricity output are limited and confined to the short-run, whereas

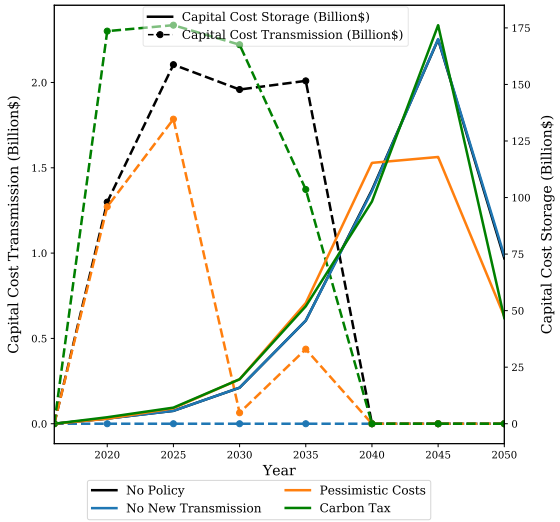

Fig. 2.9. Annual capital investments for battery storage and transmission in the whole continental U.S.

battery storage is the preferred strategy in the long-run.

In terms of annual capital investments in transmission and storage, Fig. 2.9 confirms that the electricity sector will devote more resources to expanding long-distance transmission in the short-run, but eventually shift to allocating investment to storage in the long-run. The scale of the total storage investment through 2050 is also much larger than the scale of the total transmission investment. Of course, significant costs might be incurred in reality to expand transmission and distribution within each region, a level of spatial granularity that our model cannot be used to investigate.

2.4.6.5 Sensitivity analysis: Transmission capital cost and capacity additions

A notable outcome under all our scenarios is that new investments in the long-distance transmission network are insignificant relative to the broader electricity system transformation. Since the capital cost of building new transmission in the future is uncertain, we test how sensitive our finding is to this assumption by reducing the capital cost of transmission

(a) Sensitivity of total transmission capacity additions to transmission capital cost

(b) Sensitivity of total cost to targeted % reduction in 2050 CO_2 emissions

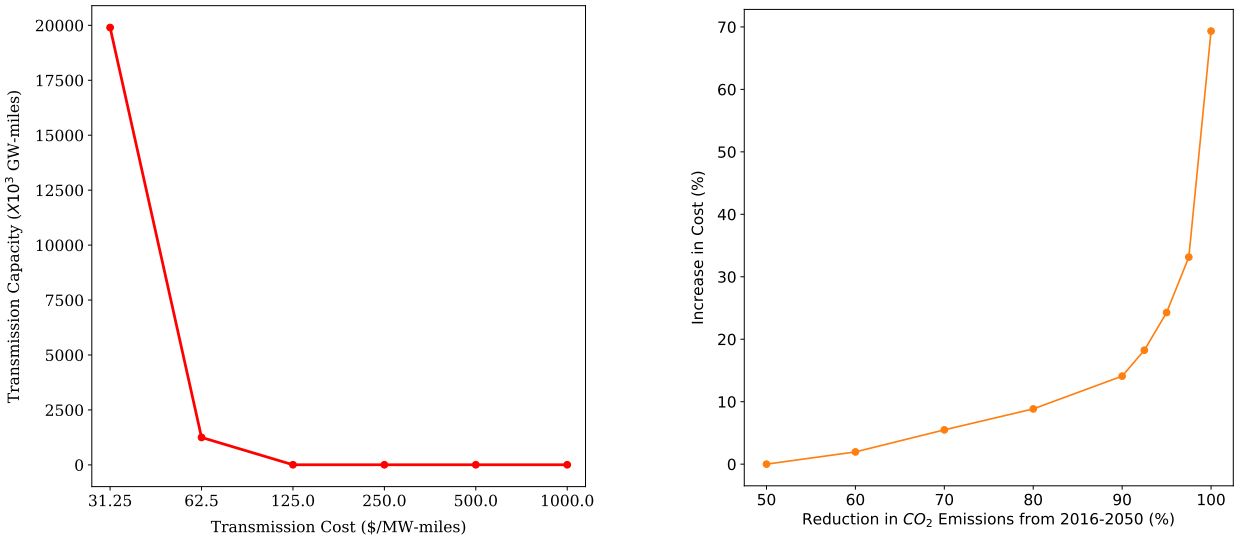

Fig. 2.10. Sensitivity analysis results showing how total transmission capacity additions respond to the capital cost of transmission (a), and how the increase in total cost (objective value) responds to the targeted percentage reduction in CO_2 emissions by 2050 (b).

below its $1000/GW-mile reference value and re-running the No Policy scenario. Fig. 2.10a shows how much total transmission capacity the model adds over the full analysis timeframe as a function of its assumed capital cost. The x-axis is logarithmic. These sensitivity results suggest that transmission would have to be many times cheaper, available at a cost unlikely to be plausible, in order for significantly more transmission capacity to be constructed. We thus conclude that the minor role of long-distance transmission expansion in the scenario results is robust to its capital cost.

2.4.6.6 Sensitivity analysis: CO_2 emissions reduction and total cost

Even in the No Policy scenario, annual U.S. electricity sector CO_2 emissions are 53% lower in 2050 than in the 2016 base year. In this sensitivity analysis, we specify increasingly stringent CO_2 reduction targets that must be reached by the 2050 time horizon, and explore

how the corresponding total cost objective values rise as emissions are reduced toward zero. The allowed total CO_2 emissions are assumed to linearly decline over time from the initial 2016 level down to the specified 2050 target. Fig. 2.10b illustrates the percentage increase in total cost relative to the No Policy scenario as CO_2 emissions are reduced more and more. The relationship between emissions reduction and cost is approximately linear until about a 90% reduction (similar to the reduction achieved under our Carbon Tax scenario), but begins to rise much more steeply after that. Eliminating the last remaining emissions from the electricity sector is very expensive because it rules out the use of relatively low-carbon technologies like fossil generation equipped with CCS, biomass, and natural gas peaking plants, and essentially demands either enough battery storage to balance all intermittent renewables or a generation mix dominated by nuclear power. As (Clack et al., 2017) suggests, it is extremely difficult to achieve complete decarbonization (zero CO_2 emissions) of the electricity system using currently available technologies, even if substantial decarbonization can be achieved at fairly moderate cost. For more results from this sensitivity analysis, see Table A.3.

2.5 Discussion

As with any mathematical model, our framework has its limitations. The sheer scope of the analysis requires considerable temporal and spatial aggregation that limits its applicability to issues that are highly resolved in either space or time. For example, our model cannot shed light on the value of transmission and distribution investments at scales smaller than each of our 13 regions, or complications associated with ramp rates on time scales less than one hour. The optimization paradigm assumes perfect foresight of future parameter values and seamless coordination across regions governed in reality by many different decision makers. Therefore, the pathways produced by the model should be viewed as idealized transformations of the U.S. electricity system rather than predictions of how it will evolve in

practice. Parameter assumptions become more uncertain as the analysis progresses toward its 2050 time horizon. While we have performed scenario and sensitivity analyses to explore how model outcomes vary with certain important assumptions, there are many other parameters in the model whose assumed values may end up being poor representations of what ends up transpiring in reality. Similarly, we employ a five-year time step for investment decisions to reduce the computational complexity associated with solving a model of this size. While using a shorter investment time step would allow us to capture varying construction lead times for different technologies, this additional granularity would be unlikely to affect the results significantly given the long analysis timeframe and assumption of perfect foresight. The values of some model parameters – such as the maximum capacity growth rates for power plant types and the fractional contribution of import transmission capacity to satisfying the reserve margin – are fairly subjective values that are either adopted from previous studies or established to approximate reality. As is the case in essentially any energy modeling study that develops long-term scenarios, we cannot predict the emergence of fundamentally new technologies that could be introduced before 2050. Despite these limitations, we have compared results across a number of different parameterizations to obtain major, policy-relevant insights about the future of U.S. electricity infrastructure. The following subsections clearly assert what we view as the five key takeaways from our analysis, and discuss their policy implications.

2.5.1 The U.S. electricity sector can be substantially decarbonized at modest cost, but complete decarbonization is very costly

In our scenario results, U.S. electricity sector CO_2 emissions in 2050 are 53% below their 2016 level even without a policy stimulus. This reflects the rapidly declining costs of renewable and storage technologies. Additional emissions reductions can be achieved at fairly moderate cost. For instance, annual CO_2 emissions can be reduced by 80% from 2016 to 2050 with only a 9% increase in total present discounted costs (see Fig. 2.10b).

However, beyond a 90% reduction, marginal abatement costs rise very steeply. We find that complete decarbonization of the U.S. electricity sector by 2050 would raise total costs by 69% relative to the No Policy case. It is not surprising that costs escalate significantly as the last remaining CO_2 emissions must be eliminated. Complete decarbonization rules out low-carbon technologies like fossil generation with CCS, and requires massive capacity additions of electricity storage to ensure that reliability standards are met.

To put the high cost of reducing the last few percent of CO_2 emissions in perspective, it is instructive to compare this cost to mainstream estimates of the social cost of carbon, which quantifies the benefits of reducing emissions in monetary terms. In terms of the cumulative CO_2 emissions from 2016–2050, raising the 2050 emissions reduction target from 97.5% to 100% entails an average abatement cost of \$2108/tCO_2 for eliminating the last 2.5% of emissions. This figure is an order of magnitude greater than even the high end of currently accepted social cost of carbon estimates (Nordhaus, 2017).

Overall, our findings indicate that the U.S. electricity sector will undergo significant decarbonization, and that policies to reduce annual emissions by 80–90% by 2050 are achievable at moderate cost but pursuing a zero-emissions electricity sector under current technology cost projections would risk major increases in electricity costs.

2.5.2 Significant expansion of solar PV and wind to combine for at least 40% of the generation mix by 2050 is fairly certain, although solar PV and battery storage are more affected by economic and policy assumptions than wind

Renewable technologies expand considerably through 2050 regardless of the scenario, but solar PV and battery storage growth are more sensitive to assumptions than wind deployment. Furthermore, future technology cost trajectories appear to be stronger drivers of renewables expansion than the climate policy. Compared to the No Policy setting, the Carbon Tax scenario does not increase renewable capacity and generation as much as the

Pessimistic Costs scenario decreases them. While wind and solar PV still grow in the latter case, their cumulative capacity investments are 40% lower in the Pessimistic Costs scenario than in the No Policy setting. Most of this difference is attributed to lower solar PV deployment, with wind less affected. Wind is a more mature technology than solar PV and its future growth is less dependent on further cost reductions. In addition, with its more extreme diurnal capacity factor variations, solar PV expansion relies more heavily on falling costs of battery storage, which also decrease less in the Pessimistic Costs scenario.

The increase in CO_2 emissions in the Pessimistic Costs case is limited because nuclear power offsets most of the decline in wind and solar generation. This outcome suggests that nuclear generation can be a reasonably cost-effective, carbon-free substitute for intermittent renewables and storage if costs develop as projected by the NREL Annual Technology Baseline. This is of course far from guaranteed, but the results do demonstrate that the extensive decarbonization of U.S. electricity is robust to the costs of any one technology, as long as other economically competitive mitigation options exist.

2.5.3 Investments in long-distance transmission are very limited, while investments in battery storage are significant, under a wide range of assumptions

In contrast to some other studies (MacDonald et al., 2016), we find that expansion of the long-distance transmission network does not play a major role in future electricity infrastructure pathways. The scenario results show that, due to rapidly falling wind, solar PV, and battery storage costs, investing in renewable generation closer to the loads it serves is generally more economical than installing renewables further away to take advantage of higher capacity factors, but needing to install new transmission capacity. Our model results thus support Lovins (Lovins, 2017), who essentially advanced this same argument. The diminishing importance of long-distance transmission should come as a relief to policymakers, since siting and approval of inter-state transmission projects has been politically challenging

due to public opposition and having to navigate multiple complex regulatory environments (Vajjhala and Fischbeck, 2007; Zichella and Hladik, 2013).

On the other hand, investments in battery storage are much greater and accelerate over the next several decades. Given the considerable value that storage offers to the electricity system, policymakers and system operators should ensure that market mechanisms fully compensate storage providers for the many valuable services it can provide. As Sioshansi (2017) describes, storage owners must often decide whether to earn revenue through competitively priced services (e.g., energy arbitrage) or services subject to rate-based cost recovery (e.g., transmission deferral) since they are not allowed to be compensated for both sets of activities. As a result, the range of valuable services that storage can provide is constrained, which discourages storage investments. Market design solutions to this artificial separation of competitive and regulated services have been proposed, such as auctioning storage capacity rights to third parties (Sioshansi, 2017), and their effective implementation will become more important as the need for storage intensifies.

2.5.4 Natural gas capacity growth is strong and robust, but utilization of gas capacity declines steadily and significantly

Our results consistently show that large investments in natural gas capacity continue to be part of the optimal system transformation, but that average utilization rates of this gas capacity decline steadily and significantly through 2050. Utilization drops as intermittent renewables expand and continue to be dispatched first due to near-zero variable costs. Cost-effective storage improves utilization of wind and solar generation, which further erodes the utilization of gas-fired power plants. However, gas capacity is still required to maintain system reliability during hours of high demand and low variable renewable power output. This constitutes another market design challenge for policymakers, who must have mechanisms in place to properly remunerate natural gas generation facilities for the reliability services

they provide. There is some doubt as to whether the high wholesale electricity prices available during a few peak net load hours when power is scarce will allow gas plants to recover their costs in energy-only markets such as the Electric Reliability Council of Texas and the Southwest Power Pool (Ela et al., 2015). Capacity markets and creative approaches for rewarding flexible, dispatchable capacity (such as the flexible ramping product introduced by the California Independent System Operator) can help overcome the *missing money* problem and ensure resource adequacy (Brown, 2018; Hobbs and Oren, 2019; Newbery, 2016). Policymakers should actively learn from successes and failures in other jurisdictions and adopt market design approaches that incentivize sufficient capacity investments.

2.5.5 Electricity system costs shift away from operating expenditures and toward capital expenditures over time, especially in the presence of climate policy

As fossil fuel generation is replaced by renewables, storage, and nuclear power in the future, costs will shift away from operating expenditures and toward capital expenditures. This trend makes access to financing critical and threatens to extend payback periods, which could be at odds with one another in an increasingly competitive electricity landscape where market-based prices present considerable risk. Investment is increasingly directed toward renewable and natural gas generation projects that are smaller than traditionally large coal and nuclear units (Rhodes, 2018), a shift that helps manage project risk. This investment trend is currently well aligned with emissions reduction goals. In the future, however, if less granular technologies like fossil plants with CCS or nuclear power are expected to form part of the decarbonization portfolio, then policymakers might need to help insulate these capital-intensive projects from risk in competitive market areas. This would become more important if wind, solar PV, and battery storage costs do not decline as much as anticipated.

2.6 Conclusions

In this chapter, we developed a customized and expanded version of the core OSeMOSYS framework (Howells et al., 2011), which is a least-cost optimization model of the integrated U.S. electricity generation and transmission system, and used it to study the evolution of U.S. electricity infrastructure through 2050. We represented 13 regions distinguished by their electricity demand profiles, wind and solar PV capacity factors, hydro and geothermal resources, and existing generation capacities. Our model incorporates the long-distance transmission network that links these regions and balances supply and demand across them. A major advantage of our framework compared to existing tools is its temporal resolution that represents time on multiple levels, from five-year capacity investment decision periods, to inter-seasonal variability in loads and capacity factors, to 24-hour dispatch in each season. We applied this model to run and compare results from four main scenarios (No Policy, No New Transmission, Pessimistic Costs, Carbon Tax) as well as additional sensitivity analyses.

Based on the model results, we affirmed five key takeaways and discussed their policy implications in the previous section. Here, they serve to summarize our most important findings.

1. The U.S. electricity sector can be substantially decarbonized at modest cost, but complete decarbonization is very costly.

2. Significant expansion of solar PV and wind to combine for at least 40% of the generation mix by 2050 is fairly certain, although solar PV and battery storage are more affected by economic and policy assumptions than wind.

3. Investments in long-distance transmission are very limited, while investments in battery storage are much greater, under a wide range of assumptions.

4. Natural gas capacity growth is strong and robust, but utilization of gas capacity declines steadily and significantly.

5. Electricity system costs shift away from operating expenditures and toward capital expenditures over time, especially in the presence of climate policy.

Chapter 3

Strategic interactions between liquefied natural gas and domestic gas markets: A bilevel model

3.1 Introduction

Natural gas is a major energy resource and is extensively used for diverse applications including residential and commercial heating, industrial processes, electricity generation, and transportation. Natural gas production in the United States (U.S.) has increased steadily over the past decade and is expected to grow another 32% from 2019 to 2050 (EIA, 2018b). This includes a 36% increase in natural gas use for U.S. electricity generation as gas continues to substitute for coal and provides dispatchable power to balance intermittent renewable generation from wind and solar (EIA, 2018b). Meanwhile, global natural gas consumption is expected to increase by more than 40% between 2018 and 2050 (IEA, 2019). In addition to its expanding role in electricity generation, natural gas use is expected to grow significantly in the industrial sector. As natural gas producers seek out new markets and natural gas importers seek out new sources of gas, liquefied natural gas (LNG) trade is growing rapidly and beginning to integrate regional gas markets into a global market. In the U.S., substantial LNG export infrastructure is slated to come online, and an increasing fraction of domestically produced gas will be sold to LNG operators for export to foreign markets.

Global LNG consumption has risen steadily over the past six years to reach 354.7 million tonnes (MT) in 2019 (IGU, 2020). The largest LNG exporters in 2019 were Qatar (77.8 MT)

This chapter is under revision at the *Computers & Operations Research* journal.

and Australia (75.4 MT), followed by the U.S. (13.1 MT) (IGU, 2020). On the other side, Japan (76.9 MT) and China (61.7 MT) were the largest importers of LNG (IGU, 2020). The global LNG market is expected to grow by 3.6% annually until 2035 (McKinsey & Company, 2019) and U.S. LNG exports are expected to increase by approximately 250% over that period (EIA, 2018b). While the U.S. only began exporting LNG in 2016 with the opening of the Sabine Pass terminal in Louisiana, five facilities are currently under construction and more are in various phases of planning and approval. Once these facilities become operational, they will cater to sharply rising LNG demand from Asia (EIA, 2018b). As LNG exports grow, they will exert increasing influence on domestic gas markets including production, infrastructure investments, and prices. It is therefore important to understand how the additions of LNG export facilities, which significantly raise demand for gas at individual locations in the network, affect the decisions of market actors further upstream, and in turn what this means for LNG operators choosing whether and where to construct terminals.

The purpose of this chapter is to develop a modeling framework that effectively captures the strategic interactions between an LNG operator and a natural gas (NG) producer. The LNG operator procures natural gas from the NG producer in the domestic network, liquefies the gas, and exports the LNG to overseas markets. LNG facilities are lumpy investments with very high upfront costs, making decisions about whether and where to construct them highly consequential. To make these decisions, LNG operators should not only consider historical prices available at potential facility locations, but should also anticipate the effects of a new export terminal's gas demand on those prices, including the reaction of domestic supply. The NG producer sells gas to the LNG operator in addition to the consumers in the domestic market, with production and demand locations connected via a pipeline network. The strategic interactions between the LNG operator and NG producer are certainly non-cooperative, as gas sales from the producer to the LNG operator appear as revenues in the former's profit maximization problem and as costs in the latter's problem. In this

environment with conflicting strategic interests, it is crucial for market agents to anticipate the responses of others when making their own decisions.

In this chapter, we model the non-cooperative relationship between the LNG operator and NG producer as a sequential game using a bilevel programming framework. Since LNG terminals are large-scale, long-lived, lumpy investments that will interact with the domestic gas market for several decades, we represent the LNG operator as the leader who faces the upper-level problem. The LNG operator's decisions involve locating LNG facilities, procuring gas for liquefaction, and selling LNG to foreign markets. The NG producer is the follower. In the lower-level problem, the NG producer makes decisions about production quantities, pipeline infrastructure, and gas sales to domestic consumers and the LNG operator. Since we are more interested in seeing how the LNG player integrates into the setting where the NG producer caters only to the local spot markets, the decisions that have more value in analyzing correspond to those of the LNG operator. The bilevel structure aids the LNG operator in making profitable decisions while anticipating the NG producer's response to those decisions. Our main contributions to the literature are summarized below.

1. We develop a bilevel model to study the strategic interactions between an LNG operator and an NG producer.

2. Using a preliminary model with one production node and one demand node, we derive analytical insights on optimal gas pricing for the NG producer.

3. We provide a general bilevel model for a network with multiple possible locations for LNG facilities, multiple production locations, multiple LNG markets, and multiple spot markets.

4. We reformulate the bilevel program into a tractable, convex QMIP and demonstrate that it can be solved efficiently for relatively large networks.

5. We apply our framework to a case study of the Gulf-Southwest region of the U.S. and evaluate several decision making scenarios to quantify the benefits of the bilevel methodology.

The remainder of the chapter is organized as follows. Section 3.2 reviews the literature on natural gas infrastructure optimization, natural gas market models, and bilevel programming applications in energy. In Section 3.3, we derive analytical insights on optimal gas pricing using a simple, preliminary model. Our generalized network model formulated as a bilevel program is presented in Section 3.4. Section 3.5 describes the solution strategy we employ to solve the bilevel model by reformulating it into a convex QMIP. Section 3.6 presents a case study that applies the bilevel model to the Gulf-Southwest region under several different decision making scenarios. The scenario results are analyzed and compared in Section 3.7. Finally, Section 3.8 concludes by summarizing our key findings.

3.2 Literature review

3.2.1 Natural gas infrastructure optimization

Significant work has been done to optimize the design and operation of natural gas transmission networks including models which aid in developing a natural gas network from scratch or optimally expanding an existing network to cater to increasing demand (da Silva Alves et al., 2016; Kabirian and Hemmati, 2007; Rømo et al., 2009; Üster and Dilaveroğlu, 2014). Most of these problems are hard to solve due to the nonlinearities and non-convexities associated with pipeline design elements and the dynamics of gas flows. Üster and Dilaveroğlu (2014) propose a large-scale mixed-integer nonlinear programming (MINLP) framework for transmission network expansion with an objective to minimize investment, operational, and gas procurement costs. The model instance is then solved using an online MINLP solver (Bonmin) and sensitivity analysis is conducted on various parameters.

Although a nonlinear, non-convex framework is justified to model the complexities associated with pipeline design and operation, the main drawback of these models is that there is no guaranteed way to ascertain the global optimality of the solution obtained. A common strategy is therefore to derive convex and tractable relaxations of these non-convex problems which can then be solved to optimality. Rømo et al. (2009) present a real-world example of such an approach for the decision support tool GassOpt, which is a single-period, steady-state, mixed-integer linear program (MILP) used to optimize Norwegian natural gas production and transport. It is also used as a decision making tool by StatoilHydro, a shipper of natural gas, and Gassco, a pipeline operator, to optimally route gas through their network (Rømo et al., 2009). A similar problem pertaining to the design of a natural gas transmission network is considered by da Silva Alves et al. (2016) using a multi-objective model. The first objective is to minimize the cost of transportation and the second is to maximize the volume of gas transported through the network. The demand points considered in their study represent growing markets, with demand curves that help capture the endogenous dynamic whereby higher demand causes additional infrastructure investment, which in turn leads to lower revenue in transportation. The multi-objective problem is then solved by generating a Pareto frontier using an ϵ-constraint method (da Silva Alves et al., 2016).

Gupta and Grossmann (2012) propose a model for offshore oilfield infrastructure development that is a multi-period, non-convex MINLP with an objective to maximize net present profit. They employ a linearization technique to reduce the problem to an MILP which can be solved efficiently using off-the-shelf solvers. Rothfarb et al. (1970) present a similar framework and implement solution techniques based on trees with heuristics that iteratively eliminate suboptimal solutions until the optimal solution is reached. Ulstein et al. (2007) describe a planning model which is used as a decision tool for petroleum production in Norway. The model considers multi-component flows and nonlinear functions to model the

complexities involved in processing, which are further linearized to achieve an MILP solved using Xpress. Cafaro and Grossmann (2014) address the problem of long-term infrastructure and operational planning for shale gas. They develop an MINLP model for optimizing infrastructure decisions for the shale gas supply chain starting from drilling of wells to the pipeline network that delivers the gas. A decomposition method based on piecewise linear approximation of the objective function is proposed as a solution strategy for the resulting large-scale, non-convex MINLP. A similar model of infrastructure planning for shale gas production is provided by Arredondo-Ramírez et al. (2016). Its objective is to develop a least-cost schedule for planning and development of infrastructure including production wells and a gas distribution network, considering price trajectories generated using Monte Carlo simulation.

A mixed-integer nonlinear version of the facility location problem is proposed by Camponogara et al. (2012) for optimal scheduling of compressors in oilfields. The authors use linear reformulations of constraints and piecewise linear approximations of cost functions to achieve an MILP. As we have described, most natural gas infrastructure planning models adopt the perspective of a single decision maker. Although these models attempt to capture the complexities and nonlinearities of infrastructure design and operation in detail, they fail to consider interactions between the decision maker and other market actors. Therefore, these existing frameworks could lead to suboptimal decision making by failing to account for the reactions of other agents to the decision maker's chosen strategy. In this dissertation, we attempt to overcome this limitation by proposing and analyzing a bilevel model where the LNG operator anticipates the response of the domestic gas market before choosing to construct LNG terminals.

Han et al. (2019) present a model for dynamic planning of natural gas transmission. Their non-convex, nonlinear model of the pipeline network is relaxed using a three-stage convex relaxation along with piecewise linear approximations to yield a tractable model that

can be solved in real-time for decision support. The strategy of reformulating non-convex problems to obtain tractable convex relaxations is practically useful and has been employed often in the literature. The solution strategy we develop in Section 3.5 to solve our bilevel model is based on the same general approach.

Recent applications of optimization to LNG focus on supply chain problems such as transportation and routing of LNG cargoes (Goel, Slusky, van Hoeve, Furman, and Shao, 2015; Grønhaug, Christiansen, Desaulniers, and Desrosiers, 2010; Halvorsen-Weare and Fagerholt, 2013; Mutlu, Msakni, Yildiz, Sönmez, and Pokharel, 2016). Goel et al. (2015) introduce a constraint programming approach for optimal LNG scheduling and routing. The solution method they propose for their mixed-integer program is based on an iterative search heuristic and is claimed to be computationally efficient compared to conventional methods. The LNG inventory routing problem, which deals with the optimal routing of LNG tanker fleets, has been studied by Grønhaug et al. (2010). They develop a mixed-integer program to decide on routes, production quantities, and sales quantities to maximize profit given the capacity restrictions of the LNG tanker fleet. Similarly, Halvorsen-Weare and Fagerholt (2013) also solve the LNG inventory routing problem as a mixed-integer program, but they use penalty costs to ensure that deliveries are completed within pre-specified time periods.

Lai et al. (2011) assess the value of downstream LNG storage using a Markov decision process model that incorporates the LNG inventory routing problem, natural gas prices, and sales quantities to the market. While optimization methods have been applied to natural gas infrastructure and LNG supply chains, these planning problems have typically been considered in isolation even though they are tightly intertwined in reality. To the best of our knowledge, our work is the first to use a bilevel programming structure to model the strategic interactions between an LNG operator and NG producer who both seek to maximize their own profits. Sönmez et al. (2013) consider the benefits of experimenting with new technologies and integrating them into the LNG supply chain. Their work demonstrates the

importance of evaluating alternative operational models as technological advances expand the possibilities in the industry.

3.2.2 Natural gas market models

Researchers have modeled natural gas markets using a variety of approaches including linear programming, nonlinear programming, mixed complementary problem (MCP) equilibrium modeling, and agent-based economic modeling (Busch, 2014). Linear and nonlinear programming models are unable to capture the interactions among the many decision makers who constitute gas markets since they inherently assume the perspective of a single decision maker who controls all aspects of the system (Busch, 2014). On the other hand, LP models can be quite detailed in terms of their representations of time and the gas infrastructure network. NLP models are more difficult to solve and often provide unstable results. Agent-based models depict each market player as a separate entity. They can also be parameterized with substantial detail, but agent-based models are typically solved by simulating agents' actions and behaviors, or by applying heuristics or iterative algorithms. They do not attempt to provide solutions which are system-wide optima or equilibria based on individual players' optimization problems (Busch, 2014).

A popular approach in the natural gas market modeling literature is to represent the market as an equilibrium problem formulated as an MCP. All players in the market face their own optimization problems, and the MCP consists of their Karush-Kuhn-Tucker (KKT) conditions as well as market-clearing conditions that determine prices and link the players' problems (Gabriel et al., 2005). Egging et al. (2008) develop an MCP model of the European natural gas market and use it to study the effects of a disruption in gas supplies from Russia via Ukraine. Egging et al. (2010) build the World Gas Model, which is similarly structured and includes LNG trade, long-term contracts, and explicit consideration of market power in the upstream segment. In recent years, MCP methodology has advanced to incorporate

features like endogenous capacity investments (Huppmann, 2013) and stochastic optimization under uncertainty (Egging, 2013; Gabriel et al., 2009).

Much like MCPs, our model in this chapter explicitly considers multiple players who face separate (but linked) optimization problems. But unlike an MCP, which is a simultaneous game, our bilevel model assumes that the LNG operator and NG producer act sequentially, with the former as the leader and the latter as the follower. The bilevel methodology allows the leader to make decisions while anticipating how those decisions would influence the actions of the follower. We believe that this is an important alternate perspective given the differences in the scales and longevities of infrastructure investments in different segments of the natural gas supply chain.

3.2.3 Bilevel models in the energy domain

While bilevel programming has not previously been applied to LNG and domestic gas market interactions, it has been used to study problems across the energy domain, especially in electricity. Jin and Ryan (2013) develop a trilevel model for electricity generation and transmission expansion. In their formulation, centralized transmission expansion decisions are made in the first level, decentralized generation expansion decisions are made in the second level, and operational decisions are made in the third level. To solve the problem, they consider the bilevel subproblems of the lower two levels of the original trilevel model, and reformulate them as equivalent single-level problems. Finally, the resulting problem is solved iteratively using a diagonalization method.

Maurovich-Horvat et al. (2014) explore the impacts of policy measures on investment and operational decisions of wind producers and transmission operators using a leader-follower model. The transmission operator acts as the leader, making investment decisions and setting congestion charges, while the wind producer acts as the follower, making capacity investment and operational decisions including transmission flows. The authors solve the

bilevel model using the complementarity approach by replacing the lower-level problem with its equivalent KKT conditions, converting it into a mathematical program with equilibrium constraints (MPEC), and further reducing it to an MILP. In a similar setting, Baringo and Conejo (2012) model a wind power plus transmission investment problem as an MPEC. The decision maker in this case aims to identify optimal investment projects in wind power and the transmission network in order to maximize social welfare. They propose an MILP reformulation by reformulating the nonlinear complementarity constraints using a disjunctive formulation approach, along the lines of what we implement in Section 3.5.3.

Pozo et al. (2017) provide an overview of bilevel models, their theoretical foundations, solution techniques, and applications to power systems. They describe many variations of the bilevel framework including single-leader-single-follower, single-leader-multiple-follower, and multiple-leader-single-follower problem structures. The solution strategies discussed in the paper are dominated by the approach of reformulating the bilevel problem into a single-level problem by employing KKT conditions or strong duality by using the primal constraints, dual constraints, and strong duality theorem with the lower-level problem. The authors also briefly review stochastic bilevel problems.

Beyond electricity, Bard et al. (2000) present a bilevel program for allocating tax credits to enhance biofuel production. The government serves as the leader and aims to increase biofuel production by providing subsidies in the form of annual tax credits. The agricultural sector serves as the follower and maximizes profit by making crop mix and land use decisions in response to the tax credits offered by the government. Two algorithms are proposed to solve the bilevel model: a grid search over the leader's variables and an approximate NLP formulation of the bilevel program.

In natural gas, researchers have used bilevel models to study the natural gas cash-out problem. This problem arises when a shipper, who has contracted with a pipeline company to deliver specified amounts of gas to different points throughout the network, actually

delivers more or less than the committed quantities, causing an imbalance (Dempe et al., 2005). The pipeline company penalizes the shipper for any imbalance by imposing a cash-out penalty policy. Dempe et al. (2005) investigate the natural gas cash-out problem from a leader-follower perspective where the supplier is the leader who aims to maximize revenue, and the pipeline company is the follower who aims to minimize penalties imposed due to imbalances. Their model is a mixed-discrete bilevel program which is solved by reducing it into two linear bilevel programs. The authors propose using a branch-and-bound-based algorithm to solve the resulting linear bilevel problems by enumerating over the faces of the underlying convex polyhedron. Dempe et al. (2011) extend this work by providing a linear reformulation of the problem that yields theoretical insights and is computationally easier. Kalashnikov et al. (2010a) consider a stochastic version of the natural gas cash-out problem. In the stochastic upper-level problem, the gas supplier considers different scenarios of future demand and decides on the amount of gas to extract and sell, earning revenue but leading to possible penalties for imbalances. The authors reformulate the upper- and lower-level problems so that they become LPs, then solve them iteratively.

Zhang and Zhu (1996) construct a bilevel program for pipeline network optimization where the available pipeline diameters are discrete. The initial discrete problem is then relaxed by replacing the discrete variables with continuous ones, yielding an NLP. The lower-level problems are then reformulated and solved using conjugate duality theory by taking advantage of the convexity of the lower-level problem. The upper-level problem is reformulated using a piecewise linear convex function and the resulting problem is then solved iteratively.

3.2.4 Solution strategies for bilevel models

Bilevel problems are fundamentally hard to solve due to their non-convex and non-differentiable nature (Colson et al., 2007), and most of the solution methodologies proposed

in the literature focus on simpler cases with convex objectives and constraint sets. Even the simplest case of a linear bilevel program, with linear upper- and lower-level problems, is NP-hard (Colson et al., 2007). As described in the previous subsection which focused on bilevel programming applications in energy, the most common solution approach is to reformulate the bilevel model into an equivalent single-level problem. Other strategies for solving bilevel programs that appear in the literature include extreme-point approaches (Tuy et al., 1993), branch-and-bound (Edmunds and Bard, 1991), complementarity pivoting (Bialas and Karwan, 1984), and various descent methods.

The prominent strategy of reformulating a bilevel problem into a single-level one essentially replaces the lower-level problem with its KKT conditions or Fritz-John conditions, resulting in a single-level mathematical program with complementarity constraints (MPCC) (Allende and Still, 2013; Dempe, 2002). This approach depends on the lower-level problem being convex. The solution strategy we implement in this chapter leverages this idea, as we begin by using the KKT conditions of the lower-level problem to obtain a single-level MPCC reformulation. Another approach is to use the necessary optimality conditions without Lagrange multipliers, resulting in an optimization problem with variational inequalities or an MPEC (Dempe, 2002). Colson et al. (2007) show that if the lower-level problem is convex and differentiable, then MPECs encompass bilevel problems and MPECs can also be formulated as bilevel problems. Therefore, techniques for solving MPECs can be used to solve bilevel programs under certain conditions.

3.3 Preliminary model and analysis

In this section, we analyze the simplest version of the bilevel model where an LNG operator and NG producer interact with each other in a sequential manner. The LNG operator is represented as the leader (due to the lumpy, large, and long-lived nature of LNG terminal investments) who anticipates the response of the NG producer when making his own

decisions. The NG producer is the follower who responds optimally to the LNG operator's upper-level choices. In this simple, preliminary model, we assume that the LNG operator has an operational export facility and the NG producer has unlimited production capacity. The NG producer can sell natural gas to two markets: the domestic spot market (consisting of power plants, homes with gas heating, etc.) and the LNG operator, each of which is assigned its own demand curve. The LNG operator can liquefy the gas it procures from the NG producer and sell LNG to a single overseas market, represented by a demand curve. The LNG operator's decisions are the amount of gas to procure from the NG producer, the quantity of LNG to export, and the LNG market price. The NG producer's decisions are the amounts of gas to produce, transmit, and sell to both the spot market and LNG operator (with corresponding prices).

3.3.1 Notation

Parameters

$C^{\text{prod}}(\cdot)$	NG production cost function
$C^{\text{pipe}}(\cdot)$	NG pipeline installation cost function
$C^{\text{ship}}(\cdot)$	NG shipment cost function
$C^{\text{liq}}(\cdot)$	LNG liquefaction cost function
$C^{\text{LNGship}}(\cdot)$	LNG shipment cost function
$D^{\text{spot}}(p^{\text{spot}})$	Domestic spot market demand curve
$D^{\text{LNG}}(p^{\text{LNG}})$	LNG market demand curve
$D^{\nu}(p^{\nu})$	LNG facility gas procurement demand curve

Leader's Decision Variables

ν	Natural gas procured from producer (by LNG operator)
l	LNG exported to overseas market

p_j^{LNG}	Market price of LNG

Follower's Decision Variables

f	Natural gas shipped to spot market
x	NG pipeline capacity installed
q	Quantity of NG produced
p^{spot}	Spot market price of natural gas
p^{ν}	NG procurement price for LNG operator

3.3.2 Preliminary model

$$\max_{\substack{p^{\text{LNG}},\nu,\\ l\in\mathbb{R}_+}} \; p^{\text{LNG}} l - p^{\nu}\nu - C^{\text{liq}}(\nu) - C^{\text{LNGship}}(l) \tag{3.1a}$$

subject to

$$l \leq \nu \tag{3.1b}$$

$$l = D^{\text{LNG}}(p^{\text{LNG}}) \tag{3.1c}$$

$$p^{\nu} \in \arg\max_{\substack{p^{\text{spot}},p^{\nu},\\ f,q,x\in\mathbb{R}_+}} \left\{ p^{\text{spot}} f + p^{\nu}\nu - C^{\text{prod}}(q) - C^{\text{pipe}}(x) - C^{\text{ship}}(f) \right. \tag{3.1d}$$

subject to

$$f + \nu \leq q \qquad (\alpha) \tag{3.1e}$$

$$f \leq x \qquad (\beta) \tag{3.1f}$$

$$f = D^{\text{spot}}(p^{\text{spot}}) \qquad (\gamma) \tag{3.1g}$$

$$\left. \nu = D^{\nu}(p^{\nu}) \qquad (\tau) \right\} \tag{3.1h}$$

The upper-level problem (3.1a) – (3.1c) is the optimization problem faced by the LNG operator, who maximizes the revenue earned from LNG sales minus the costs of procuring natural gas from the NG producer, liquefying it, and shipping LNG to the overseas market. The lower-level problem (3.1d) – (3.1h) belongs to the NG producer, who maximizes revenue earned from sales of natural gas to the spot market and LNG operator, minus the costs of production, pipeline investment, and shipment via the pipeline. The variables $\alpha \in \mathbb{R}_+$, $\beta \in \mathbb{R}_+$, $\gamma \in \mathbb{R}$, and $\tau \in \mathbb{R}$ are the dual variables associated with constraints (3.1e) – (3.1h), respectively. Spatially, this simple formulation assumes that gas production and the LNG terminal are located in the same place, whereas the domestic spot market demand is located elsewhere. The NG producer thus needs to build and use a pipeline to deliver gas to the spot market. Note that the spatial configuration could be changed easily by making minor modifications to the model structure. Our model naturally fits within the bilevel framework because the upper-level gas procurement quantity appears in the lower-level problem, while the lower-level price for gas sales to the LNG operator appears in the upper-level problem.

3.3.3 Analytical insights

The preliminary model allows us to derive analytical insights on optimal gas pricing in a bilevel setting. The lower-level problem is an LP, so we can replace it with its equivalent KKT conditions.

Proposition 1. *At optimality, the constraints $f+\nu \leq q$ and $f \leq x$ of the lower-level problem hold with equality.*

Proof. When the optimal production quantity $q^* = 0$ and the optimal pipeline capacity $x^* = 0$, given the non-negativity of pipeline flow f and gas procurement by the LNG operator ν, we have $f^* = x^*$ and $f^* + \nu^* = q^*$.

Next, if the optimal production quantity $q^* > 0$, then the complementarity conditions

yield $\alpha^* = \frac{dC^{\text{prod}}(q)}{dq}$ and $\alpha^* \ (f^* + \nu^* - q^*) = 0$. Assuming $\frac{dC^{\text{prod}}(q)}{dq} > 0$, we have $f^* + \nu^* = q^*$ at optimality. Similarly, if the optimal pipeline capacity $x^* > 0$, then the respective complementarity conditions yield $\beta^* = \frac{dC^{\text{pipe}}(x)}{dx}$ and $\beta^* \ (f^* - x^*) = 0$. Assuming a non-negative unit pipeline investment cost, we get $f^* = x^*$ at optimality since the objective has a negative term in x with the associated constraint $x \geq f$, so the lowest value x can take on is f^*. □

We see from Proposition 1 that the NG producer will only produce as much gas as he sells to the spot market and LNG operator, and will only invest in as much pipeline capacity as he will actually use to ship gas from the production location to the spot market.

Proposition 2. *Under optimal pricing, the change in the NG producer's revenue from selling the marginal unit of gas to the spot market is equal to the total marginal cost of producing and shipping the gas.*

Proof. When the optimal flow $f^* > 0$, the complementarity condition yields an expression for the optimal spot market price $p^{\text{spot}*}$, which is

$$p^{\text{spot}*} - \gamma^* = \frac{dC^{\text{prod}}(q)}{dq} + \frac{dC^{\text{pipe}}(x)}{dx} + \frac{dC^{\text{ship}}(f)}{df}. \tag{3.2}$$

Similarly, when $p^{\text{spot}*}, p^{\nu*} > 0$, we have

$$\gamma^* = \frac{-1}{\frac{dD^{\text{spot}}(p^{\text{spot}})}{dp^{\text{spot}}}} \ f^*,$$

$$\tau^* = \frac{-1}{\frac{dD^{\nu}(p^{\nu})}{dp^{\nu}}} \ \nu^*.$$

Observe that $f^* + \nu^*$ represents total sales in both markets, $\frac{dp^{\text{spot}}}{dD^{\text{spot}}(p^{\text{spot}})}$ represents the change in spot price when an additional unit of gas is sold in the spot market, and $\frac{dp^{\nu}}{dD^{\nu}(p^{\nu})}$ represents

the change in LNG facility gas procurement price when an additional unit of gas is sold to the LNG operator. Thus, we can interpret γ^* and τ^* as the losses in revenue from existing sales when an additional unit of gas is sold to the spot market and LNG operator, respectively (because selling more gas depresses the price). We can see that Eq. (3.2) represents the condition equating marginal revenue to marginal cost, where marginal revenue ($p^{\text{spot}^*} - \gamma^*$) is the price of the marginal unit sold in the spot market minus the effect of that one unit increase in spot sales on the revenue earned from all previous units of gas sold. □

3.4 Generalized network model

In this section, we formulate a far more expansive version of the bilevel model. We generalize the preliminary model to a network wherein the nodes represent geographical regions and arcs represent the pipeline network that transmits gas across regions. Here are some simplifying assumptions our model entails. We ignore the nonlinearities associated with modeling the physical characteristics of pipelines and gas compressibility for mathematical tractability. The model considers a single LNG operator and a single NG producer in the upper and lower level, respectively, leading to both the leader and the follower acting as monopolists. We consider quadratic production costs for the NG production and linear costs for the remaining parameters, including NG and LNG shipments, liquefaction, and capacity investments. We consider linear demand curves for all markets. The LNG operator decides whether to open an export terminal in each region where one is allowed, and if a terminal is added, then the NG producer can sell gas to both the spot market and LNG facility in that region.

3.4.1 Notation

Sets

$\mathcal{N}$	Set of production nodes; $\mathcal{N} = \{1, 2, \ldots, N\}$
$\mathcal{M}$	Set of LNG market nodes; $\mathcal{M} = \{1, 2, \ldots, M\}$

Parameters

K_j	Maximum production capacity at node $j \in \mathcal{N}$
K_j^{LNG}	Maximum capacity of LNG facility that can be built at node $j \in \mathcal{N}$
A_{ij}	Adjacency matrix, $\mathcal{N} \times \mathcal{N}$
C_j^{unit}	Unit cost of installing production capacity at node $j \in \mathcal{N}$
$C_j^{\text{prod}}(\cdot)$	Production cost at node $j \in \mathcal{N}$ ($C_j^{\text{prod}}(.) = C_{a_j}^{\text{prod}} q_j^2 + C_{b_j}^{\text{prod}} q_j$)
C_{ij}^{pipe}	Unit cost of installing pipeline on link $(i, j) \in \mathcal{N} \times \mathcal{N}$
C_{ij}^{ship}	Variable cost of shipping gas through pipeline link $(i, j) \in \mathcal{N} \times \mathcal{N}$
C_j^{liq}	Cost of liquefaction at node $j \in \mathcal{N}$
C_j^{LNGfixed}	Fixed cost of investment in LNG facility at node $j \in \mathcal{N}$
C_j^{LNGunit}	Unit cost of installing capacity in LNG facility at node $j \in \mathcal{N}$
C_{ij}^{LNGship}	Variable cost of LNG shipment between node $j \in \mathcal{N}$ and market $i \in \mathcal{M}$
η_j	Loss during liquefaction process at node $j \in \mathcal{N}$
a_j^{spot}	Intercept of spot market demand curve at node $j \in \mathcal{N}$
b_j^{spot}	Slope of spot market demand curve at node $j \in \mathcal{N}$
a_j^{LNG}	Intercept of LNG market demand curve at node $j \in \mathcal{M}$
b_j^{LNG}	Slope of LNG market demand curve at node $j \in \mathcal{M}$
a_j^{ν}	Intercept of LNG facility gas procurement demand curve at node $j \in \mathcal{N}$
b_j^{ν}	Slope of LNG facility gas procurement demand curve at node $j \in \mathcal{N}$

Leader's Decision Variables

ν_j	Natural gas procured at node $j \in \mathcal{N}$ (by LNG operator)
l_{ij}	LNG shipped from node $i \in \mathcal{N}$ to market $j \in \mathcal{M}$

z_j	Binary variable taking value 1 if LNG facility is opened at node $j \in \mathcal{N}$, 0 otherwise
μ_j	Capacity installed in LNG facility at node $j \in \mathcal{N}$
d_j^{LNG}	Demand for LNG in market $j \in \mathcal{M}$
p_j^{LNG}	Price of LNG in market $j \in \mathcal{M}$

Follower's Decision Variables

f_{ij}	Flow in pipeline $(i,j) \in \mathcal{N} \times \mathcal{N}$ (from node i to j)
x_{ij}	Pipeline capacity installed in link $(i,j) \in \mathcal{N} \times \mathcal{N}$
Q_j	Production capacity installed at node $j \in \mathcal{N}$
q_j	Production at node $j \in \mathcal{N}$
d_j^{spot}	Demand for natural gas in spot market $j \in \mathcal{N}$
p_j^{spot}	Spot price of natural gas at node $j \in \mathcal{N}$
p_j^{ν}	LNG facility gas procurement price in node $j \in \mathcal{N}$

3.4.2 Model

3.4.2.1 Upper-level problem

$$\max \sum_{j\in\mathcal{M}} p_j^{\text{LNG}} d_j^{\text{LNG}} - \sum_{j\in\mathcal{N}} p_j^{\nu}\nu_j - \sum_{j\in\mathcal{N}} C_j^{\text{LNGfixed}} z_j - \sum_{j\in\mathcal{N}} C_j^{\text{LNGunit}} \mu_j - \sum_{j\in\mathcal{N}} C_j^{\text{liq}} \nu_j - \sum_{i\in\mathcal{N}} \sum_{j\in\mathcal{M}} C_{ij}^{\text{LNGship}} l_{ij} \tag{3.3a}$$

subject to

$$\sum_{i\in\mathcal{M}} l_{ji} \leq (1-\eta_j)\ \nu_j \qquad \forall \quad j \in \mathcal{N} \tag{3.3b}$$

$$\nu_j \leq \mu_j \qquad \forall \quad j \in \mathcal{N} \tag{3.3c}$$

$$\mu_j \leq K_j^{\text{LNG}} z_j \qquad \forall \quad j \in \mathcal{N} \tag{3.3d}$$

$$\sum_{i \in \mathcal{N}} l_{ij} = d_j^{\text{LNG}} \qquad \forall \quad j \in \mathcal{M} \tag{3.3e}$$

$$d_j^{\text{LNG}} = a_j^{\text{LNG}} - b_j^{\text{LNG}} p_j^{\text{LNG}} \qquad \forall \quad j \in \mathcal{M} \tag{3.3f}$$

$$z_j \in \{0, 1\} \qquad \forall \quad j \in \mathcal{N} \tag{3.3g}$$

$$p_j^{\text{LNG}}, \nu_j, \mu_j, d_j^{\text{LNG}} \in \mathbb{R}_+ \qquad \forall \quad j \in \mathcal{N} \tag{3.3h}$$

$$l_{ij} \in \mathbb{R}_+ \qquad \forall \quad i \in \mathcal{N}, j \in \mathcal{M} \tag{3.3i}$$

Eq. (3.3a) represents the total profit earned by the LNG operator (leader), where the term $p_j^{\text{LNG}} d_j^{\text{LNG}}$ is the revenue earned from LNG exports to overseas market j and the term $p_j^{\nu} \nu_j$ is the cost of procuring gas from the NG producer (follower) at node j, where the variable p_j^{ν} is set by the NG producer in response to the LNG operator's decisions. $C_j^{\text{LNGfixed}} z_j$ denotes the fixed cost of opening an LNG facility at node j and $C_j^{\text{LNGunit}} \mu_j$ is the cost of adding capacity to the LNG facility opened there. The term $C_j^{\text{liq}} \nu_j$ captures the cost of liquefying the gas procured at node j and the term $C_{ij}^{\text{LNGship}} l_{ij}$ represents the cost of shipping LNG from the export facility at node i to the LNG market at node j.

Constraint (3.3b) stipulates that the total LNG shipments from any node j to the LNG markets are bounded by the total gas procured at that node, accounting for losses during the liquefaction process. Constraints (3.3c) – (3.3d) ensure that the gas procured by the LNG facility at node j does not exceed the capacity available at the facility. Constraints (3.3e) – (3.3f) compute the total sales in each LNG market and specify the LNG demand curves faced by the LNG operator. Constraint (3.3g) declares the binary variable z_j, whose value denotes whether the LNG operator opens an export terminal at node j or not. We incorporate these binary variables into the model to reflect the lumpy nature of LNG terminal investments, which have very high fixed costs.

3.4.2.2 Lower-level problem

$$\max \sum_{j\in\mathcal{N}} p_j^{\text{spot}} d_j^{\text{spot}} + \sum_{j\in\mathcal{N}} p_j^{\nu}\nu_j - \sum_{j\in\mathcal{N}} C_j^{\text{unit}} Q_j - \sum_{j\in\mathcal{N}} C_{a_j}^{\text{prod}} q_j^2 - \sum_{j\in\mathcal{N}} C_{b_j}^{\text{prod}} q_j$$
$$- \sum_{i\in\mathcal{N}}\sum_{j\in\mathcal{N}} C_{ij}^{\text{pipe}} x_{ij} - \sum_{i\in\mathcal{N}}\sum_{j\in\mathcal{N}} C_{ij}^{\text{ship}} f_{ij} \tag{3.4a}$$

subject to

$$\sum_{i\in\mathcal{N}} f_{ij} + q_j = \sum_{i\in\mathcal{N}} f_{ji} + d_j^{\text{spot}} + \nu_j \qquad \forall \quad j \in \mathcal{N} \qquad (\lambda_j) \tag{3.4b}$$

$$q_j \le Q_j \qquad \forall \quad j \in \mathcal{N} \qquad (\theta_j) \tag{3.4c}$$

$$Q_j \le K_j \qquad \forall \quad j \in \mathcal{N} \qquad (\alpha_j) \tag{3.4d}$$

$$f_{ij} \le A_{ij} x_{ij} \qquad \forall \quad i,j \in \mathcal{N} \qquad (\beta_{ij}) \tag{3.4e}$$

$$d_j^{\text{spot}} = a_j^{\text{spot}} - b_j^{\text{spot}} p_j^{\text{spot}} \qquad \forall \quad j \in \mathcal{N} \qquad (\kappa_j) \tag{3.4f}$$

$$\nu_j = a_j^{\nu} - b_j^{\nu} p_j^{\nu} \qquad \forall \quad j \in \mathcal{N} \qquad (\tau_j) \tag{3.4g}$$

$$q_j, Q_j, p_j^{\text{spot}}, p_j^{\nu}, d_j^{\text{spot}} \in \mathbb{R}_+ \qquad \forall \quad j \in \mathcal{N} \tag{3.4h}$$

$$x_{ij}, f_{ij} \in \mathbb{R}_+ \qquad \forall \quad i,j \in \mathcal{N} \tag{3.4i}$$

Eq. (3.4a) represents the total profit earned by the NG producer (follower), where the term $p_j^{\text{spot}} d_j^{\text{spot}}$ is the revenue from spot market sales at node j and $p_j^{\nu}\nu_j$ is the revenue earned from sales to the LNG operator. $C_j^{\text{unit}} Q_j$ denotes the cost of adding production capacity at node j and the term $C_j^{\text{prod}} q_j$ represents the production cost at node j. The terms $C_{ij}^{\text{pipe}} x_{ij}$ and $C_{ij}^{\text{ship}} f_{ij}$ are the costs of adding pipeline capacity and shipping gas, respectively, from node i to node j.

Constraint (3.4b) ensures flow balance among production, shipments, and sales at any node j. Constraints (3.4c) – (3.4d) ensure that the total production at node j does not exceed the production capacity available there. Constraints (3.4f) – (3.4g) specify the demand curves

for the spot market and LNG facility gas procurement at node j. The variables $\lambda_j \in \mathbb{R}$, $\theta_j \in \mathbb{R}_+$, $\alpha_j \in \mathbb{R}_+$, $\beta_{ij} \in \mathbb{R}_+$, $\kappa_j \in \mathbb{R}$, and $\tau_j \in \mathbb{R}$ are the dual variables associated with constraints (3.4b) – (3.4g), respectively.

3.5 Solution strategy

This section describes in detail how we reformulate our bilevel program from the previous section into a tractable, convex QMIP through a combination of (i) replacing the convex lower-level problem with its KKT conditions to yield an MPCC, (ii) using piecewise linear approximations to eliminate the non-convex terms from the objective, and (iii) using a disjunctive reformulation to eliminate the complementarity constraints from the original lower-level problem.

3.5.1 Mathematical program with complementarity constraints

Finding the optimal solution to the bilevel program presented in Section 3.4.2 requires jointly solving the upper-level problem (3.3) and lower-level problem (3.4). The lower-level problem in which the NG producer maximizes profit has a convex quadratic objective function and a linear constraint set, and is therefore convex. To solve the bilevel program, we transform it into a single-level problem by replacing the lower-level problem with its KKT conditions, which yields an MPCC.

Proposition 3. *The lower–level problem (3.3) of the NG producer is convex.*

Proof. The objective function of the lower-level problem can be written as

$$\begin{aligned} F\Big(\begin{bmatrix} p^{\text{spot}} & p^{\nu} & Q & q & x & f \end{bmatrix}^{\top} \Big) \; &= a^{\text{spot}\top} p^{\text{spot}} - p^{\text{spot}\top} \operatorname{Diag}\left(b^{\text{spot}}\right) p^{\text{spot}} + a^{\nu\top} p^{\nu} \\ &\quad - p^{\nu\top} \operatorname{Diag}\left(b^{\nu}\right) p^{\nu} - C^{\text{unit}\top} Q - q^{\top} \operatorname{Diag}\left(C_a^{\text{prod}}\right) q \\ &\quad - C_b^{\text{prod}\top} q - C^{\text{pipe}\top} x - C^{\text{ship}\top} f, \end{aligned} \tag{3.5}$$

where Diag$(\cdot)$ is the diagonal matrix. The Hessian of the function F has non-zero rows only corresponding to the variables $p^{\text{spot}} \in \mathbb{R}_+^{\mathcal{N}}$, $p^{\nu} \in \mathbb{R}_+^{\mathcal{N}}$, and $q \in \mathbb{R}_+^{\mathcal{N}}$. The non-zero rows of the Hessian of the objective function F are given by

$$\operatorname{Hess} F = \begin{bmatrix} -2\ \operatorname{Diag}(b^{\text{spot}}) & 0 & 0 \\ 0 & -2\ \operatorname{Diag}(b^{\nu}) & 0 \\ 0 & 0 & -2\ \operatorname{Diag}(C_a^{\text{prod}}) \end{bmatrix}.$$

The parameters b^{spot} and b^{ν} represent the slopes of the demand curves for the spot market and LNG facility gas procurement, respectively, and both parameters are non-negative (slopes are negative). Similarly, C_a^{prod} is the coefficient for the quadratic term of the production cost function and each term in C_a^{prod} is non-negative as well. Therefore, the matrix $\operatorname{Hess} F$ is negative semidefinite (NSD) since it is a diagonal matrix with all eigenvalues negative. Also, the constraints associated with the lower–level problem are all linear. Hence, the problem of maximizing the objective function F subject to linear constraints is convex. □

3.5.2 Piecewise linear convex relaxation

In this subsection, we develop a relaxation scheme to solve the non-convex, nonlinear, single-level MPCC described in Section 3.5.1, which arises after the lower-level problem is replaced with its KKT conditions. We start by analyzing this MPCC, with a quadratic objective function (3.6).

Proposition 4. *The MPCC that maximizes the objective function* (3.6) *is non-convex.*

Proof. The objective function of the MPCC can be written as

$$\begin{aligned} G\Big(\begin{bmatrix} p^{\text{LNG}} & p^{\nu} & z & \mu & \nu & l \end{bmatrix}^{\top} \Big) &= a^{\text{LNG}\top} p^{\text{LNG}} - p^{\text{LNG}\top} \operatorname{Diag}\left(b^{\text{LNG}}\right) p^{\text{LNG}} - a^{\nu\top} p^{\nu} \\ &\quad + p^{\nu\top} \operatorname{Diag}\left(b^{\nu}\right) p^{\nu} - C^{\text{LNGfixed}\top} z - C^{\text{LNGunit}\top} \mu \\ &\quad - C^{\text{liq}\top} \nu - C^{\text{LNGship}\top} l. \end{aligned} \tag{3.6}$$

The Hessian of the function G has non-zero rows only corresponding to the variables $p^{\text{LNG}} \in \mathbb{R}_+^{\mathcal{M}}$ and $p^\nu \in \mathbb{R}_+^{\mathcal{N}}$. The non-zero rows of the Hessian of the objective function G are given by

$$\operatorname{Hess} G = \begin{bmatrix} -2\ \operatorname{Diag}(b^{\text{LNG}}) & 0 \\ 0 & 2\ \operatorname{Diag}(b^\nu) \end{bmatrix}.$$

The parameters b^{LNG} and b^ν represent the slopes of the demand curves for the LNG market, $D^{\text{LNG}}(p^{\text{LNG}}) = a^{\text{LNG}} - b^{\text{LNG}} p^{\text{LNG}}$, and LNG facility gas procurement, $D^\nu(p^\nu) = a^\nu - b^\nu p^\nu$, and both parameters are non-negative (slopes are negative). Therefore, the matrix $\operatorname{Hess} G$ is not NSD since $\operatorname{Hess} G$ is a diagonal matrix with both negative and positive eigenvalues. Hence, the objective function G to be maximized is not concave and thus the problem of maximizing it is non-convex. □

To make the problem tractable, we replace the non-convex terms in the objective function (3.6) with piecewise linear convex approximations. Let $\mathcal{S}$ be the index set of segments. Now, for each node j, we approximate the quadratic terms in (3.6) with the linear segments $a_{sj}^{\text{pw}} + b_{sj}^{\text{pw}} p_j^\nu$ for all $s \in \mathcal{S}$, as shown in Fig. 3.1, where the superscript "pw" is an abbrebiation for "piecewise." The slopes b_{sj}^{pw} and intercepts a_{sj}^{pw} of the pieces, along with the breakpoints, are estimated by solving an MILP with the objective of minimizing the absolute error: $\min \sum_{i \in \boldsymbol{N}} |y_i - \hat{y}_i|$. Using this method, we now achieve a convex objective function by replacing each of the non-convex terms $b_j^\nu (p_j^\nu)^2$ with u_j, such that Eq. (3.7) holds true:

$$\begin{aligned}
&u_j \le a_{sj}^{\text{pw}} + b_{sj}^{\text{pw}} p_j^\nu && \forall \quad s \in \mathcal{S}, j \in \mathcal{N}, \\
&u_j \ge a_{sj}^{\text{pw}} + b_{sj}^{\text{pw}} p_j^\nu - M(1 - \xi_{sj}) && \forall \quad s \in \mathcal{S}, j \in \mathcal{N}, \\
&\sum_{s \in \mathcal{S}} \xi_{sj} = 1 && \forall \quad j \in \mathcal{N}, \\
&\xi_{sj} \in \{0, 1\} && \forall \quad s \in \mathcal{S}, j \in \mathcal{N}.
\end{aligned} \tag{3.7}$$

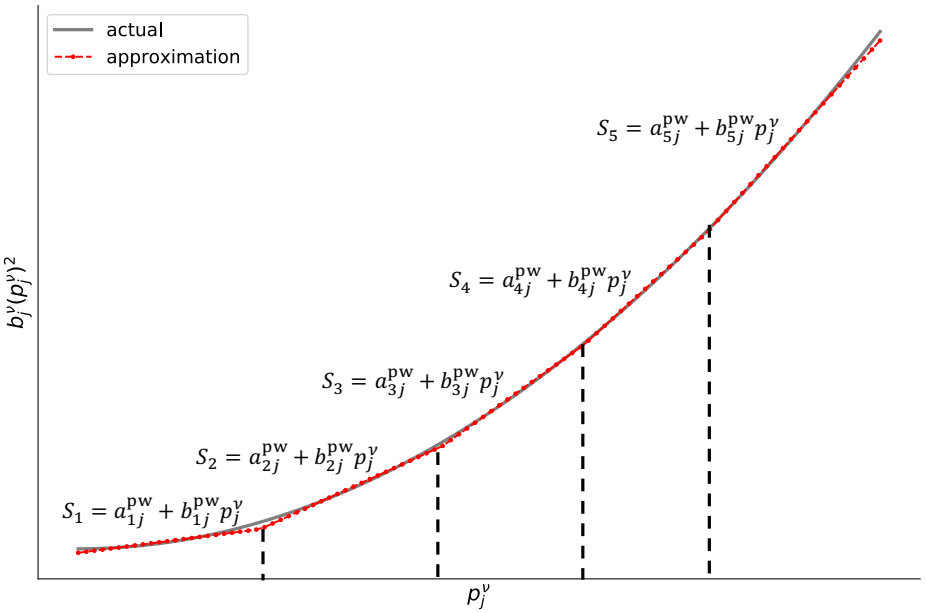

Fig. 3.1. An example piecewise linear approximation of $b_j^{\nu} p_j^{\nu 2}$ with $|\mathcal{S}| = 5$

.

3.5.3 Quadratic mixed-integer program

In this subsection, we carry out our final reformulation of the problem into a convex QMIP, which is computationally tractable. First, we prove that the objective function of the MPCC is convex when the piecewise linear relaxation scheme from Eq. (3.7) is used. Then, we employ a disjunctive reformulation of the complementarity constraints to obtain the convex QMIP.

Proposition 5. *In the single-level MPCC reformulation of the bilevel program, incorporating the piecewise linear relaxation scheme from Eq. (3.7) makes the objective function convex.*

Proof. With the piecewise linear relaxation, the objective function of the MPCC can be

written as

$$H\Big(\begin{bmatrix} p^{\text{LNG}} & p^{\nu} & u & z & \mu & \nu & l \end{bmatrix}^{\top}\Big) = a^{\text{LNG}\top} p^{\text{LNG}} - p^{\text{LNG}\top} \operatorname{Diag}(b^{\text{LNG}}) p^{\text{LNG}} - a^{\nu\top} p^{\nu} + u^{\top} - C^{\text{LNGfixed}\top} z - C^{\text{LNGunit}\top} \mu - C^{\text{liq}\top} \nu - C^{\text{LNGship}\top} l. \tag{3.8}$$

The Hessian of the function H has non-zero rows only corresponding to the variables $p^{\text{LNG}} \in \mathbb{R}_{+}^{\mathcal{N}}$. The non-zero rows of the Hessian are given by $\operatorname{Hess} H = -2 \operatorname{Diag}(b^{\text{LNG}})$, which is an NSD matrix since the Hessian is a diagonal matrix with all eigenvalues negative. Hence, the objective function H is concave and thus the problem of maximizing it has a convex objective function. □

The resulting relaxed MPCC with a convex quadratic objective function is written as follows:

$$\max \sum_{j\in\mathcal{M}} a_j^{\text{LNG}} p_j^{\text{LNG}} - \sum_{j\in\mathcal{M}} b_j^{\text{LNG}} (p_j^{\text{LNG}})^2 - \sum_{j\in\mathcal{N}} a_j^{\nu} p_j^{\nu} + \sum_{j\in\mathcal{N}} u_j - \sum_{j\in\mathcal{N}} C_j^{\text{LNGfixed}} z_j - \sum_{j\in\mathcal{N}} C_j^{\text{LNGfixed}} \mu_j - \sum_{j\in\mathcal{N}} C_j^{\text{liq}}\ \nu_j - \sum_{i\in\mathcal{N}} \sum_{j\in\mathcal{M}} C_{ij}^{\text{LNGship}} l_{ij} \tag{3.9a}$$

$$\text{s.t.}\quad u_j \le a_{sj}^{\text{pw}} + b_{sj}^{\text{pw}} p_j^{\nu} \qquad \forall\ \ s\in\mathcal{S}, j\in\mathcal{N} \tag{3.9b}$$

$$u_j \ge a_{sj}^{\text{pw}} + b_{sj}^{\text{pw}} p_j^{\nu} - M(1-\xi_{sj}) \qquad \forall\ \ s\in\mathcal{S}, j\in\mathcal{N} \tag{3.9c}$$

$$\sum_{s\in\mathcal{S}} \xi_{sj} = 1 \qquad \forall\ \ j\in\mathcal{N} \tag{3.9d}$$

$$\sum_{i\in\mathcal{M}} l_{ji} \le (1-\eta_j)\ \nu_j \qquad \forall\ \ j\in\mathcal{N} \tag{3.9e}$$

$$\nu_j \le \mu_j \qquad \forall\ \ j\in\mathcal{N} \tag{3.9f}$$

$$\mu_j \le K_j^{\text{LNG}} z_j \qquad \forall\ \ j\in\mathcal{N} \tag{3.9g}$$

$$\sum_{i\in\mathcal{N}} l_{ij} = a_j^{\text{LNG}} - b_j^{\text{LNG}} p_j^{\text{LNG}} \qquad \forall\ \ j\in\mathcal{N} \tag{3.9h}$$

$$0 \le p_j^{\text{spot}} \perp -d_j^{\text{spot}} + b_j^{\text{spot}} \kappa_j \ge 0 \qquad \forall\ \ j\in\mathcal{N} \tag{3.9i}$$

$$0 \le p_j^{\nu} \perp -\nu_j - b_j^{\nu} \tau_j \ge 0 \qquad \forall\ \ j\in\mathcal{N} \tag{3.9j}$$

$$0 \leq d_j^{\text{spot}} \perp -p_j^{\text{spot}} + \lambda_j + \kappa_j \geq 0 \qquad \forall \quad j \in \mathcal{N} \qquad (3.9k)$$

$$0 \leq Q_j \perp C_j^{\text{unit}} - \theta_j + \alpha_j \geq 0 \qquad \forall \quad j \in \mathcal{N} \qquad (3.9l)$$

$$0 \leq q_j \perp 2\, C_{a_j}^{\text{prod}} q_j + C_{b_j}^{\text{prod}} + \theta_j - \lambda_j \geq 0 \qquad \forall \quad j \in \mathcal{N} \qquad (3.9m)$$

$$0 \leq x_{ij} \perp C_{ij}^{\text{pipe}} - A_{ij}\beta_{ij} \geq 0 \qquad \forall \quad j \in \mathcal{N} \qquad (3.9n)$$

$$0 \leq f_{ij} \perp C_{ij}^{\text{ship}} + \lambda_i - \lambda_j + \beta_{ij} \geq 0 \qquad \forall \quad j \in \mathcal{N} \qquad (3.9o)$$

$$0 \leq \theta_j \perp Q_j - q_j \geq 0 \qquad \forall \quad j \in \mathcal{N} \qquad (3.9p)$$

$$0 \leq \alpha_j \perp K_j - Q_j \geq 0 \qquad \forall \quad j \in \mathcal{N} \qquad (3.9q)$$

$$0 \leq \beta_{ij} \perp A_{ij}x_{ij} - f_{ij} \geq 0 \qquad \forall \quad j \in \mathcal{N} \qquad (3.9r)$$

$$\sum_{i \in \mathcal{N}} f_{ij} + q_j = \sum_{i \in \mathcal{N}} f_{ji} + d_j^{\text{spot}} + \nu_j \qquad \forall \quad j \in \mathcal{N} \qquad (3.9s)$$

$$d_j^{\text{spot}} = a_j^{\text{spot}} - b_j^{\text{spot}} p_j^{\text{spot}} \qquad \forall \quad j \in \mathcal{N} \qquad (3.9t)$$

$$\nu_j = a_j^{\nu} - b_j^{\nu} p_j^{\nu} \qquad \forall \quad j \in \mathcal{N} \qquad (3.9u)$$

$$z_j \in \{0, 1\} \qquad \forall \quad j \in \mathcal{N} \qquad (3.9v)$$

$$\xi_{sj} \in \{0, 1\} \qquad \forall \quad s \in \mathcal{S}, j \in \mathcal{N} \qquad (3.9w)$$

$$l_{ij}, x_{ij}, f_{ij}, \beta_{ij} \in \mathbb{R}_+ \qquad \forall \quad i, j \in \mathcal{N} \qquad (3.9x)$$

$$\nu_j, \mu_j, p_j^{\text{LNG}}, p_j^{\text{spot}}, p_j^{\nu}, q_j, Q_j, d_j^{\text{spot}}, \theta_j, \alpha_j \in \mathbb{R}_+ \qquad \forall \quad j \in \mathcal{N} \qquad (3.9y)$$

$$\lambda_j, \tau_j, \kappa_j, u_j \in \mathbb{R} \qquad \forall \quad j \in \mathcal{N} \qquad (3.9z)$$

Lastly, the MPCC model (3.9) is reformulated into an MILP by implementing a disjunctive reformulation of the nonlinear complementarity constraints from the original lower-level problem. The reformulation scheme shown in Eq. (3.10) is applied to all of the complementarity constraints, (3.9i) – (3.9r), of the MPCC model (3.9):

$$
\begin{aligned}
& & x &\leq M\ \delta, \\
x \perp b - Ax,\ x \geq 0 \quad & \iff & b - Ax &\leq M\ (1-\delta), \\
& & b - Ax &\geq 0,\ x \geq 0,\ \delta \in \{0,1\}.
\end{aligned} \tag{3.10}
$$

Therefore, the combination of applying piecewise linear approximations to the objective function and a disjunctive reformulation to the complementarity constraints yields an MILP with a convex quadratic objective function and linear constraints. This "convex QMIP" is computationally tractable using off-the-shelf commercial solvers.

3.5.4 Computational experiments

We perform computational experiments on randomly generated instances of the convex QMIP to investigate how the problem size and solution time scale with the numbers of nodes in the network and LNG markets. Each instance is randomly generated in the following sequence: (1) an $\mathcal{N} \times \mathcal{N}$ network is generated such that each node $i \in \mathcal{N}$ has a local spot market with a demand curve, (2) potential locations for LNG facilities are randomly selected within the network, (3) generate investment costs, capacity costs, production costs, and production capacity limits for the LNG operator and NG producer for each node in the network, (4) generate a node-node incidence matrix for the network along with pipeline and shipping costs, and (5) define LNG markets with demand curves where open LNG facilities can sell LNG. The computational experiments are executed using a single 2.6 GHz Intel Core i7 processor with 16 GB memory, with Gurobi 8.1.1 as the QMIP solver. We generate 10 random instances each for different problem sizes, and the average runtime in seconds is reported in Table 3.1. It is worth noting that the solution time increases significantly with the number of nodes but does not vary considerably with the addition of LNG markets. The greater sensitivity to the number of domestic nodes arises because the lower-level problem grows exponentially with this number. Our model is intended as a decision support tool

Table 3.1. Results of computational experiments on randomly generated instances.

# of nodes	# of LNG markets	# of int. vars (upper)	# of cont. vars (upper)	# of vars (lower)	Solution time (s)
5	1	5	17	75	0.026
	2	5	24	75	0.031
	3	5	31	75	0.023
10	1	10	32	250	0.558
	2	10	44	250	0.695
	3	10	56	250	0.604
15	1	15	47	525	7.364
	2	15	64	525	7.976
	3	15	81	525	7.565
25	1	25	77	1375	85.05
	2	25	104	1375	87.26
	3	25	131	1375	87.92
50	1	50	152	5250	1848.92
	2	50	204	5250	2108.79
	3	50	256	5250	1979.56
100	1	100	302	20500	8496.24
	2	100	404	20500	8725.63
	3	100	506	20500	8805.04

for long-run strategic infrastructure planning rather than real-time operations. Therefore, even the solution times for the largest instances in Table 3.1, which are on the order of 2–3 hours, are acceptable given the application. Although the case study presented in the next section features only nine nodes and two LNG markets, we emphasize that the results of our computational experiments confirm that the model could include significantly more of them without becoming too computationally burdensome. The limited numbers of nodes

and LNG markets in the case study have far more to do with the difficulty of obtaining high-quality, publicly available input data.

3.6 Case study

In this section, we apply our bilevel framework to model the interactions between an LNG operator and NG producer in a real-world setting. As a case study, we focus on the Gulf-Southwest region of the U.S., which is a major producer and exporter of natural gas. This area of interest is divided into nine regions, where each region is represented as a node in the network. The regions are defined according to state boundaries, namely, New Mexico (NM), Oklahoma (OK), Arkansas (AR), Louisiana (LA), and Texas. Since Texas covers a large area with multiple production clusters and suitable LNG export locations, it is further subdivided into North Texas (NT), East Texas (ET), West Texas (WT), and South Texas (ST) based on the oil and gas division district boundaries established by the Railroad Commission of Texas (2020). For the case study, LNG facilities can only be constructed in the three regions with coastlines, which are LA, ET, and ST. All regions feature spot markets with associated demand curves. We consider two distinct LNG markets representing exports to Atlantic (e.g., Europe) and Pacific (e.g., Asia) destinations.

Table 3.2 documents all of the data sources that we use to parameterize the case study input database. All of these sources are publicly available.

3.6.1 Scenario analysis

In this scenario analysis for the Gulf-Southwest case study, we compare and contrast results from five scenarios that differ according to their decision making structures and assumptions about existing infrastructure. In particular, these scenarios are designed to shed light on the differences between cooperative and non-cooperative outcomes, the benefits of using the bilevel model instead of single-agent optimization to make costly and lumpy

Table 3.2. Documentation of data sources for the case study input database.

Parameter	Source
Production capacity	EIA (2018a)
Unit cost of production capacity	EIA (2018a)
Production costs	IEA (2017)
Pipeline installation & shipment cost	Jaremko (2019)
Liquefaction costs	IEA (2017)
LNG facility costs (fixed & unit)	Songhurst (2018)
LNG shipment costs	Moryadee and Gabriel (2017)
Demand curve parameters	Government of Canada (2018), Baker (2018), EIA (2018), Statistics Canada (2018), Canadian Gas Association (2018)

investment decisions, and the general effects of LNG additions on the domestic gas market. The five scenarios we assess are outlined in Table 3.3.

The Bilevel scenario captures the strategic conflict between the LNG operator and NG producer which is present in the real-world market, so we consider it the baseline scenario against which all other scenarios are compared. This is the generalized network model we presented in Section 3.4, in which the LNG operator and NG producer compete in a non-cooperative, leader-follower game.

The Cooperative scenario assumes that a single optimizing agent is given control of all decisions that belong to both the LNG operator and NG producer in the Bilevel scenario. This agent optimizes the entire system to maximize total profits from gas and LNG sales. In reality, this scenario would describe situations where the LNG operator and NG producer are two divisions of the same company, so that they jointly coordinate their decisions with the goal of maximizing their combined profit. The strategic conflict over the price at which

Table 3.3. Summary of the five main scenarios we investigate.

Scenario name	**Description**
Bilevel Scenario	• A scenario with two players, the LNG operator (leader) and NG producer (follower), who aim to maximize their own profits. • Interpreted as the baseline scenario against which the other scenarios are compared.
Cooperative Scenario	• A scenario with a single optimization agent who jointly makes all NG and LNG decisions to maximize total profit. • Serves as a counterfactual to the Bilevel scenario to elucidate the effects of conflicting strategic interests in the latter.
No LNG Scenario	• A single-agent optimization problem in which the NG producer maximizes profit by selling to the spot markets only. • Used to study spot market outcomes in the absence of an LNG export industry and provide prices for the Naïve LNG scenario.
Naïve LNG Scenario	• A scenario where the LNG operator makes decisions assuming that gas procurement prices will be the same as the spot prices in the solution to the No LNG scenario. • Compared to the Bilevel scenario to quantify the losses incurred by the LNG operator for failing to anticipate the effects of his demand on prices across the network.
Existing Pipeline Network Scenario	• This is the same as the Bilevel scenario, except it assumes that a pipeline network already exists to transmit gas across regions. • Used to study the impact of having an existing pipeline network instead of having to build this infrastructure from scratch.

the NG producer sells gas to the LNG operator is absent in this Cooperative scenario.

As very large purchasers of natural gas at specific locations in the network, LNG terminals can have profound effects on the local spot markets in the region. These effects are captured in the Bilevel scenario, but in order to compare its results to a case without the

LNG industry present, we run the No LNG scenario. This scenario omits the LNG operator and adopts the single-agent perspective of the NG producer, who can only sell gas to the domestic spot markets. In other words, the No LNG scenario is just the lower-level problem from the bilevel formulation, but without sales to the LNG operator. The spot prices featured in the solution to this scenario can be interpreted as the gas prices that prevail before any LNG facilities are added to the region.

The primary advantage of using the bilevel formulation to make decisions about LNG investments is that it allows the LNG operator to anticipate the effects of LNG facility demands on the prices at which they would be able to procure gas. This is important because their large demands would put upward pressure on prices, although the effect could be somewhat mitigated if the NG producer responds by increasing production. To quantify the benefits of using the bilevel framework to aid LNG investment decisions, we compare the Bilevel scenario results against those of a Naïve LNG scenario. In this case, the LNG operator makes LNG terminal investment decisions based on the spot prices from the solution to the No LNG scenario, naïvely assuming that he will be able to procure gas at these prices. Once the LNG operator and NG producer engage in leader-follower competition with LNG facility capacities fixed at their suboptimal values, the LNG operator will not be able to earn as much profit as in the Bilevel scenario.

A common assumption in the four scenarios described above is that both players begin without any infrastructure and must invest in production, pipeline, and LNG capacities from scratch. However, the model proposed in this chapter can flexibly represent either cases of new gas development or cases with existing gas infrastructure. For example, the Gulf-Southwest region which is the focus of our case study already has an extensive pipeline network which has been built up over the years to transmit gas across locations. Therefore, in the Existing Pipeline Network scenario, we assume that the NG producer inherits the initial pipeline network instead of having to construct all pipelines from scratch. This sce-

nario allows us to examine how the initial infrastructure configuration influences the spatial distributions of production and prices.

3.7 Case study scenario results

This section presents and compares results from the five scenarios to obtain relevant strategy insights. Natural gas production levels are described in Section 3.7.1 while Section 3.7.2 examines infrastructure investments. Natural gas and LNG consumption levels and prices are reported in Section 3.7.3. Section 3.7.4 compares the profits earned by the players in each scenario.

3.7.1 Natural gas production

Natural gas and LNG production levels are higher in the Cooperative scenario shown in Fig. 3.2b than in the Bilevel scenario shown in Fig. 3.2a. This is expected, since the Cooperative scenario removes the strategic conflict over the price at which the NG producer sells gas to the LNG operator in the Bilevel scenario. As a result, the single optimizing agent in the Cooperative case can seamlessly increase gas production to supply more feedstock to the LNG facilities. By contrast, in the Bilevel scenario, as the LNG operator seeks to procure more gas, the NG producer has an interest in limiting his gas production response to keep the price of their exchange higher. Fig. 3.2 also indicates that the LNG operator only chooses to add terminals in two of the three coastal regions (ST and LA) in the Bilevel scenario, whereas terminals are constructed in all three of them in the Cooperative scenario. The strategic conflict over LNG facility gas procurement prices in the Bilevel case thus reduces LNG infrastructure investment relative to the Cooperative counterfactual.

Fig. 3.2c reports production volumes for the No LNG scenario, where the NG producer is the lone player and sells gas only to the domestic spot markets. Compared to the Bilevel scenario, gas production in the No LNG scenario is significantly different only in the coastal

(a) Bilevel Scenario

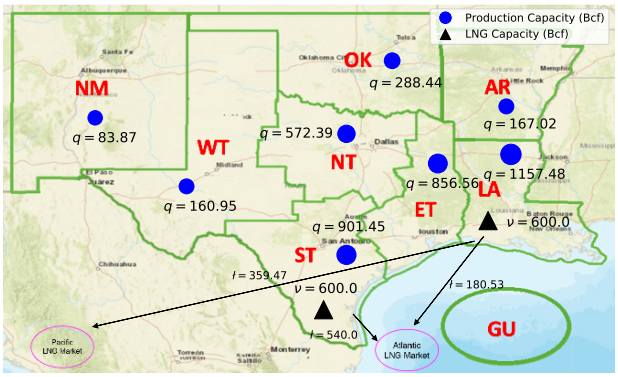

(b) Cooperative Scenario

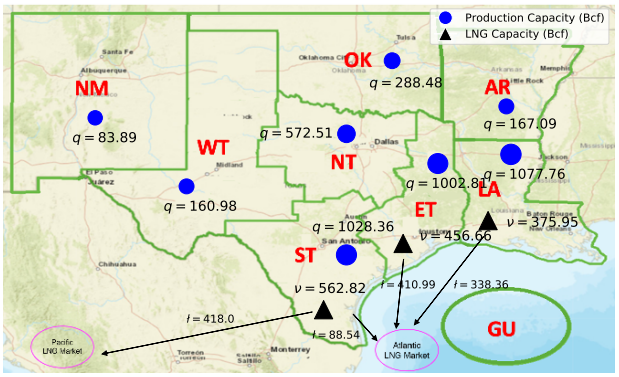

(c) No LNG Scenario

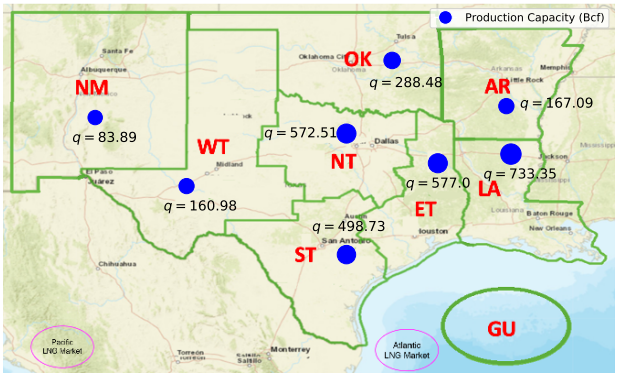

(d) Naïve LNG Scenario

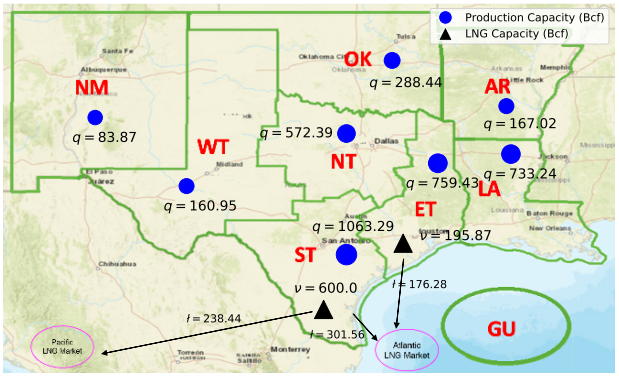

(e) Existing Pipeline Network Scenario

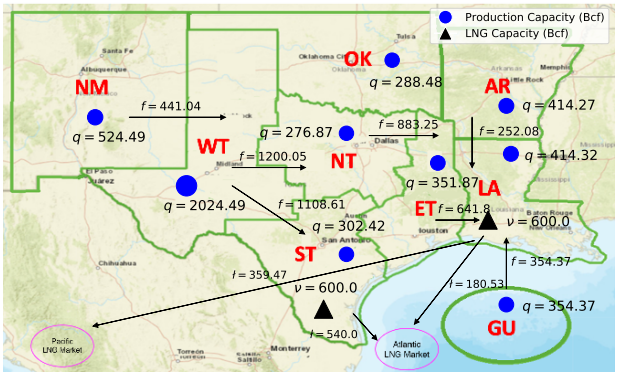

Fig. 3.2. Natural gas and LNG production levels across the scenarios.

regions where LNG terminals are allowed to be built in the Bilevel setting. The presence of the LNG operator in the Bilevel scenario increases gas production in the regions with a potential LNG facility, but in the interior regions with only spot markets, production volumes are not affected by the addition of an LNG export industry. The response of gas production to the presence of the LNG operator in the Bilevel scenario is limited to the potential LNG exporting regions because the NG producer chooses to satisfy increased demand for gas there by ramping up local production within these regions rather than by investing in a pipeline network to produce gas elsewhere and transmit it to the LNG facilities.

Fig. 3.2d shows natural gas and LNG production levels in the Naïve LNG scenario. Interestingly, the locations of the constructed LNG terminals are not the same in this case as in the Bilevel scenario depicted in Fig. 3.2a. Specifically, the Naïve LNG solution features LNG terminals in ST and ET instead of ST and LA, as in the Bilevel solution. By failing to anticipate the effects of his LNG terminals on gas procurement prices, the LNG operator in the Naïve LNG scenario locates facilities suboptimally. As a result, once those capacity investments are fixed and the sequential game for the Naïve LNG scenario takes place, the LNG operator faces higher procurement prices than anticipated. Consequently, the LNG operator procures much less gas and exports less LNG than in the Bilevel case. Therefore, natural gas production is lower as well in the Naïve LNG case.

A noteworthy feature of the solutions to the first four scenarios is that the model does not find it economical to invest in a pipeline network to transmit gas across regions. Instead, the model prefers to produce enough gas in each region to satisfy that region's demands, essentially making all regions self-sufficient. The decision to not invest in pipelines is naturally influenced by many factors in the model including (but not limited to) the cost of adding pipeline capacity, the maximum production capacity in each region, relative production costs in each region, and the fact that our model does not capture pipeline exports from the Gulf-Southwest to other areas of the U.S. and Mexico, which are substantial in real life.

Therefore, to understand how results change if we incorporate the existing pipeline capacities in these regions rather than require the model to build them from scratch, we consider the Existing Pipeline Network scenario. Its production volumes are shown in Fig. 3.2e. The LNG operator's optimal decisions in this scenario are the same as in the Bilevel scenario; regardless of where the NG producer extracts gas, the LNG operator is only concerned about the prices at which its facilities in selected locations can procure gas. Furthermore, the LNG operator makes the same discrete investments in terminals in ST and LA in the Bilevel and Existing Pipeline Network scenarios, and these terminals are at their maximum capacity limits, so there is limited flexibility to adjust operational decisions to whatever differences in gas procurement prices arise between these two cases. Meanwhile, for the NG producer, it is clear that inheriting the underlying pipeline network increases overall natural gas production and shifts it toward the interior regions with lower production costs (e.g. WT). So, while it is apparently not profitable to invest in pipelines from scratch under our reference parameter assumptions, having these pipelines in place is valuable because it links high-demand nodes to low-cost production areas.

3.7.2 Infrastructure investments

Fig. 3.3a reports total investments in gas production and LNG production capacities in each scenario. Compared to the No LNG scenario, the presence of the LNG export industry in all other scenarios leads to far greater investment in natural gas production. This effect is strong because the demand for gas from LNG facilities is sizable relative to the size of the overall domestic spot market, and especially relative to the spot markets within the LNG exporting regions. In the Bilevel scenario, the LNG operator accounts for 29% of total natural gas consumption, and approximately 50% of gas consumption in the regions where LNG terminals are located. Therefore, LNG exports serve as a major stimulus for upstream investment in natural gas production capacity, especially in the regions where

(a) Production capacity and LNG capacity installed

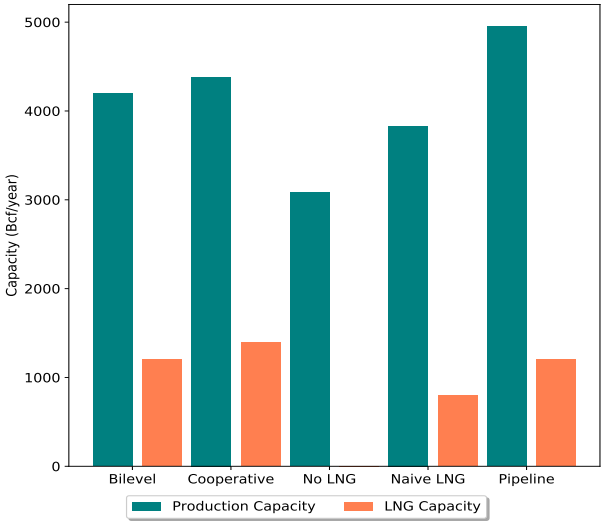

(b) Natural gas consumption

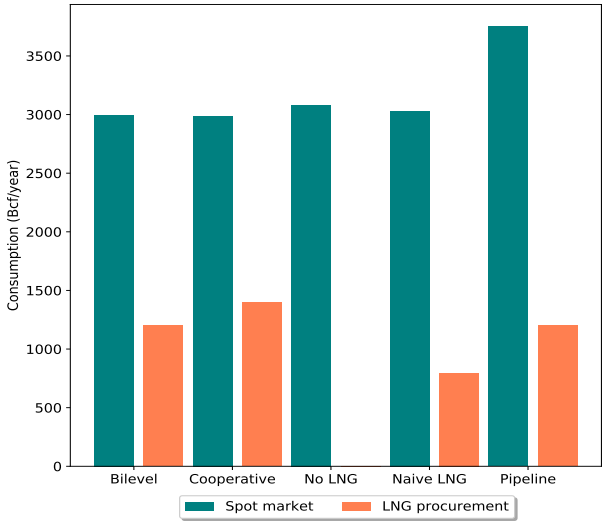

Fig. 3.3. Comparison of annual production capacity and annual LNG capacity installed (a) and annual gas consumption (b) across the scenarios.

export terminals are sited.

Total LNG capacity investment is greatest in the Cooperative scenario. As previously described, this scenario removes the strategic conflict over LNG facility gas procurement prices that shapes the non-cooperative scenarios. As a result, the LNG operator can invest more extensively without worrying about increasing the prices for feedstock gas. The Existing Pipeline Network solution features the most investment in natural gas production capacity. Since the capital costs of shipping gas across regions are sunk in this scenario, the NG producer is able to produce gas in low-cost regions and transmit it to high-demand regions, leading to greater overall production capacity investment as the optimal market equilibria shift to higher quantities sold.

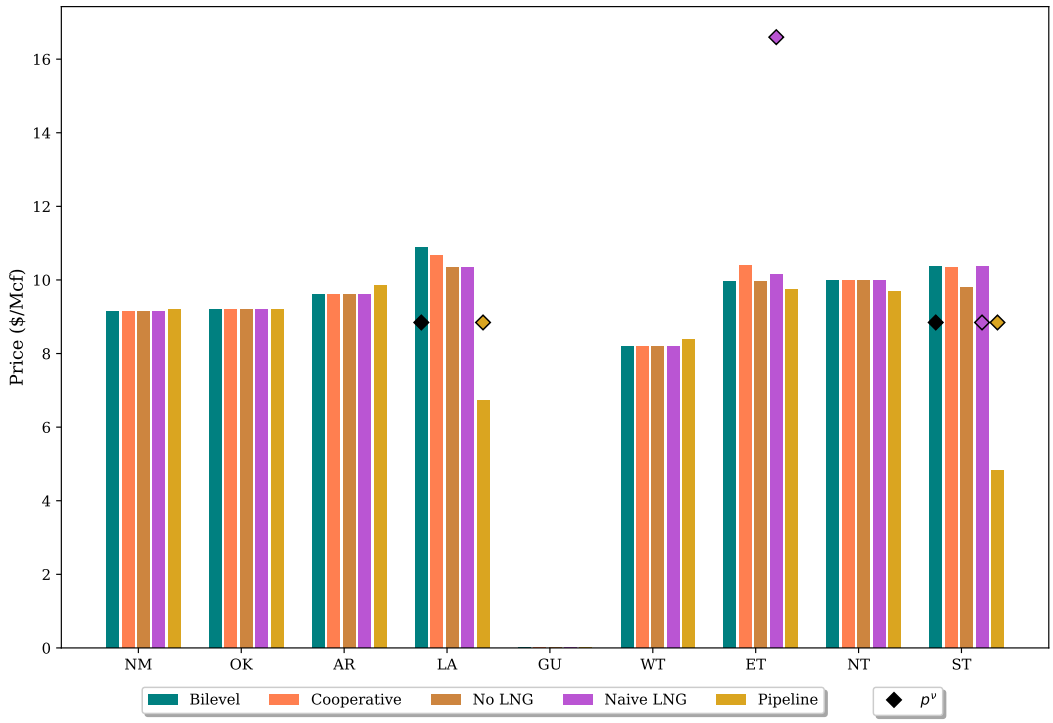

Fig. 3.4. Spot prices (bars) and LNG procurement prices (markers) by region across the scenarios.

3.7.3 Consumption and prices

3.7.3.1 Spot markets and LNG facility gas procurement

Fig. 3.4 plots natural gas spot prices (bars) in each region by scenario, and where applicable, also plots the LNG facility procurement prices (markers). Please note that the gas procurement prices for LNG facilities only exist for the regions and scenarios which result in an LNG facility being opened. It can be seen that the addition of LNG terminals to a region drives up the local spot market prices. For instance, in Fig. 3.4, the spot prices in the ST and LA regions are higher in the Bilevel scenario than in the No LNG scenario. This effect is intuitive, since the LNG facilities are large users of natural gas that compete with local consumers for gas supplies. A more general observation is that the prices in Fig. 3.4 are higher than the actual current market prices in these regions. There are several reasons for

these price differences between the model and reality, the most important of which is likely that our model features a single NG producer who acts as a monopolist, which is far more market power than exists in the real upstream segment. Since our aim in this case study is to understand the impact of LNG industry growth on domestic natural gas markets, and assess the importance of using a bilevel model to plan LNG infrastructure investments, we emphasize relative changes in prices from one scenario to another rather than the absolute price levels.

Fig. 3.4 further elucidates the pitfalls of failing to anticipate production and price responses to new LNG terminals when deciding whether and where to construct these facilities. In the Naïve LNG scenario, the LNG operator suboptimally locates an LNG terminal in ET instead of LA (see Fig. 3.2d), assuming that the spot market prices from the No LNG solution will remain available for gas procurement. However, as seen in Fig. 3.4, once the LNG operator puts a terminal in ET, the NG producer charges almost double the original spot price for sales to this LNG terminal. Therefore, we infer that the naïve approach of failing to anticipate the price effects of constructing new LNG terminals can lead to suboptimal performance by underestimating the prices that these facilities would need to pay to procure gas. The availability of existing pipelines in the Existing Pipeline Network scenario leads to much lower spot prices in the LNG exporting regions ST and LA. The pipelines allow gas to be transmitted in large quantities from low-cost production regions to these regions with high demands, thus reducing spot prices. However, LNG procurement prices do not change in the Existing Pipeline Network scenario, as the NG producer can price separately for sales to the spot market and the LNG operator.

Fig. 3.3b shows overall gas consumption in each scenario. The Existing Pipeline Network scenario features the highest total consumption, mainly due to the spot market as access to low-cost production regions enabled by the pipeline network results in spot market equilibria with higher quantities. Out of the four scenarios that lack an initial pipeline infrastructure,

the Cooperative scenario has the most total gas consumption. While it features slightly less spot market consumption than the No LNG scenario, the Cooperative case has the highest consumption by the LNG operator. With the strategic conflict over gas sales to the LNG operator eliminated, the single optimizing agent in the Cooperative scenario can effectively supply gas to the LNG terminals at cost, leading to more procurement and liquefaction. Gas procurement by LNG facilities is much lower in the Naïve LNG scenario than in the Bilevel scenario because export infrastructure in the former is suboptimally located in regions where the NG producer charges high procurement prices.

3.7.3.2 LNG markets

(a) LNG market price by market

(b) LNG market sales by market

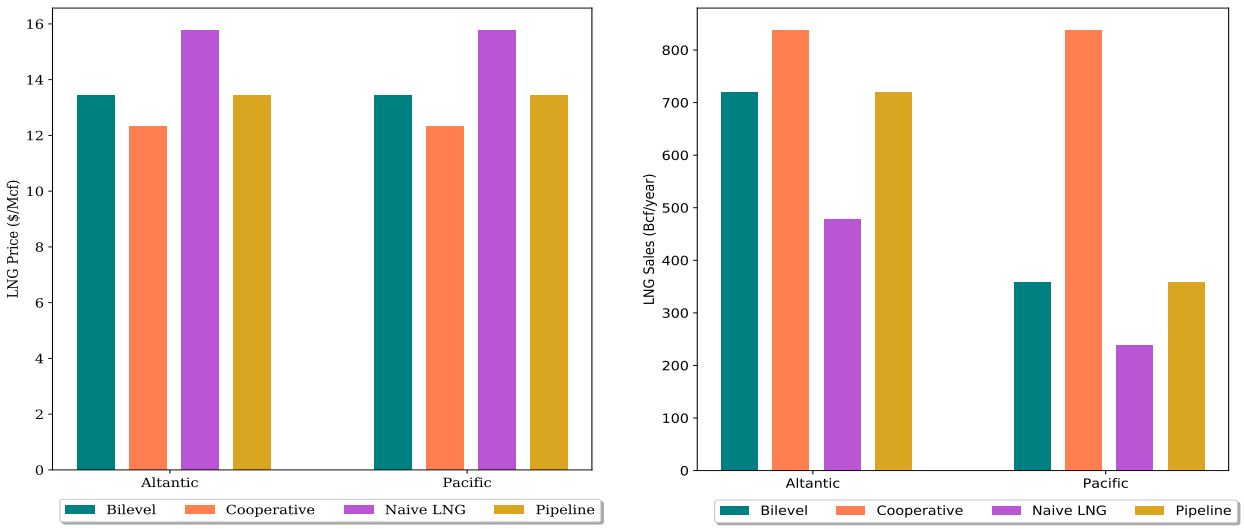

Fig. 3.5. Comparison of LNG market price (a) and total LNG market sales (b) by export market across the scenarios.

Figs. 3.5a and 3.5b show the LNG prices and total LNG sales, respectively, for the two LNG export markets in each scenario. The lowest LNG prices and highest export volumes occur in the Cooperative scenario in which LNG infrastructure investments are greatest and there is no conflict over procurement prices. On the other hand, the highest LNG prices and

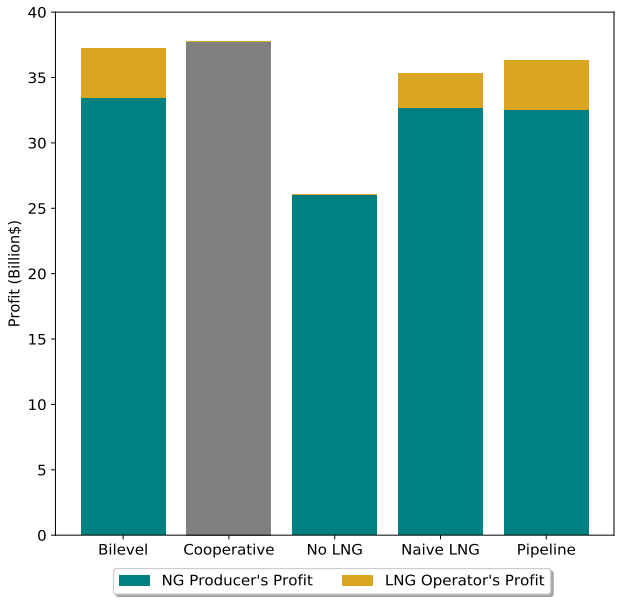

Fig. 3.6. Profits earned by the LNG operator and NG producer in each scenario.

lowest export volumes arise in the Naïve LNG scenario where LNG infrastructure investments are lower and gas procurement prices are higher, discouraging liquefaction.

3.7.4 Profits

The profits earned by the LNG operator and NG producer in each scenario are shown in Fig. 3.6. The highest combined profit is earned in the Cooperative scenario where a single agent jointly optimizes all decisions on behalf of the two players, resulting in greater natural gas production, more LNG exports, and higher profit. The profits in the Bilevel scenario are split between the LNG operator and NG producer, and their combined profit is lower than in the Cooperative case due to their strategic conflict over the LNG facility gas procurement price. Profits are the lowest by far in the No LNG scenario, since the NG producer cannot sell to overseas LNG markets without the LNG operator, and the total demand for the NG producer's gas is significantly lower. The reduction in the LNG operator's profit from the

Bilevel scenario to the Naïve LNG scenario captures (in annualized terms) the loss that the LNG operator would incur by failing to anticipate the effect of his LNG terminal investments on the prices at which they would be able to procure gas. The Existing Pipeline Network scenario does not affect outcomes for the LNG operator, and its effect on the NG producer is insignificant. While overall production and spot market consumption increase compared to the Bilevel scenario, these greater quantities are largely offset by lower spot prices, and the NG producer's profit barely changes. Consumer surplus, however, expands because the pipeline network provides access to low-cost gas, which increases domestic spot market consumption.

3.8 Discussion and conclusions

In this chapter, we have developed a bilevel model to study the strategic interactions between an LNG operator and an NG producer in a leader-follower setting. The model helps both players determine optimal strategies when they operate in a non-cooperative environment wherein their objectives conflict with one another. To solve the bilevel program, we proposed and demonstrated a solution strategy based on (i) replacing the convex lower-level problem with its KKT conditions to yield an MPCC, (ii) using piecewise linear approximations to eliminate the non-convex terms from the objective, and (iii) using a disjunctive reformulation to eliminate the complementarity constraints from the original lower-level problem. These steps ultimately generate a tractable, convex QMIP reformulation. By carrying out computational experiments on randomly generated problem instances, we showed that our method can obtain optimal solutions to instances with a hundred nodes and several LNG markets within reasonable runtimes.

We then applied our bilevel framework to a real-world case study of the Gulf-Southwest region of the U.S. Focusing on this case study, we evaluated five scenarios distinguished by their decision making structures and assumptions about existing infrastructure. Scenario

results show that the addition of LNG export terminals to the region can significantly increase demand for domestic gas and raise prices, although this effect is somewhat mitigated by the NG producer's endogenous production response to higher demand. If the LNG operator does not properly account for the effect of his infrastructure additions on gas prices when deciding whether and where to construct new LNG terminals, then LNG operator profits can suffer due to suboptimal capacity investments that face higher-than-expected prices to procure gas from the NG producer. This finding underscores the usefulness of our bilevel framework for informing discrete decisions about very costly LNG infrastructure, as it captures domestic market responses to LNG investment alternatives. While the NG producer does not find it economical to invest in a pipeline network when he would need to build it from scratch, inheriting existing pipelines expands access to low-cost gas production regions and benefits domestic consumers while leaving the LNG operator unaffected.

In terms of energy market insights, our goals in this dissertation have been to understand the strategic interactions between an LNG operator and NG producer, develop a tractable model capable of informing their optimal infrastructure investments, and analyze how the growth of an LNG export industry affects domestic gas markets under a variety of scenarios. Restricting the model structure to just two players helped us accomplish these goals with a computationally tractable bilevel program, but entailed a number of limitations. Most notably, our model assumes that there is just one LNG operator and one NG producer, effectively acting as monopolists in their respective segments of the supply chain. In reality, natural gas markets are often quite competitive, with many producers and multiple LNG exporters operating in a given country or region. Furthermore, our bilevel framework gives the NG producer control over the pipeline network, which is often constructed and operated by a separate midstream company in real-world market environments. An extension of the work described in this chapter could expand the number of market actors represented in the model by incorporating multiple decision makers into the upper- and/or lower-level problems.

For instance, Pozo et al. (2017) provide examples of bilevel models in power systems with multiple-leader-single-follower and single-leader-multiple-follower structures. Applying these ideas to extend the model presented in this chapter could lead to a richer formulation with more comprehensive market interactions.

Chapter 4

Risk-averse stochastic bilevel programming: An application to natural gas markets

4.1 Introduction

The natural gas market comprises a variety of players and a plethora of moving parts. The natural gas sector in the U.S. has seen extensive changes and shifts in trends in the past decade (Finley, 2013). The global natural gas demand has been growing over the past decade and is expected to continue to rise over the years to come. The shale gas revolution has changed the role of the U.S. from a major importer of natural gas to a major exporter (Conti et al., 2018). The U.S. Energy Information Administration (EIA) anticipates the natural gas production in the U.S. to continue to grow through 2050. With this growth trajectory, the EIA contemplate the U.S. to become a net energy exporter by 2022 (Conti et al., 2018). A similar growth trend is expected in the global liquefied natural gas (LNG) market, with the demand expected to grow by over 3.6% annually (McKinsey & Company, 2019). The growth in the growing global natural gas demand will essentially pave the way to an increase in LNG exports from the U.S., making it a major exporter of LNG. In 2019, the U.S. became the third-largest LNG exporter after Qatar and Australia (EIA, 2020). Multiple LNG projects in the U.S. have become operational in 2019 and 2020, with more expected to come online in the subsequent years. With these additions, the U.S. LNG exports are expected to increase by approximately 250% over the next 15 years (EIA, 2018a).

Although the overall demand forecasts and market growth trends are valuable tools in future infrastructure planning, investment and operational decisions are often vastly affected

by various uncertainties associated with these forecasts. In practice, it is often hard to accurately forecast the demand in different markets. We often approximate future demands by extrapolating the historical data along with other economic signals. However, in reality, the demand often has inherent randomness associated with it that can significantly impact the decisions and the repercussions associated with those decisions. A very recent example is the COVID-19 pandemic and how it affected the global natural gas market in 2020. The natural gas production in the U.S. had been growing steadily in the past decade. The natural gas production in 2019 grew by almost 10 % compared to 2018 (EIA, 2021), but the trend did not continue in 2020. The natural gas consumption by LNG operators in the U.S. has fallen from 9.8 billion cubic feet per day (Bcf/d) in late March 2020 to 4.0 Bcf/d in June due to the decline in the global natural gas demand (EIA, 2020). The extremely low natural gas prices globally in 2020 have also affected the economic viability of U.S. LNG exports (EIA, 2020). Hence, it is of paramount importance for both the LNG operator and the NG producer to consider these demand uncertainties when making investment and operational decisions.

LNG plants require considerable capital investments and generally involve multiple stakeholders. Setting up an LNG facility generally takes about 6-10 years (U.S. Department of Energy, 2018) and are usually planned and structured with an approximate estimated 20-40 years of usage. The average construction cost of an LNG facility is about $US1.5B per 1 MM tonnes per annum (mtpa). Other costs associated with building an LNG facility include the receiving terminal costs and LNG vessels costs for transportation (Naghash, 2017). The average size of LNG facilities is about 5 mtpa, resulting in an average total cost of approximately $US10B - $US15B (U.S. Department of Energy, 2018). Due to the long time frames and extremely high costs associated with these projects, the structuring of these projects would need to anticipate and account for the various risks associated with the project's different aspects. Thus, the consideration of risk is of extreme importance while considering

the decisions of the LNG operator.

In this chapter, we propose a multi-stage stochastic modeling framework that captures the strategic interactions between an LNG operator and NG producer under demand uncertainty while accounting for the players' risk behavior. The LNG operator makes large-scaled, high fixed cost investment decisions and hence is considered the leader. The LNG operator makes investments, gas procurement, LNG export, and pricing decisions. The NG producer produces gas and sells it in the spot market and to the LNG operator. The production, sales, and prices for both players are directly impacted by the market conditions, which are by no means deterministic. Hence, we capture the stochastic behavior in these models by introducing uncertainty in demand for each player's respective markets. We capture the demand uncertainty using scenarios that correspond to various demand conditions in the market. Our main contributions to the literature are summarized below.

1. We develop a stochastic bilevel model to study the strategic interactions between an LNG operator and an NG producer under uncertain demand.

2. We explore the optimal strategies under risk-neutral and risk-averse decision-making approaches.

3. We provide a stochastic bilevel model for an $\mathcal{N} \times \mathcal{N}$ network with multiple potential LNG locations, production locations, spot markets, and LNG markets for multiple demand scenarios. We further reformulate the problem into a convex QMIP.

4. We propose an algorithm that finds "good" feasible solutions to the stochastic bilevel problem within a reasonable amount of time.

5. We apply our framework to a case study of the Gulf-Southwest region of the U.S. and study the effect of the decision maker's risk behavior on the investment and operational decisions.

The remainder of the chapter is organized as follows. Section 4.2 presents the literature review on general stochastic optimization, stochastic bilevel programming, and its applications in energy. Section 4.4 presents the model formulations under the risk-neutral and risk-averse strategies. The solution strategy and algorithm to solve the stochastic bilevel problem are described in Section 4.5. Section 4.6 reports the computational experiments run to study the solution algorithm's efficiency. Section 4.7 presents a case study that applies the stochastic risk-based bilevel model to the Gulf-Southwest region, and the results for the risk-neutral and risk-averse strategies are summarized in Section 4.7.2. Finally, Section 4.8 concludes by summarizing our key findings.

4.2 Literature review

Stochastic programming deals with solving optimization problems in the presence of uncertainty. There has been a plethora of literature available on applying stochastic optimization framework to real-world problems. In this section, we provide a brief review of the different methodologies and techniques that are related to the risk-based stochastic bilevel optimization framework we are attempting to develop. The topic of risk-based stochastic bilevel optimization on falls at the intersection of three different methodologies in the literature. The literature review presented in this section is divided into three sections, summarizing some of the prominent work in each of these methodology, as shown in Fig. 4.1.

4.2.1 Risk-based stochastic optimization

Stochastic optimization has been very frequently used to model many problems arising in the energy sector. Powell and Meisel (2016a) provides a summary of some of the significant problems in the power sector that employ the stochastic optimization framework. Some examples include but are not limited to the unit commitment problem, bidding en-

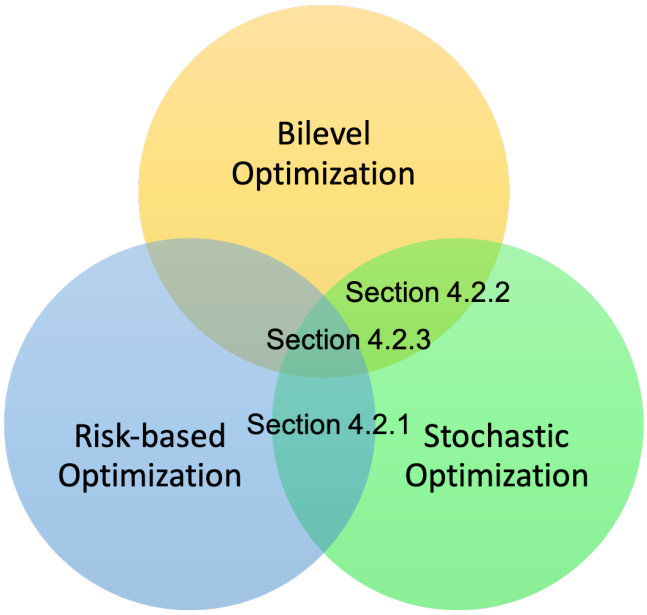

Fig. 4.1. Venn diagram representation of literature review

ergy resources, infrastructure investment planning, and pricing electricity contracts. Powell and Meisel (2016a) provide a standard canonical framework using the Markov decision process theory that could be generalized to a variety of stochastic optimization problems. The methodology is then applied to an energy storage problem (Powell and Meisel, 2016b) and tested on five variants of the problem to demonstrate a particular policy class's suitability for specific problems.

Pozo and Contreras (2012) solve a unit commitment problem with chance constraints with $n - K$ reliability constraints for the day-ahead market with wind and demand uncertainties. An alpha confidence level chance-constrained optimization problem is developed to solve the problem, which the authors reformulate into a mixed-integer linear programming (MILP) problem. They employ different case studies to demonstrate the methodology to highlight the model's performance under increasing wind penetration. Huang et al. (2014) study a two-stage unit commitment problem with the conditional value at risk (CVaR) con-

straints. They incorporate demand response (DR) and energy storage (ES) in the model and employ risk constraints to account for the intermittency of solar and wind resources. The mathematical properties of the CVaR are crucial in attaining a linear convex reformulation of the CVaR constraints, which does not require integer variables, unlike the VaR constraints. The effects of DR and ES on generator schedules are studied using the model to quantify the total expected costs with risk consideration.

Roustai et al. (2018) present a scenario-based optimization framework for real-time electricity and natural gas prices along with electricity demand where the smart energy hub aims to minimize the cost of energy and the net penalty for emissions. The authors consider the CVaR technique to account for the operational risk of the smart energy hub. The authors further test the methodology on a simulation of an office building.

A risk-based stochastic scheduling problem of an energy hub is explored by (Tian et al., 2019), where the energy hub comprises a wind turbine, electricity market, electrical and heat storage systems, along with the electrical and heat demand response programs. The risk-in-cost and the energy hub's operational costs are incorporated using the downside risk constraints, and these constraints are employed to minimize the risk associated with the uncertainties. The methodology is tested on simulated data to study the impact of the downside risk constraints on the problem. Jabr (2005) proposes a model for the robust self-scheduling problem under price uncertainty using the CVaR technique. The objective of the problem is to identify bidding strategies and robust self-schedules under price uncertainties that have lower risk associated with them. Hence, optimal schedules would need to provide a trade-off between maximizing the net profit while minimizing the risk. The problem is reformulated into a second-order cone program (SOCP) and solved using interior-point methods.

4.2.2 Stochastic bilevel optimization

Stochastic bilevel frameworks have been extensively used in the literature to study a variety of problems arising in the energy sector and other fields like structural engineering, supply chain, etc. There have been multi-period stochastic bilevel models developed for the electricity sector for infrastructure planning and operation. Still, the application of these models to natural gas markets has not been that prevalent.

Valinejad and Barforoushi (2015) present a multi-period stochastic bilevel framework for generation expansion planning of restructured power systems. The upper-level problem is a profit maximization problem for investment decisions, and the lower-level problem maximizes the system's social welfare. The solution approach converts the bilevel problem into a stochastic MPEC whose objective and constraints are further linearized, resulting in a MILP. A similar problem is explored by Wogrin et al. (2011) where the upper level represents a generation company that makes investment decisions to maximize profits. The lower level represents an oligopolistic market with other companies making generation decisions and competing in the market. The resulting problem is solved by reformulating it into a stochastic MPEC by replacing the lower-level problem with its equivalent KKT conditions. The stochastic MPEC is then solved by further reformulating it into a MILP.

Carrión et al. (2009) propose a stochastic bilevel framework to solve the medium-term decision-making problem faced by a power retailer. The model considers uncertainties in demand, future prices, and rival-retailer prices and explicitly attempts to model the client response to the retail price offered and the competition among rival retailers. The retailer operates intending to maximize the expected profit at a specified risk level while making decisions pertaining to the level of future involvement in markets and the prices offered to its potential clients. The resulting bilevel programming formulation is solved by transforming it into an equivalent single-level non-linear problem by replacing the lower-level problem with its KKT optimality conditions. The single-level non-linear problem is further reformulated

into a MILP using binary variables.

Zhan and Zheng (2018) propose a bilevel model for the long-term investment planning problem in power generation under uncertainty. The upper-level problem is a multi-stage stochastic expansion planning problem, and the lower-level problems include a collection of economic dispatch problems. This model seeks the optimal sizing and siting for both thermal and wind power units to be built to maximize the expected profit for a profit-oriented power generation investor. A decision-dependent stochastic programming approach is employed to address the uncertainties in the system. The scenario tree's non-stationary transition probabilities are calculated based on discrete choice theory and the economies of scale theory in electricity systems. The problem is solved by reformulating it into a single-level optimization problem and employing decomposition algorithms.

Other than the energy sector, stochastic bilevel models are also seen in other applications, including agriculture, structural engineering, and supply chain. Christiansen et al. (2001) attempt to mathematically model robust and cost-optimizing structural design problems. The problem is modeled using a stochastic bilevel optimization framework that optimally picks structural designs in response to a given probability distribution. The authors propose a heuristic-based solution algorithm that uses the problem's structure and its differentiability properties. The proposed algorithm is efficient and is parallelizable across the scenarios. Numerical experiments illustrate the benefits of considering a stochastic system compared to a deterministic one that considers the average-case. The results show that using a stochastic model to pick structural design optimally leads to increased robustness in the designs.

In the natural gas space, Kalashnikov et al. (2010b) present a multi-stage stochastic bilevel framework for the natural gas cash-out problem. The upper-level problem is associated with the natural gas shipping company making decisions about gas purchase and injection decisions into the pipeline. The lower-level problem then optimizes the operational decisions of the pipeline operator. Any change in the requested extraction and injection

decisions to the actual amount required in real-time causes imbalances in the system, which is then penalized. The non-linear natural gas problem is solved by reducing it to a linear bilevel problem and solved by employing a scenario tree with stochastic demand and prices. The model then compares the decisions made in the face of uncertainty to those made under a deterministic system.

Yeh et al. (2015) study the supply allocation problem for a timber-lands supply chain with harvesters and manufacturers under a leader-follower setting. The harvesters act as the leader and make decisions pertaining to the amount to be harvested. The manufacturers act as the followers and decide on the quantities they need to buy from the harvester. Each player has conflicting objectives, and they attempt to maximize their respective individual profits. The problem is set up as a multi-stage stochastic problem with the bio-refinery investment decisions, including logistical decisions like location and capacity are considered in the first-stage problem and the second-stage problem involves a bilevel timberlands model with parameter uncertainty. The resulting problem is solved by replacing the lower-level problem in the second-stage bilevel problem with its equivalent KKT conditions and reformulating the resulting mathematical program with complementarity constraints (MPCC) into a MILP using binary variables.

Nishi and Yoshida (2016) explore a multi-period stochastic bilevel model for a multi-echelon supply chain. The supplier is the leader, and the upper-level problem is associated with maximizing the profit for the supplier who makes decisions, including the production quantities and inventory levels for various products. The retailer is the lower-level player who makes decisions of order quantities and logistics under uncertain demand. They suggest an iterative solution algorithm to solve the proposed model, which solves the lower-level non-linear problem and uses that solution to solve the upper-level mixed-integer program using a branch and bound scheme. The algorithm proposed in Section 4.5.2 of this chapter is similar to some extent to the algorithm proposed in (Nishi and Yoshida, 2016). Instead

of solving the lower-level problem and upper-level problem separately, we attempt to solve them simultaneously by creating a restricted problem by fixing some lower-level problem variables and solving the resulting MILP while ensuring the feasibility of the solutions.

4.2.3 Risk-based stochastic bilevel optimization

Kardakos et al. (2015) provide a three-stage stochastic bilevel optimization model with uncertainty in the day-ahead production and load consumption in distributed energy resources and real-time balancing prices. The upper-level problem is associated with profit maximization of the virtual power plant problem, and the lower level represents the independent system operator's day-ahead market-clearing problem. The conditional value-at-risk (CVaR) metric captures the risk associated with the virtual power plant profit variability. The bilevel problem is reformulated using the KKT conditions and strong duality of the lower-level problem and solved as a MILP. The solution methodology we develop in Section 4.5 follows a similar approach. We reformulate the bilevel problem into a MILP using the KKT conditions and the lower-level problem's convexity. Although this is a commonly effective approach, it often does not scale well with the number of scenarios.

A bilevel model for micro-grid planning under uncertainty is explored by Gazijahani and Salehi (2017). The paper explores risk-based strategies for the operation of micro-grids, where the upper-level problem is associated with the optimal planning of distributed energy resources. The lower level represents the problem of partitioning the traditional distribution system into multiple micro-grids. The authors develop a cuckoo optimization algorithm to optimize the upper-level problem and an imperialist competitive algorithm to solve the lower-level problem. Although the overall problem structure is similar to what we are looking at in this chapter, most solution methodologies presented in the space of stochastic bilevel programming problems often make use of the inherent structure of the problem and have problem-specific assumptions that do not generalize well to other problems.

In this chapter, we consider a risk-based multi-stage stochastic bilevel model with an underlying spatial network structure for decision making in the presence of two players acting under a non-cooperative setting. We develop a customized heuristic based algorithm to find high quality feasible solution to instances of the stochastic bilevel model. The algorithm finds feasible solutions to the stochastic bilevel problem by iteratively solving restricted versions of the problem until feasibility is achieved. The model focuses on analyzing the optimal strategies for different risk preferences of the LNG operator (leader), who makes high-cost decisions.

4.3 Problem Description

In this section, the bilevel problem's general framework is described, then the stochastic framework is incorporated into the problem. The bilevel problem consists of two players acting in a leader-follower setting. The players make investment and operational decisions to set up an infrastructure network with markets to buy and sell goods. The leader or manufacturer starts the game and operates to maximize the profit, subject to a set of constraints that can include capacity constraints and other constraints associated with the network capacity restrictions. The leader makes decisions concerning facility location, capacity installation at these facilities, how much raw materials to procure from the follower, and the sales and pricing decisions for its finished goods. Since the manufacturing facilities' locations affect the prices at which they can purchase raw materials from the supplier or follower, which in turn affects the costs of delivering goods to consumers, the leader's decisions have to be made with much anticipation of the response from the follower. In light of the leader's decisions, the follower then responds in a manner that maximizes his profit function subject to his operational constraints. The follower's decisions include capacity investments, production decisions, and the sales and pricing decisions in the different consumer markets.

The choice of facility locations for the leader or manufacturer mainly depends on the

dynamics of the leader's market and the follower's infrastructure decisions, production decisions, and strategic market decisions involving the prices and sales. These factors often have stochasticity associated with them, which is introduced into this setting by considering the demand uncertainty faced by both players in their respective markets. Uncertainty in demand is captured through a set of scenarios that correspond to different demand levels in markets, which we consider to be uncorrelated to each other. Considering a leader who makes more capital-heavy and long-term investment decisions naturally paves the way to a risk-based stochastic model where the leader makes decisions while considering the high risk associated with his investments.

This chapter develops a multi-stage stochastic bilevel model formulation that captures the strategic interactions between an LNG operator or leader and an NG producer or follower under demand uncertainty. The underlying spatial network of the problem can be represented as a graph $G(V, A)$ as shown in Fig. 4.2. The nodes $V \in \{v_1, v_2, v_3, v_4, v_5\}$ represent geographical regions where the NG producers are operational, with each of these nodes also representing a local spot market. The subset of nodes $V' \in \{v_2, v_5\}$ shown in red in Fig. 4.2 represent potential locations for opening LNG facilities. The node v_6 represents the overseas LNG market. The arcs represent the pipeline network that connects different production regions and is assumed to be owned and operated by the NG producer. The blue arcs in Fig. 4.2 represent the LNG transportation that links possible LNG locations to the LNG market.

The first-stage decisions comprise the capacity investment decisions for both the players, which need to be made before the demand uncertainty in the markets is revealed and hence are not scenario specific. The LNG terminal location decisions are represented using a set of binary decision variables, each one corresponding available locations for opening the terminal. The LNG operator also makes decisions pertaining to the capacity to be invested at each opened location. The NG producer's first-stage decisions are the production capacity invest-

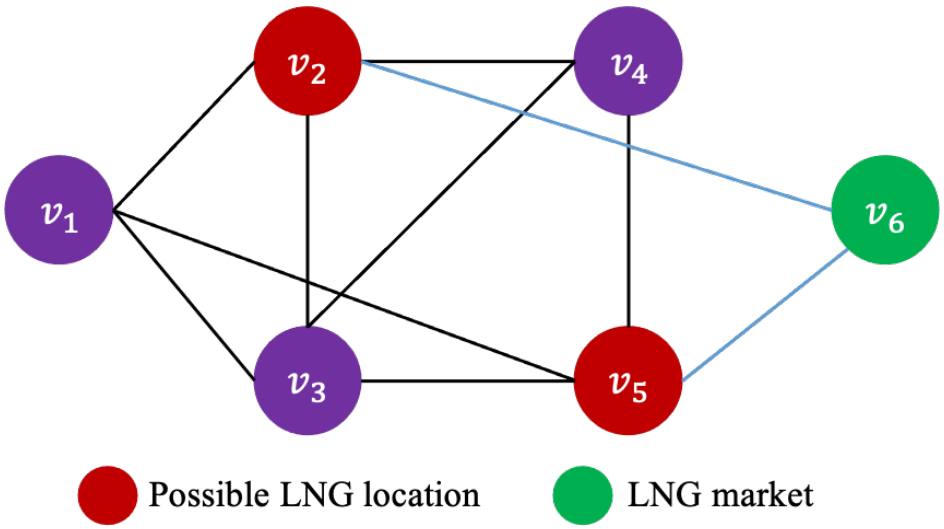

Fig. 4.2. Graphical representation of NG producers, possible LNG locations, LNG market, and pipeline network.

ment decisions. The leader and follower's operational decisions are wait-and-see decisions and are made once the uncertainty in demand is revealed. The LNG operator's operational decisions are the gas procurement quantities, sales, and prices in the LNG market. The NG producer's second-stage decisions include production quantities, sales to the local spot market, sales to the LNG operator's gas procurement market, and prices in both markets. The stochastic bilevel model proposed in this chapter is formulated by incorporating the stochastic framework into the bilevel model described in Chapter 3, to study the strategic interactions between an LNG operator and NG producer.

We model the demand uncertainties in the different markets using stochastic scenario-based optimization. The scenarios reflect the state of demand in the spot market, the gas procurement market for the LNG player, and the LNG market and follow a discrete probability distribution. The chance of every scenario occurring has a non-zero probability, which exacerbates the risk associated with high-cost decisions. This study will consider two decision-making approaches, risk-neutral and risk-averse, to conduct risk analysis and

examine the impact of considering risk when making decisions.

4.4 Stochastic bilevel model

In this section, we provide the formulation for the stochastic bilevel model. The sets, parameters, and decision variables of the leader and follower are given in Section 4.4.1. Sections 4.4.2 and 4.4.3 presents the model formulations for the risk-neutral and risk-averse decision making approaches respectively.

4.4.1 Notation

Sets

$\mathcal{N}$	Set of production nodes; $\mathcal{N} = \{1, 2, \ldots, N\}$
$\mathcal{M}$	Set of LNG market nodes; $\mathcal{M} = \{1, 2, \ldots, M\}$
Ω	Set of scenarios; $\Omega = \{\text{High}, \text{Medium}, \text{Low}\}$

Parameters

K_j	Maximum production capacity at node $j \in \mathcal{N}$
K_j^{LNG}	Maximum capacity of LNG facility that can be built at node $j \in \mathcal{N}$
K_{ij}^{pipe}	Pipeline capacity available on link $(i, j) \in \mathcal{N} \times \mathcal{N}$
C_j^{unit}	Unit cost of installing production capacity at node $j \in \mathcal{N}$
$C_j^{\text{prod}}(\cdot)$	Production cost at node $j \in \mathcal{N}$ ($C_j^{\text{prod}}(.) = C_{a_j}^{\text{prod}} q_j^2 + C_{b_j}^{\text{prod}} q_j$)
C_{ij}^{ship}	Variable cost of shipping gas through pipeline link $(i, j) \in \mathcal{N} \times \mathcal{N}$
C_j^{liq}	Cost of liquefaction at node $j \in \mathcal{N}$
C_j^{LNGfixed}	Fixed cost of investment in LNG facility at node $j \in \mathcal{N}$
C_j^{LNGunit}	Unit cost of installing capacity in LNG facility at node $j \in \mathcal{N}$
C_{ij}^{LNGship}	Variable cost of LNG shipment between node $j \in \mathcal{N}$ and market $i \in \mathcal{M}$
η_j	Loss during liquefaction process at node $j \in \mathcal{N}$

$a_{j\omega}^{\text{spot}}$ Intercept of spot market demand curve at node $j \in \mathcal{N}$ for scenario ω

$b_{j\omega}^{\text{spot}}$ Slope of spot market demand curve at node $j \in \mathcal{N}$ for scenario ω

$a_{j\omega}^{\text{LNG}}$ Intercept of LNG market demand curve at node $j \in \mathcal{M}$ for scenario ω

$b_{j\omega}^{\text{LNG}}$ Slope of LNG market demand curve at node $j \in \mathcal{M}$ for scenario ω

$a_{j\omega}^{\nu}$ Intercept of LNG facility gas procurement demand curve at node $j \in \mathcal{N}$ for scenario ω

$b_{j\omega}^{\nu}$ Slope of LNG facility gas procurement demand curve at node $j \in \mathcal{N}$ for scenario ω

Leader's Decision Variables

$\nu_{j\omega}$ LNG procured at node $j \in \mathcal{N}$ for scenario ω (by LNG operator)

$l_{ij\omega}$ LNG shipped from node $i \in \mathcal{N}$ to market $j \in \mathcal{M}$ for scenario ω

z_j Binary variable taking value 1 if LNG facility is opened at node $j \in \mathcal{N}$, 0 otherwise

μ_j Capacity installed in LNG facility at node $j \in \mathcal{N}$

$d_{j\omega}^{\text{LNG}}$ Demand for LNG in market $j \in \mathcal{M}$ for scenario ω

$p_{j\omega}^{\text{LNG}}$ Price of LNG in market $j \in \mathcal{M}$ for scenario ω

Follower's Decision Variables

$f_{ij\omega}$ Flow in pipeline $(i, j) \in \mathcal{N} \times \mathcal{N}$ for scenario ω (from node i to j)

Q_j Production capacity installed at node $j \in \mathcal{N}$

$q_{j\omega}$ Production at node $j \in \mathcal{N}$ for scenario ω

$d_{j\omega}^{\text{spot}}$ Demand for natural gas in spot market $j \in \mathcal{N}$ for scenario ω

$p_{j\omega}^{\text{spot}}$ Spot price of natural gas at node $j \in \mathcal{N}$ for scenario ω

$p_{j\omega}^{\nu}$ LNG facility gas procurement price in node $j \in \mathcal{N}$ for scenario ω

4.4.2 Risk neutral strategy

In this section, we develop the model formulation for a risk-neutral decision maker who optimizes the expected profit across all scenarios and does not explicitly consider any particular scenario when making decisions. In other words, a risk-neutral decision-maker considers the different scenarios and makes decisions to maximize the expected profit across all scenarios.

4.4.2.1 Upper-level problem

$$\max \ \mathbb{E}_{\omega}\Bigg[\sum_{j\in\mathcal{M}} p^{\mathrm{LNG}}_{j\omega} d^{\mathrm{LNG}}_{j\omega} - \sum_{j\in\mathcal{N}} p^{\nu}_{j\omega}\nu_{j\omega} - \sum_{j\in\mathcal{N}} C^{\mathrm{LNGfixed}}_{j} z_j - \sum_{j\in\mathcal{N}} C^{\mathrm{LNGunit}}_{j}\mu_j - \sum_{j\in\mathcal{N}} C^{\mathrm{liq}}_{j}\nu_{j\omega} - \sum_{i\in\mathcal{N}}\sum_{j\in\mathcal{M}} C^{\mathrm{LNGship}}_{ij} l_{ij\omega}\Bigg] \tag{4.1a}$$

subject to

$$\sum_{i\in\mathcal{M}} l_{ji\omega} \leq (1-\eta_j)\ \nu_{j\omega} \qquad \forall \quad j\in\mathcal{N}, \omega\in\Omega \tag{4.1b}$$

$$\nu_{j\omega} \leq \mu_j \qquad \forall \quad j\in\mathcal{N}, \omega\in\Omega \tag{4.1c}$$

$$\mu_j \leq K^{\mathrm{LNG}}_{j} z_j \qquad \forall \quad j\in\mathcal{N} \tag{4.1d}$$

$$\sum_{i\in\mathcal{N}} l_{ij\omega} = d^{\mathrm{LNG}}_{j\omega} \qquad \forall \quad j\in\mathcal{M}, \omega\in\Omega \tag{4.1e}$$

$$d^{\mathrm{LNG}}_{j\omega} = a^{\mathrm{LNG}}_{j\omega} - b^{\mathrm{LNG}}_{j\omega} p^{\mathrm{LNG}}_{j\omega} \qquad \forall \quad j\in\mathcal{M}, \omega\in\Omega \tag{4.1f}$$

$$z_j \in \{0,1\} \qquad \forall \quad j\in\mathcal{N} \tag{4.1g}$$

$$p^{\mathrm{LNG}}_{j\omega}, \nu_{j\omega}, \mu_j, d^{\mathrm{LNG}}_{j\omega} \in \mathbb{R}_{+} \qquad \forall \quad j\in\mathcal{N}, \omega\in\Omega \tag{4.1h}$$

$$l_{ij\omega} \in \mathbb{R}_{+} \qquad \forall \quad i\in\mathcal{N}, j\in\mathcal{M}, \omega\in\Omega \tag{4.1i}$$

Equation (4.1a) represents the expected total profit earned by the LNG operator (leader), where the term $p_{j\omega}^{\text{LNG}} d_{j\omega}^{\text{LNG}}$ is the revenue earned from LNG exports to overseas market j under scenario ω. The term $p_{j\omega}^{\nu} \nu_{j\omega}$ is the cost of procuring gas from the NG producer (follower) at node j under scenario ω. $C_j^{\text{LNGfixed}} z_j$ is the fixed cost of opening an LNG facility at node j and $C_j^{\text{LNGunit}} \mu_j$ is the cost of adding capacity to the LNG facility opened there. The cost of liquefaction of the gas at node j is given by $C_j^{\text{liq}} \nu_{j\omega}$ and cost of shipping LNG from the export facility at node i to the LNG market at node j is represented by the term $C_{ij}^{\text{LNGship}} l_{ij}$.

Constraint (4.1b) ensures that the total LNG shipments from any node j to all LNG markets are bounded by the total gas procured at that node, accounting for losses during the liquefaction process. Constraints (4.1c) – (4.1d) ensure that the gas procured by the LNG facility at node j does not exceed the capacity available at the facility. Constraints (4.1e) – (4.1f) compute the total sales in each LNG market and specify the demand curves faced by the LNG operator. Constraint (4.1g) represents the binary variable z_j, which denotes whether an LNG export terminal is open at node j or not.

4.4.2.2 Lower-level problem

$$\max \ \mathbb{E}_{\omega}\Bigg[\sum_{j\in\mathcal{N}} p_{j\omega}^{\text{spot}} d_{j\omega}^{\text{spot}} + \sum_{j\in\mathcal{N}} p_{j\omega}^{\nu}\nu_{j\omega} - \sum_{j\in\mathcal{N}} C_j^{\text{unit}} Q_j - \sum_{j\in\mathcal{N}} C_{a_j}^{\text{prod}} q_{j\omega}^2 - \sum_{j\in\mathcal{N}} C_{b_j}^{\text{prod}} q_{j\omega} - \sum_{i\in\mathcal{N}}\sum_{j\in\mathcal{N}} C_{ij}^{\text{ship}} f_{ij\omega}\Bigg] \tag{4.2a}$$

subject to

$$\sum_{i\in\mathcal{N}} f_{ij\omega} + q_{j\omega} = \sum_{i\in\mathcal{N}} f_{ji\omega} + d_{j\omega}^{\text{spot}} + \nu_{j\omega} \qquad \forall \quad j\in\mathcal{N}, \omega\in\Omega \qquad (\lambda_{j\omega}) \tag{4.2b}$$

$$q_{j\omega} \le Q_j \qquad \forall \quad j\in\mathcal{N}, \omega\in\Omega \qquad (\theta_{j\omega}) \tag{4.2c}$$

$$Q_j \le K_j \qquad \forall \quad j\in\mathcal{N} \qquad (\delta_j) \tag{4.2d}$$

$$f_{ij\omega} \leq K_{ij}^{\text{pipe}} \qquad \forall \quad i,j \in \mathcal{N}, \omega \in \Omega \qquad (\beta_{ij\omega}) \quad (4.2e)$$

$$d_{j\omega}^{\text{spot}} = a_{j\omega}^{\text{spot}} - b_{j\omega}^{\text{spot}} p_{j\omega}^{\text{spot}} \qquad \forall \quad j \in \mathcal{N}, \omega \in \Omega \qquad (\kappa_{j\omega}) \quad (4.2f)$$

$$\nu_{j\omega} = a_{j\omega}^{\nu} - b_{j\omega}^{\nu} p_{j\omega}^{\nu} \qquad \forall \quad j \in \mathcal{N}, \omega \in \Omega \qquad (\tau_{j\omega}) \quad (4.2g)$$

$$q_{j\omega}, Q_j, p_{j\omega}^{\text{spot}}, p_{j\omega}^{\nu}, d_{j\omega}^{\text{spot}} \in \mathbb{R}_+ \qquad \forall \quad j \in \mathcal{N}, \omega \in \Omega \qquad (4.2h)$$

$$f_{ij\omega} \in \mathbb{R}_+ \qquad \forall \quad i,j \in \mathcal{N}, \omega \in \Omega \qquad (4.2i)$$

Equation (4.2a) represents the expected total profit earned by the NG producer (follower), where the term $p_{j\omega}^{\text{spot}} d_{j\omega}^{\text{spot}}$ is the revenue from spot market sales at node j and $p_{j\omega}^{\nu}\nu_{j\omega}$ is the revenue earned from sales to the LNG operator. $C_j^{\text{unit}} Q_j$ denotes the cost of adding production capacity at node j and the term $C_j^{\text{prod}}(q_{j\omega})$ represents the production cost at node j. $C_{ij}^{\text{ship}} f_{ij}$ represents the costs of shipping gas from node i to node j.

Constraint (4.2b) ensures flow balance among production, shipments, and sales at any node j for all scenarios. Constraints (4.2c) – (4.2d) ensure that the total production at node j under any scenario does not exceed the production capacity available there. Constraints (4.2f) – (4.2g) specify the demand curves for the spot market and LNG facility gas procurement at node j. The variables $\lambda_{j\omega} \in \mathbb{R}$, $\theta_{j\omega} \in \mathbb{R}_+$, $\delta_j \in \mathbb{R}_+$, $\beta_{ij\omega} \in \mathbb{R}_+$, $\kappa_{j\omega} \in \mathbb{R}$, and $\tau_{j\omega} \in \mathbb{R}$ are the dual variables associated with constraints (4.2b) – (4.2g), respectively.

4.4.3 Risk averse strategy

The LNG operator makes high fixed cost investment decisions that are influenced by factors including natural gas availability, natural gas prices, and the LNG market demand. Due to their high cost nature, the LNG operator's decisions have a high risk. Hence, it becomes necessary to consider how these decisions would change in the face of uncertainty if we consider different risk behaviors for the LNG operator. Unlike the risk-neutral decision-

maker, a risk-averse decision-maker makes decisions while keeping in mind the worst possible scenarios and attempting to avoid high-risk decisions associated with extreme losses.

The value-at-risk (VaR) at a confidence-level α represents the α^{th} quantile of the distribution over the expected loss. The CVaR represents the conditional expected loss over the VaR, and it penalizes larger losses more, unlike the VaR, which penalizes all losses bigger than VaR equally. In this chapter, we use the conditional value at risk (CVaR) to account for the risk associated with decisions for the LNG operator (leader) under a risk-averse decision making approach. We assume that the NG producer is a risk-neutral decision-maker who attempts to maximize the expected profit. The $\alpha - \text{CVaR}$ of loss function F is defined as (Krokhmal et al., 2002):

$$\begin{aligned} \text{CVaR}_\alpha(F) &= y + (1-\alpha)^{-1}\mathbb{E}[F(.) - y]^+ \\ \text{where,}\ \ \mathbb{E}[F(.) - y]^+ &= max\{0, \mathbb{E}[F(.) - y]\} \end{aligned} \tag{4.3}$$

The CVaR is a coherent risk measure and is convex if the function F is convex (Krokhmal et al., 2002). We attain a convex objective function for the LNG operator shown in Eq. (4.1a) by employing a piecewise linear approximation of the quadratic term ${p_\omega^\nu}^\top \text{Diag}\,(b_\omega^\nu) p_\omega^\nu$ as shown in preposition 5 in chapter 3. Hence, using the CVaR risk measure on this function does not affect the risk-averse LNG operator's objective function's convexity. Hence, the resulting CVaR problem described in Eq. (4.4a) – Eq. (4.4d) retains the mathematical properties of the risk-neutral decision-makers problem and both problems can be solved using a similar approach.

$$\min\ \ y + (1-\alpha)^{-1} \sum_{\omega \in \Omega} \psi_{j\omega} w_\omega \tag{4.4a}$$

subject to

$$w_\omega + y + \sum_{j\in\mathcal{M}} d^{\text{LNG}}_{j\omega} p^{\text{LNG}}_{j\omega} - \sum_{j\in\mathcal{N}} \nu_{j\omega} p^{\nu}_{j\omega} - \sum_{j\in\mathcal{N}} C^{\text{LNGfixed}}_{j} z_j - \sum_{j\in\mathcal{N}} C^{\text{LNGunit}}_{j} \mu_j$$
$$- \sum_{j\in\mathcal{N}} C^{\text{liq}}_{j} \nu_{j\omega} - \sum_{i\in\mathcal{N}} \sum_{j\in\mathcal{M}} C^{\text{LNGship}}_{ij} l_{ij\omega} \geq 0 \tag{4.4b}$$

$$y, w_\omega \in \mathbb{R}_+ \qquad \forall \quad \omega \in \Omega \tag{4.4c}$$

$$\text{Eq.(4.1b)} - \text{Eq.(4.1i)} \tag{4.4d}$$

4.5 Solution strategy

4.5.1 MPCC Formulation

We can solve the bilevel model described in section 4.4 by reducing it to a single-level problem. The lower-level problem described in Eq. (4.2a) – (4.2i) is convex, and therefore, we can replace the lower–level problem by the equivalent KKT conditions to achieve a mathematical model with complementarity constraints (MPCC). The resulting MPCC shown in Eq. (4.5a) – (4.5z) has non–linear complementarity constraints Eq. (4.5i) – (4.5q) which can be converted to a set of linear constraints using binary variables and big-M terms as shown in Eq. (3.10) in chapter 3. The resulting problem is a convex quadratic mixed-integer program (QMIP) with a quadratic objective function and a set of linear constraints. The QMIP is solvable for reasonably sized problems but becomes intractable as the number of scenarios increases under the stochastic setting.

$$\max \mathbb{E}_\omega \Bigg[\sum_{j\in\mathcal{M}} a^{\text{LNG}}_{j\omega} p^{\text{LNG}}_{j\omega} - \sum_{j\in\mathcal{M}} b^{\text{LNG}}_{j\omega} (p^{\text{LNG}}_{j\omega})^2 - \sum_{j\in\mathcal{N}} a^{\nu}_{j\omega} p^{\nu}_{j\omega} + \sum_{j\in\mathcal{N}} u_{j\omega} - \sum_{j\in\mathcal{N}} C^{\text{LNGfixed}}_{j} z_j$$
$$- \sum_{j\in\mathcal{N}} C^{\text{LNGfixed}}_{j} \mu_{j\omega} - \sum_{j\in\mathcal{N}} C^{\text{liq}}_{j}\ \nu_{j\omega} - \sum_{i\in\mathcal{N}} \sum_{j\in\mathcal{M}} C^{\text{LNGship}}_{ij} l_{ij\omega} \Bigg] \tag{4.5a}$$

$$\text{s.t.} \quad u_{j\omega} \leq a^{\text{pw}}_{sj} + b^{\text{pw}}_{sj} p^{\nu}_{j\omega} \qquad \forall \quad s \in \mathcal{S}, j \in \mathcal{N}, \omega \in \Omega \tag{4.5b}$$

$$u_{j\omega} \geq a_{sj}^{\mathrm{pw}} + b_{sj}^{\mathrm{pw}} p_{j\omega}^{\nu} - M(1-\xi_{sj}) \qquad \forall \quad s \in \mathcal{S}, j \in \mathcal{N}, \omega \in \Omega \tag{4.5c}$$

$$\sum_{s \in \mathcal{S}} \xi_{sj} = 1 \qquad \forall \quad j \in \mathcal{N} \tag{4.5d}$$

$$\sum_{i \in \mathcal{M}} l_{ji\omega} \leq (1-\eta_j)\ \nu_{j\omega} \qquad \forall \quad j \in \mathcal{N}, \omega \in \Omega \tag{4.5e}$$

$$\nu_{j\omega} \leq \mu_j \qquad \forall \quad j \in \mathcal{N}, \omega \in \Omega \tag{4.5f}$$

$$\mu_j \leq K_j^{\mathrm{LNG}} z_j \qquad \forall \quad j \in \mathcal{N} \tag{4.5g}$$

$$\sum_{i \in \mathcal{N}} l_{ij\omega} = a_{j\omega}^{\mathrm{LNG}} - b_{j\omega}^{\mathrm{LNG}} p_{j\omega}^{\mathrm{LNG}} \qquad \forall \quad j \in \mathcal{N}, \omega \in \Omega \tag{4.5h}$$

$$0 \leq p_{j\omega}^{\mathrm{spot}} \perp -\psi_\omega d_{j\omega}^{\mathrm{spot}} + b_{j\omega}^{\mathrm{spot}} \kappa_{j\omega} \geq 0 \qquad \forall \quad j \in \mathcal{N}, \omega \in \Omega \tag{4.5i}$$

$$0 \leq p_{j\omega}^{\nu} \perp -\psi_\omega \nu_{j\omega} - b_{j\omega}^{\nu} \tau_{j\omega} \geq 0 \qquad \forall \quad j \in \mathcal{N}, \omega \in \Omega \tag{4.5j}$$

$$0 \leq d_{j\omega}^{\mathrm{spot}} \perp -\psi_\omega p_{j\omega}^{\mathrm{spot}} + \lambda_{j\omega} + \kappa_{j\omega} \geq 0 \qquad \forall \quad j \in \mathcal{N}, \omega \in \Omega \tag{4.5k}$$

$$0 \leq Q_j \perp \psi_\omega C_j^{\mathrm{unit}} - \sum_{\omega \in \Omega} \theta_{j\omega} + \delta_j \geq 0 \qquad \forall \quad j \in \mathcal{N} \tag{4.5l}$$

$$0 \leq q_{j\omega} \perp 2\ \psi_\omega C_{a_j}^{\mathrm{prod}} q_{j\omega} + \psi_\omega C_{b_j}^{\mathrm{prod}} + \theta_{j\omega} - \lambda_{j\omega} \geq 0 \qquad \forall \quad j \in \mathcal{N}, \omega \in \Omega \tag{4.5m}$$

$$0 \leq f_{ij\omega} \perp \psi_\omega C_{ij}^{\mathrm{ship}} + \lambda_{i\omega} - \lambda_{j\omega} + \beta_{ij\omega} \geq 0 \qquad \forall \quad j \in \mathcal{N}, \omega \in \Omega \tag{4.5n}$$

$$0 \leq \theta_{j\omega} \perp Q_j - q_{j\omega} \geq 0 \qquad \forall \quad j \in \mathcal{N}, \omega \in \Omega \tag{4.5o}$$

$$0 \leq \delta_j \perp K_j - Q_j \geq 0 \qquad \forall \quad j \in \mathcal{N} \tag{4.5p}$$

$$0 \leq \beta_{ij\omega} \perp K_{ij}^{\mathrm{pipe}} - f_{ij\omega} \geq 0 \qquad \forall \quad j \in \mathcal{N}, \omega \in \Omega \tag{4.5q}$$

$$\sum_{i \in \mathcal{N}} f_{ij\omega} + q_{j\omega} = \sum_{i \in \mathcal{N}} f_{ji\omega} + d_{j\omega}^{\mathrm{spot}} + \nu_{j\omega} \qquad \forall \quad j \in \mathcal{N}, \omega \in \Omega \tag{4.5r}$$

$$d_{j\omega}^{\mathrm{spot}} = a_{j\omega}^{\mathrm{spot}} - b_{j\omega}^{\mathrm{spot}} p_{j\omega}^{\mathrm{spot}} \qquad \forall \quad j \in \mathcal{N}, \omega \in \Omega \tag{4.5s}$$

$$\nu_{j\omega} = a_{j\omega}^{\nu} - b_{j\omega}^{\nu} p_{j\omega}^{\nu} \qquad \forall \quad j \in \mathcal{N}, \omega \in \Omega \tag{4.5t}$$

$$z_j \in \{0,1\} \qquad \forall \quad j \in \mathcal{N} \tag{4.5u}$$

$$\xi_{sj} \in \{0,1\} \qquad \forall \quad s \in \mathcal{S}, j \in \mathcal{N} \qquad (4.5v)$$

$$l_{ij\omega}, f_{ij\omega}, \beta_{ij\omega} \in \mathbb{R}_+ \qquad \forall \quad i,j \in \mathcal{N}, \omega \in \Omega \qquad (4.5w)$$

$$\mu_j, Q_j, \delta_j \in \mathbb{R}_+ \qquad \forall \quad j \in \mathcal{N} \qquad (4.5x)$$

$$\nu_{j\omega}, p_{j\omega}^{\text{LNG}}, p_{j\omega}^{\text{spot}}, p_{j\omega}^{\nu}, q_{j\omega}, d_{j\omega}^{\text{spot}}, \theta_{j\omega} \in \mathbb{R}_+ \qquad \forall \quad j \in \mathcal{N}, \omega \in \Omega \qquad (4.5y)$$

$$\lambda_{j\omega}, \tau_{j\omega}, \kappa_{j\omega}, u_{j\omega} \in \mathbb{R} \qquad \forall \quad j \in \mathcal{N}, \omega \in \Omega \qquad (4.5z)$$

4.5.2 Algorithm

Bilevel programs are strongly NP hard, even for the simplest case where both the upper and lower-level problems are linear programs Ben-Ayed and Blair (1990). Since the stochastic bilevel problem presented in this chapter involves an integer program in the upper-level and a convex program in the lower level, it is NP-hard. This makes it rather hard to find optimal solutions to large instances of the problem. Hence, we turn our attention to developing a heuristic-based approach to identify "good" feasible solutions to the stochastic bilevel problem, which can be attained in a reasonable amount of time. In this section, we develop a heuristic-based algorithm to find feasible solutions to the stochastic bilevel problem described in Section 4.5.1. We further explore the tractability of the algorithm and the goodness of the feasible solutions attained in section 4.6

The MILP described in Eq. (4.5a)–Eq. (4.5z) is not tractable and cannot be solved to optimality even for small networks when the number of scenarios increases. Thus, in this section, we will exploit the underlying structure of the problem to develop an iterative algorithm that would help attain feasible solutions in a reasonable amount of time. The lower-level problem's size increases exponentially with the size of the network and the number of scenarios, leading to the increased size of the stochastic bilevel problem (SBLP). There are a total of $\mathcal{N} \times \mathcal{N} \times \Omega$ flow variables in the lower-level problem that capture the flow of gas

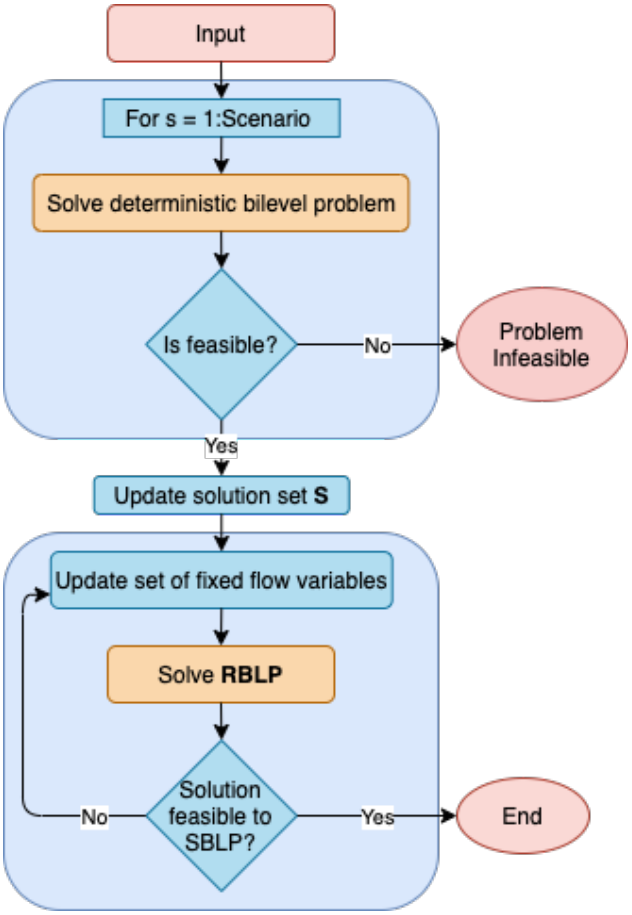

Fig. 4.3. Flowchart of the proposed heuristic algorithm to solve the SBLP

between regions based on the pipeline capacity. A large subset of these flow variables retains the value of zero in all the best-case deterministic solutions. Hence, we create a restricted bilevel problem (RBLP) by fixing a subset of the flow variables in the original SBLP to zeros. Under this setting, we can iteratively update the subset of flow variables set to zero until we attain a feasible solution to the original SBLP.

Algorithm 1: Algorithm for finding feasible solutions for the SBLP

Initialization:
Deterministic solution set, $\mathcal{S} = \emptyset$;
Flow subset, $\mathcal{F} = \emptyset$;
for $\omega = 1 : \Omega$ **do**
  solve deterministic BLP $\rightarrow$ s_ω ;
  if $s_\omega \rightarrow \emptyset$ **then**
    INFEASIBLE ;
    break ;
  else
    update $\mathcal{S} \leftarrow \mathcal{S} \cup \{s_\omega\}$;
  end
end
for $j \in (\mathcal{N} \times \mathcal{N} \times \Omega)$ **do**
  for $s = 1 : \mathcal{S}$ **do**
    if $f_j = 0$ **then**
      update $\mathcal{F} \leftarrow \mathcal{F} \cup \{f_j\}$;
    else
      continue ;
    end
  end
end
Solve RBLP $\rightarrow sol^{\mathrm{RBLP}}$;
Fix leader's decisions and solve lower–level problem $\rightarrow sol^{\mathrm{LL}}$;
if $sol^{RBLP} = sol^{LL}$ **then**
  Feasible solution found ;
  break;
else
  for $j \in (\mathcal{N} \times \mathcal{N} \times \Omega)$ **do**
    if $(f_j \in sol^{RBLP}) \,! = (f_j \in sol^{LL})$ **then**
      if $(f_j \in sol^{LL}) = 0$ **then**
        update $\mathcal{F} \leftarrow \mathcal{F} \cup \{f_j\}$;
      else
        update $\mathcal{F} \leftarrow \mathcal{F} \setminus \{f_j\}$;
      end
    else
      continue;
    end
  end
end

In the proposed algorithm, a feasible solution to the SBLP is found using a series of steps. First, we find the best-case deterministic solutions for each scenario by solving the deterministic version of the SBLP for every scenario. The solutions to all the scenario-wise deterministic problems are added to a set $\mathcal{S}$. We then use all the solutions in the set $\mathcal{S}$ to identify a subset $\mathcal{F}$ of the flow variables that remain at value zero across all solutions in $\mathcal{S}$. Fixing the flow variables in $\mathcal{F}$ to zero, we now solve the RBLP. We now check if the solution attained from the RBLP is feasible to the original SBLP by fixing the leader's variables and solving the lower–level problem. If the solution is not feasible, we update the set $\mathcal{F}$ by removing the non-zero flow variables in the lower–level problem and adding the zero flow variables not in $\mathcal{F}$ to $\mathcal{F}$. We repeat the process until we attain a feasible solution to the SBLP. The proposed algorithm's flowchart is shown in Fig. 4.3 and the pseudocode is presented in Algorithm 1.

4.6 Computational experiments

In this section, we conduct numerical experiments to study the computational tractability of the proposed algorithm. We generate random instances of the stochastic bilevel problem for different network sizes, demands, and numerous scenarios. We generate random instances of the stochastic bilevel problem in the following order: (1) generate an $\mathcal{N} \times \mathcal{N}$ network, (2) randomly select potential locations for LNG facilities within the network, (3) generate investment costs, capacity costs, production costs, and production capacity limits for the LNG operator and NG producer for each node in the network, (4) generate a node-node incidence matrix for the network along with pipeline and shipping costs, (5) define LNG markets, $\mathcal{M}$ where open LNG facilities can sell LNG, (6) define scenarios $\omega \in \Omega$ which represent the demand conditions in the markets, (7) define demand curves for the local spot

market and LNG market for each scenario. The computational study employs a single 2.6 GHz Intel Core i7 processor with 16 GB memory, using Gurobi 8.1.1.

Table 4.1. Run times for the exact solution approach and the algorithm on randomly generated instances.

# of nodes	# of LNG markets	# of scenarios	Exact solution time (s)	Algorithm solution time (s)
5	2	3	20	5
		9	75	12
		27	–	91
10	2	3	252	15
		9	–	55
		27	–	292
15	2	3	–	28
		9	–	117
		27	–	549
25	2	3	–	89
		9	–	223
		27	–	1265
50	2	3	–	176
		9	–	918
		27	–	2537

We study the solution times and the computational tractability of the algorithm proposed in Section 4.5.2 for randomly generated instances of the stochastic bilevel model. The average runtime in seconds of 10 trials for each instance is summarized in Table 4.1. The instances for which the exact solution time is not reported are the cases for which we could not find an

optimal solution after 15 hours of computational time. The runtime analysis shows that the proposed algorithm can find feasible solutions to several instances of the stochastic bilevel problem in a very reasonable amount of time. In contrast, even small-sized problems are not solvable using the exact solution methodology. The case study presented in Section 4.7 consists of a 9 node 9 scenario problem but this is because of the ease of visual representation rather than computational limitation. For illustration purposes, we have solved the 27 scenario case and the results are summarized in C.1. We also see that the runtime increases with the size of the network and its density, which is expected since the time to solve the restricted bilevel problem increases with the network's size.

The algorithm proposed in this chapter attempts to find a "good" feasible solution to the stochastic bilevel problem. It becomes necessary to analyze the quality of the solution with respect to the optimal solution. To study the quality of solutions, we compare the solution attained by employing the proposed algorithm described in Section 4.5.2 to the solution attained by exactly solving the QMIP described in Section 4.5.1. Table 4.2 presents the percentage gap between the profits achieved by the leader and the follower attained from the exact solution and the solution attained by the proposed algorithm for random instances for which we can solve the stochastic bilevel problem exactly. We use this analysis to study the quality of the feasible solution attained using the proposed algorithm. It is worth noting that for most instances, the solution attained by the algorithm is within 9% of the optimal solution. For smaller size problems, with three nodes, we achieve a solution within 4% of the optimal solution, even for a larger number of scenarios. For some instances of the problem, we achieve the optimal solution by applying the proposed algorithm. We repeated the same experiments with changes in different model parameters like the investment costs, demand curve parameters, and operational costs. We find that the results obtained are robust to a wide range of parameter values.

Table 4.2. Percentage gap between solution found from the exact solution approach and the algorithm on instances solvable by exact method.

# of nodes	# of scenarios	Leader's profit		% gap	Follower's profit		% gap
		Exact solution	Heuristic solution		Exact solution	Heuristic solution	
3	3	4.376	4.376	0.00%	15.580	15.580	0.00%
	9	7.975	7.975	0.00%	14.672	14.672	0.00%
	27	6.453	6.268	2.87%	15.398	15.857	-2.98%
	64	6.589	6.379	3.18%	15.160	15.387	-1.49%
4	3	4.873	4.873	0.00%	19.595	19.595	0.00%
	9	5.454	4.991	8.50%	19.375	19.580	-1.06%
9	3	4.679	4.295	8.22%	38.743	39.870	-2.91%

4.7 Case study

In this section, the stochastic bilevel model developed in this chapter is applied to a real-world problem to study the interactions between an LNG operator and an NG producer under demand uncertainty. We will employ the model to study the Gulf-Southwest region of the U.S., using similar regional definitions and data discussed in Section 3.6 of Chapter 3. The nine regions included in the study are New Mexico (NM), Oklahoma (OK), Arkansas (AR), Louisiana (LA), and Texas. Texas is further subdivided into North Texas (NT), East Texas (ET), West Texas (WT), and South Texas (ST) based on the oil and gas division district boundaries established by the Railroad Commission of Texas (2020).

The potential locations to open LNG terminals are limited to LA, ET, and ST. Similar to the problem described in Chapter 3, each region has a local spot market with an associated demand curve. We also consider two distinct LNG markets, each representing exports to

Atlantic (e.g., Europe) and Pacific (e.g., Asia) destinations.

4.7.1 Scenario generation

In this chapter, we propose a model that models uncertainties in demand by considering scenarios representing the state of demand in each market. We define high demand (H), medium demand (M), and low demand (L) levels that each market could face with a given probability ($\psi^{\text{market}}_{\text{demand}}$). Each scenario ($\omega$) is the realization of demand levels in the spot market and the LNG market. We construct the scenarios such that the LNG market's demand uncertainties are not correlated with the demand uncertainties in the NG spot market and vice versa. These set of demand uncertainties considered for both the LNG market and the NG spot market leads to a total of nine scenarios. We define a discrete probability distribution across all scenarios as described below:

$$\omega^{\text{LNG}} = \{(\mathbf{H},\ \psi_H^{\text{LNG}}), (\mathbf{M},\ \psi_M^{\text{LNG}}), (\mathbf{L},\ \psi_L^{\text{LNG}})\}$$

$$\psi_H^{\text{LNG}} + \psi_M^{\text{LNG}} + \psi_L^{\text{LNG}} = 1 \tag{4.6a}$$

$$\omega^{\text{spot}} = \{(\mathbf{H},\ \psi_H^{\text{spot}}), (\mathbf{M},\ \psi_M^{\text{spot}}), (\mathbf{L},\ \psi_L^{\text{spot}})\}$$

$$\psi_H^{\text{spot}} + \psi_M^{\text{spot}} + \psi_L^{\text{spot}} = 1 \tag{4.6b}$$

$$\Omega = \omega^{\text{LNG}} \times \omega^{\text{spot}}$$

$$\sum_{\omega \in \Omega} \psi_\omega^{\text{LNG}} \times \psi_\omega^{\text{spot}} = 1 \tag{4.6c}$$

In Eq. (4.6), **H**, **M**, and **L** represents the possible states of demand in the LNG market and the spot market, whereas ψ^{LNG} and ψ^{spot} represent the respective probabilities of these demand scenarios in each market. ω^{LNG} and ω^{spot} represent the set of possible states the

LNG market and spot market can be in, respectively. Ω represents the set of all possible scenario combinations that we can achieve.

We create the scenarios by considering the actual data obtained from sources listed in table 3.2 in Chapter 3. We define the high demand (H) scenario as having twice the demand, medium scenario as having 1.5 times the demand, and the low demand scenario as having the base demand. In the spot market, we similarly define the low scenario as having the base demand, high demand (H) scenario as having twice the base demand, and the medium demand scenario as having 1.5 times the base demand. We accommodate this by parameterizing the demand curve parameters, intercept a, and the slope b, which change based on each market scenario.

4.7.2 Results

In this section, we compare the risk-neutral decision-maker's investment and operational decisions to the risk-averse decision-maker. LNG operator's high-cost decisions are prone to high-risk, and hence the results presented in this section analyze the difference in optimal strategies between the two decision-making approaches from the perspective of the LNG operator. We consider the NG producer to be a risk-neutral player who maximizes his expected profit in both approaches. The decision-maker's risk behavior has significant implications on the investment decisions, including the number of LNG facilities open, the location of these facilities, and the total capacities invested in each location. We explore the results in detail for both the LNG operator and the NG producer, including the investment decisions, profits, pricing, and sales decisions.

(a) Risk-neutral LNG operator **(b)** Risk-averse LNG operator

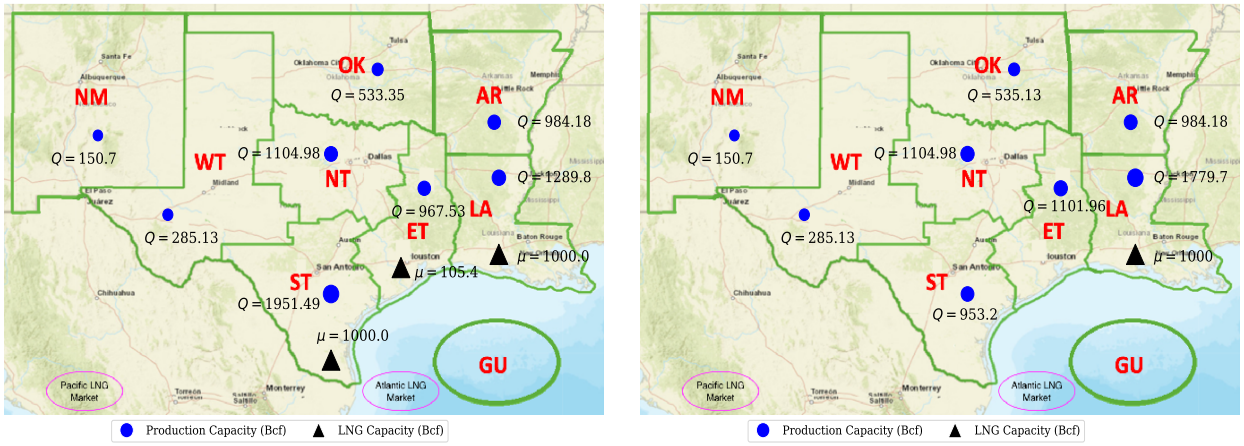

Fig. 4.4. Comparison of LNG operator's and NG producer's capacity investments when the LNG operator is considered to be (a) risk-neutral decision-maker (b) and risk-averse decision-maker.

4.7.2.1 Investment decisions

Figures 4.4a and 4.4b show the capacity investment decisions by region of the LNG operator and the NG producer under the risk-neutral and risk-averse strategy. Table 4.3 shows the total capacity investments under both risk strategies. In an attempt to minimize the chances of huge losses at a 95% confidence level under the risk-averse strategy, the LNG operator chooses to invest in only one LNG facility, which is quite in contrast with the three facilities that are open under a risk-neutral strategy. The lower investments, in turn, leads to a lower LNG capacity being available in the risk-averse strategy. Since the available LNG capacity is lower in the CVaR solution, the amount of gas demand that the LNG operator contributes is also lower, leading to lower capacity investments by the NG producer. The NG production capacity investments in the risk-neutral strategy are 5% higher than those of the risk-averse strategy.

Table 4.3. Investment decisions when the LNG operator is considered to be a risk-neutral vs. risk-averse decision-maker.

Variable	**Risk-neutral LNG operator (EV solution)**	**Risk-averse LNG operator (CVaR solution)**
Number of LNG facilities open	3	1
Total LNG capacity open	2105.4 Bcf	1000.0 Bcf
Total production capacity	7267.161 Bcf	6894.977 Bcf

4.7.2.2 Profits

Figures 4.5a and 4.5b show the profits earned by the LNG operator and the NG producer for each scenario under the risk-neutral and risk-averse strategies, respectively. The LNG operator earns an expected profit of 7.9569 Billion$ under the risk-neutral strategy and 4.3953 Billion$ under the risk-averse strategy. The NG producer earns an expected profit of 50.0506 Billion$ under the risk-neutral strategy and 46.9584 Billion$ under the risk-averse strategy. Although the profits earned by both players are higher under the risk-neutral strategy, we can see from Fig. 4.5a that this strategy leads to a negative profit for the LNG operator in the ('L', 'H') scenario where the LNG market is at low demand and the spot market is at high demand. Under this scenario, the NG producer charges higher gas prices

The scenario definitions are represented using tuples (L_1, L_2) that show demand levels for the different markets. The first element of the tuple (L_1) represents the demand level of the overseas LNG market and the second element (L_2) represents the demand level for the local spot markets. For instance, the scenario ('H','L') represents the case where the LNG market demand levels are high and the local spot market demand levels are low.

to the LNG operator. Since the LNG operator already makes the investment decisions, he ends up operating at a loss, which is the precise scenario a risk-averse decision-maker aims to avoid. Hence, the risk-averse decision-maker chooses to invest more conservatively at the expense of a lower profit to minimize the chances of incurring losses.

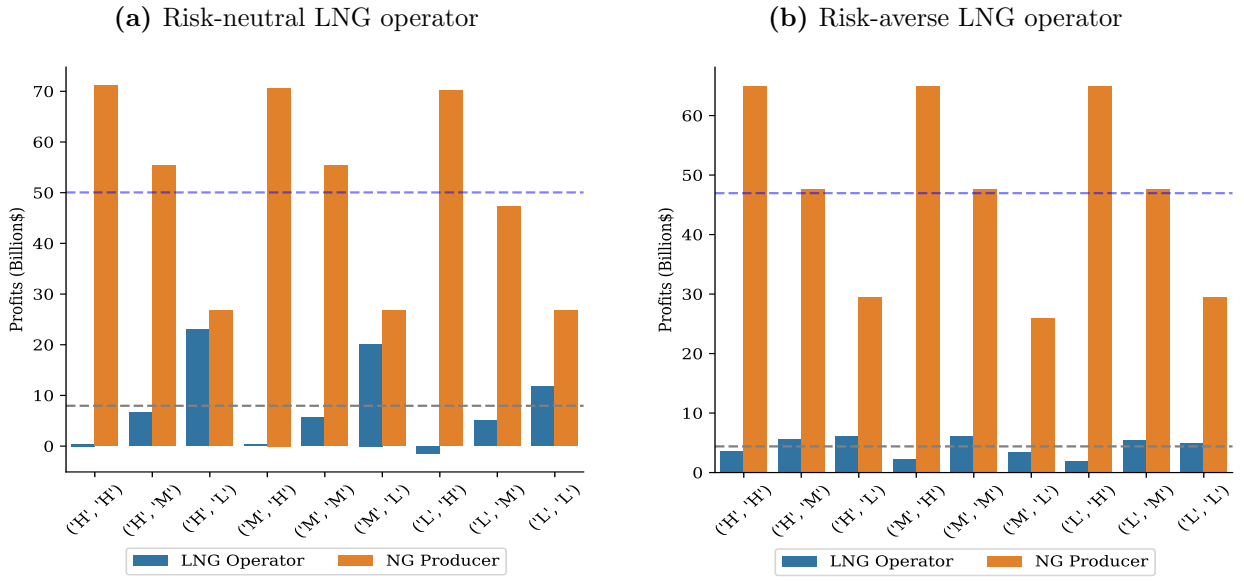

Fig. 4.5. Comparison of LNG operator's and NG producer's profit when the LNG operator is considered to be (a) risk-neutral decision-maker (b) and risk-averse decision-maker by scenario. Each scenario represents (LNG market demand level, spot market demand level).

It is also worth noting that in the CVaR solution, the conservative investment decisions also prevent the leader's profit from increasing significantly even when the spot market is at lower demand like in the ('H','L') and ('M','L') scenarios. Under these scenarios, the LNG operator makes almost double the profit under the risk-neutral strategy compared to the risk-averse strategy due to the NG producer's higher gas prices.

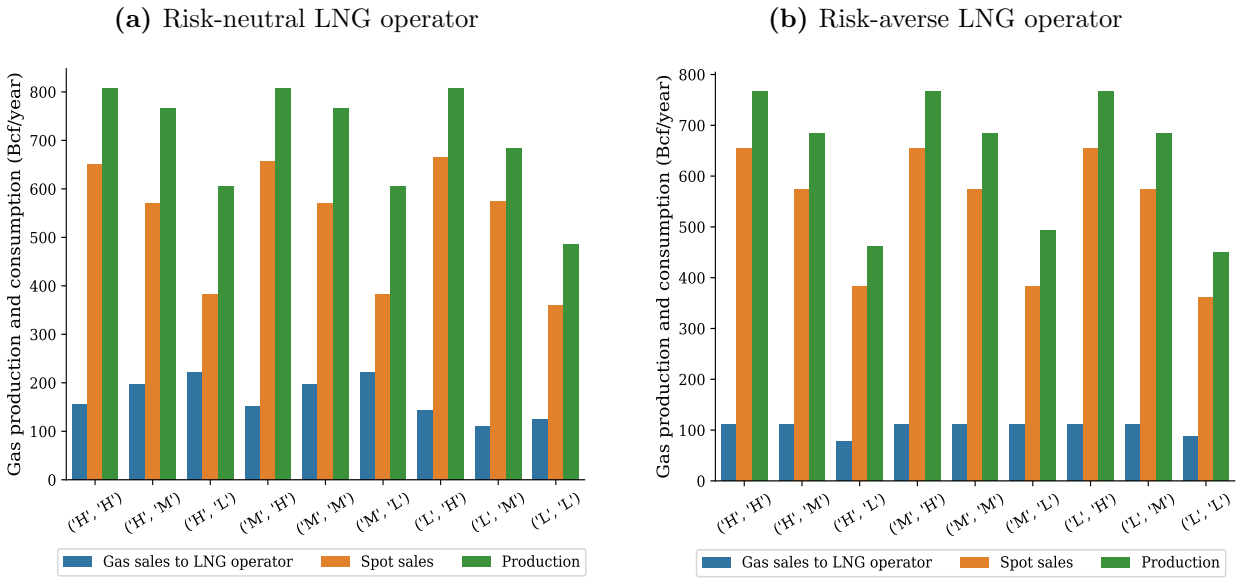

Fig. 4.6. Annual natural gas production and consumption when the LNG operator is considered to be (a) Risk-neutral decision-maker (b) and Risk-averse decision-maker.

4.7.2.3 Natural gas production and consumption

Figures 4.6a and 4.6b show the total gas produced and consumed by both the spot market and the LNG operator for each scenario under the risk-neutral and risk-averse strategies, respectively. Although the overall trends are similar under both strategies, it is worth noting the behavior of the NG producer under both strategies when faced with the scenarios ('H','L'), ('M','L') and ('L','L'), where the spot market demand is low. In the risk-averse strategy, the producer chooses to restrict production and increase the LNG operator's gas prices in contrast with the risk-neutral solution where the producer produces much more gas. This behavior of the NG producer is due to the LNG operator's decision to open only one LNG facility. Since the NG operator anticipated higher gas demand from one specific location, he can increase the prices and reduce production. In the risk-neutral case, since there are multiple facilities open, the LNG operator can now choose where to buy gas from,

and hence the NG producer loses the control he has over the prices. Therefore, the NG producer increases his profits by increasing the production instead of increasing the prices.

(a) Risk-neutral LNG operator

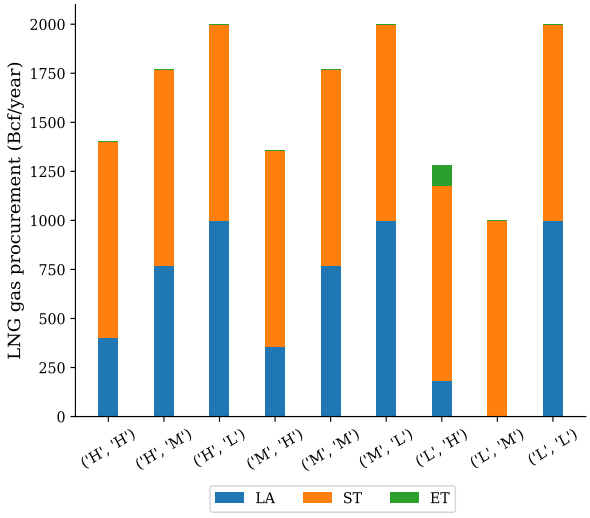

(b) Risk-averse LNG operator

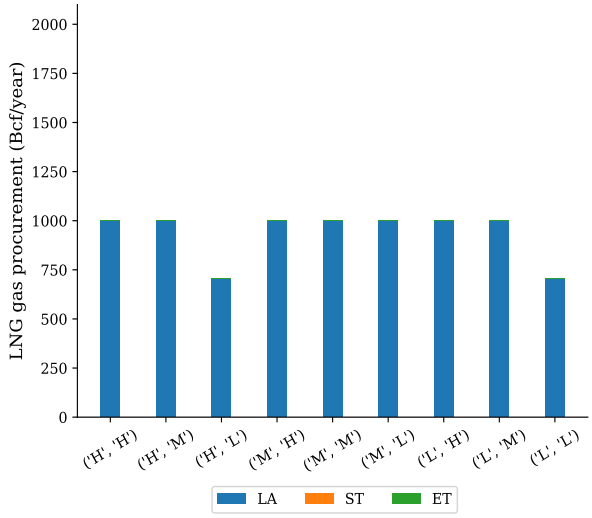

Fig. 4.7. Natural gas procured by the LNG operator when the LNG operator is considered to be (a) Risk-neutral decision-maker (b) and Risk-averse decision-maker.

Figures 4.7a and 4.7b show the amount of gas procured at each open LNG terminal by scenario under the risk-neutral and risk-averse strategies, respectively. In the risk-neutral case, with multiple facilities open, the facilities at locations ST and LA are almost always utilized to capacity. The sharp contrast in model behavior under the different risk strategies is evident under scenarios where the spot market demand is low. The CVaR solution restricts the amount of gas purchased even when the LNG market demand is high. Alternatively, the risk-neutral solution prefers buying more gas and increasing the LNG sales. In the risk-neutral solution, it is worth noting that the choice to open an LNG facility at ET is mainly to hedge against extreme gas prices charged by the producer, especially when the spot market demand is high.

4.7.2.4 Natural gas prices

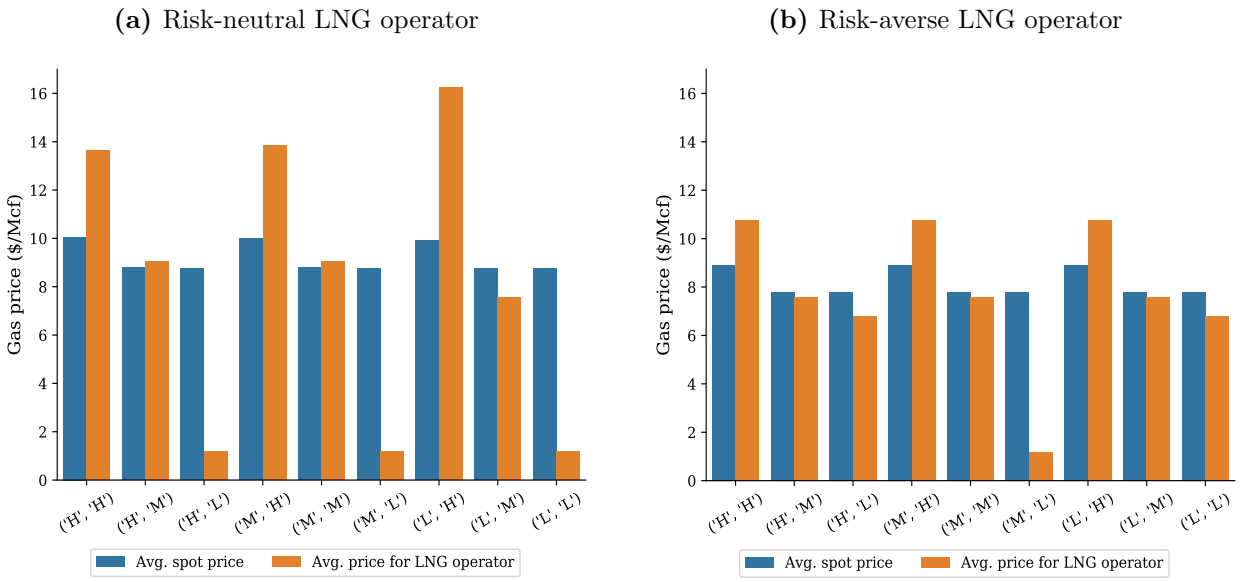

Fig. 4.8. Average natural gas price in the spot market and LNG operator's gas procurement market when the LNG operator is considered to be (a) Risk-neutral decision-maker (b) and Risk-averse decision-maker.

Figures 4.8a and 4.8b show the average gas prices faced by the LNG operator and the local spot market by scenario under the risk-neutral and risk-averse strategies, respectively. Although the NG producer's risk behavior does not change under both strategies, we still see slight changes in the spot market prices. Having a lower gas demand from the LNG player in the risk-averse case leads to lower spot prices in that case compared to the risk-neutral case. A high spot market and LNG operator's gas demand leads to higher average gas prices, especially to the LNG operator. This hike in prices is even more apparent in the risk-neutral case, where the overall gas demand is much higher than the risk-averse case. When the spot market demand is low, the LNG operator can procure gas from the NG player at lower prices in the risk-neutral case. The gas prices are higher in the risk-averse case when the

LNG market demand is high, as the NG producer charges higher prices as the LNG operator only has one open location from where to buy the gas.

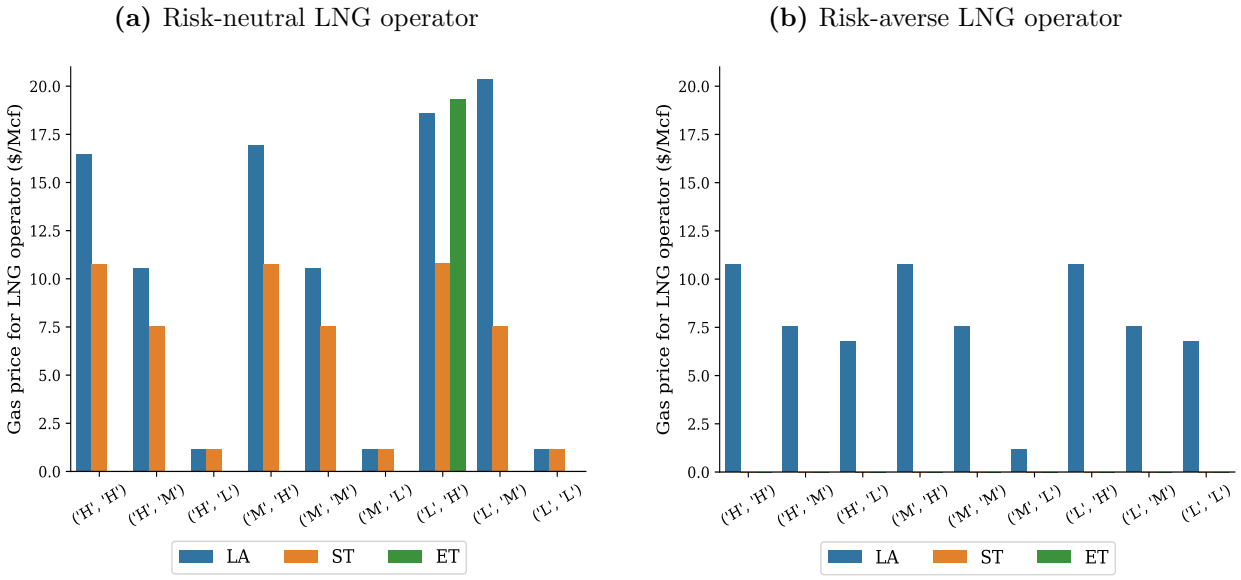

Fig. 4.9. Natural gas price faced by the LNG operator by region when the LNG operator is considered to be (a) Risk-neutral decision-maker (b) and Risk-averse decision-maker.

Figures 4.9a and 4.9b show the gas prices faced by the LNG operator at open LNG locations by scenario under the risk-neutral and risk-averse strategies, respectively. The LG operator attains the lowest gas prices when the spot market is in low demand. The low gas prices are because of the excess production capacity available and lower demand in the spot market, causing the NG producer to lower the prices he charges. Under the risk-neutral strategy, the decision to open multiple locations helps attain much lower prices at both locations when the spot market demand is low. When the LNG operator has only one location open under the risk-averse strategy, the NG producer would prefer to restrict production and increase gas prices. Thus, in this case, even with potentially high demand in the LNG market, the low prices achieved under the risk-neutral strategy are not achieved.

4.7.2.5 LNG market dynamics

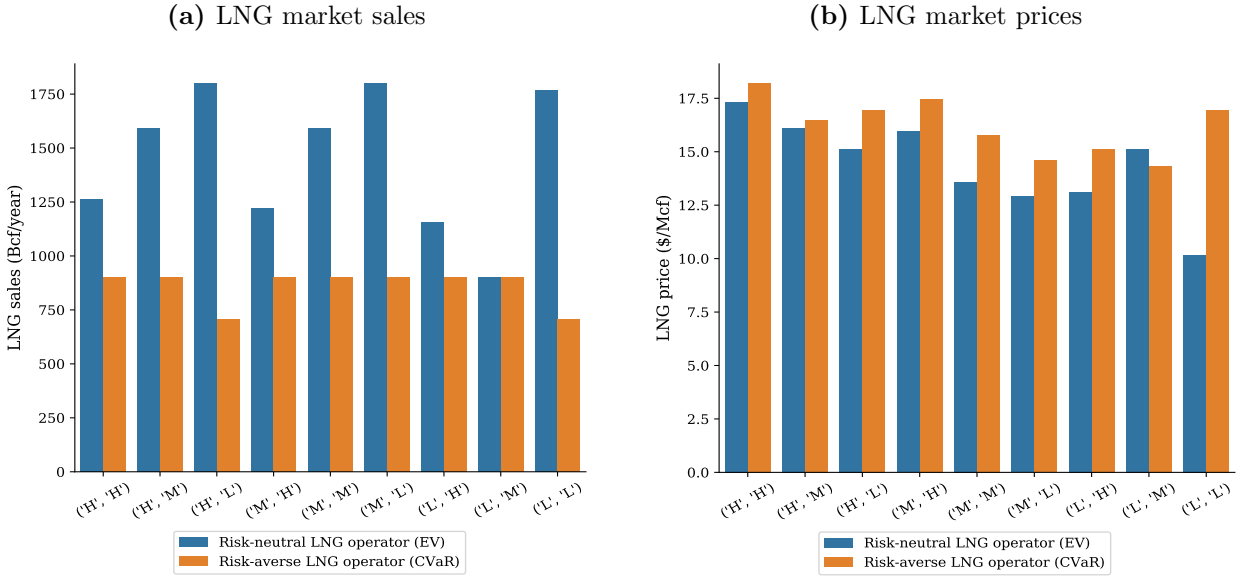

Fig. 4.10. LNG market dynamics when the LNG operator is considered to be Risk-neutral decision-maker vs. Risk-averse decision-maker including (a) LNG sales (b) and LNG market prices.

Figure 4.10a shows the total sales in the LNG market and the corresponding average market prices by scenario under the risk-neutral and risk-averse strategies. We can see that the total LNG sales are lower under the risk-averse strategy due to lower LNG capacity investments. Under the risk-neutral strategy, when the spot market demand is lower, the LNG operator can purchase a more considerable amount of gas from the NG producer at lower prices, which leads to higher sales in the LNG market in those scenarios.

The average LNG market prices across both the Atlantic and Pacific LNG markets is shown in Fig. 4.10b. Since the overall LNG sales are lower under the risk-averse strategy, the market faces higher prices. Due to the higher natural gas and subsequent LNG supply in the risk-neutral solution, the market prices are lower. The highest prices occur when the spot market is at a lower demand under the risk-averse strategy, when the gas procured by

the LNG operator is lower, leading to lower supply in the LNG market. The LNG market prices under this case reflect the reduction in the supply of natural gas.

4.8 Discussion and conclusions

In this chapter, we have developed a stochastic bilevel model to study the strategic interactions between an LNG operator and an NG producer in a leader-follower setting under demand uncertainty. The model presented in the chapter aid the LNG operator and NG producer in making capacity investment and operational decisions. It helps determine optimal locations for the LNG facilities and their capacities, the amount of gas to procure from the NG producer, sales, and market prices for the LNG operator. On the other hand, the NG producer uses the model to determine production, sales, and pricing decisions. We developed models for aid in decision-making under different risk strategies and illustrated the impact of considering risk on the decision maker's choices. To analyze the impact of risk management on the decision-maker, we employ the CVaR to study the risk-averse strategy. At the same time, we use an expected value maximization approach for the risk-neutral strategy. We propose an algorithm to find high quality feasible solutions to the stochastic bilevel problem relatively fast. We study the algorithm's computational efficiency and the quality of solutions obtained using the algorithm using randomly generated instances of the stochastic bilevel problem. We see that the algorithm is able to find quality solutions for even relatively larger instances of the problem within reasonable times. The quality of the solutions found are consistently good and within 7-9% of the optimal solution for all tested instances. The proposed algorithm utilizes the composition of the problem and the intuition that most of the network flow variables remain at zero in our specific problem instance. It is worth noting that this generalization may not hold in instances of the problem where most

flow variables are non-zero. For such cases, a variation of this algorithm can be developed, which could fix flow variables that may be non-zero yet unchanged in all the deterministic scenarios, along with the flow variables that remain at zero.

We apply the models to a real-world example of the Gulf-Southwest region of the U.S., comprising nine regions with local spot markets, three potential LNG locations, and 2 LNG markets. The results clearly show that when the LNG operator is a risk-averse decision-maker, he makes more conservative investment decisions to hedge against possible high losses. On the other hand, when the LNG operator is a risk-neutral decision-maker, his decisions are less conservative and are made so as to maximize the expected profit, without considering any chances of extreme losses explicitly. We see that both risk strategies have their advantages and disadvantages and which one to choose should be based on the decision maker's priorities. Suppose the decision-maker is mainly interested in avoiding huge losses. In that case, using the risk-averse (CVaR) strategy is better since it avoids a loss in all scenarios shown in the case study. But if the decision-maker is risk-neutral, we can see that the decision to open multiple facilities helps the LNG operator exert some control over the prices the NG producer would charge. Hence, the expected profits earned under this strategy are higher.

The model's primary aim is to analyze how the growth in the LNG sector can affect the local spot market and the NG producers' behavior under demand uncertainty. To identify insights specific to two autonomous players, namely the LNG operator and the NG producer, and how they interact with each other, we make several simplifying assumptions regarding the players and the markets. As with every model, our model also has some limitations due to these simplifying assumptions. Our model only assumes single players in each level which translates to a monopolistic assumption in both markets. In reality, both these markets

are not monopolistic and have competition. Several moving parts and components in the natural gas market are not explicitly modeled in our framework, including the pipeline operator, storage operators, etc. The model presented in this chapter can be extended to address some of these limitations. The monopolistic behavior of the LNG operator and NG producer can be tackled by introducing multiple players in the upper and lower-level which would introduce the aspect of competition in the model, leading to more realistic results. Although we consider demand uncertainty using a discrete set of scenarios, we can extend this analysis to continuous demand distributions. This can be accommodated into the model with ease based on the availability of sufficient data to render a good approximation of the demand distribution. The computational tractability of the problem can be preserved by employing scenario reduction techniques (Römisch, 2009; Gazijahani and Salehi, 2017).

Chapter 5

Conclusion

5.1 Summary of research contributions

In Chapter 2, we developed a least-cost optimization model of the U.S. electricity generation and transmission system. This model is used to study the evolution of the generation and capacity mix from 2016 until 2050. The model represents the continental U.S. using 13 regions, each created based on similarity of demand profiles, generation resources, and other factors. The temporal component in the demand profile is captured using 24-hour representative profiles for each season. The model incorporates long-distance transmission using the underlying network structure such that demand and supply are balanced across the regions. The results produced by the model include the investment decisions over five years and operational decisions, including the 24-hour dispatch for each season.

We compare the model results across four scenarios: No Policy, No New Transmission, Pessimistic Costs, and Carbon Tax. The main policy-relevant insights derived from the scenario analysis are summarized below.

1. U.S. electricity can be substantially decarbonized at modest cost, but complete decarbonization is very costly.

2. Significant expansion of solar PV and wind to combine for at least 40% of the generation mix by 2050 is fairly certain, although solar PV and battery storage are more affected by economic and policy assumptions than wind.

3. Investments in long-distance transmission are very limited, while investments in battery storage are much greater, under a wide range of assumptions.

4. Optimal solutions include large investments in natural gas capacity, but gas capacity utilization rates decline steadily and significantly.

5. Cost structures shift away from operating expenditures and toward capital expenditures, especially under climate policy.

Chapter 3 proposed a bilevel programming framework to investigate the strategic interactions between an LNG operator and an NG producer under a leader-follower setting. The model assumes the LNG operator to be the leader and the NG producer to be the follower and helps both players make optimal investment and operational decisions under a non-cooperative environment. The bilevel problem is solved by replacing the lower-level problem with its equivalent KKT conditions, followed by reformulating the complementarity constraints into linear constraints using a disjunctive formulation employing binary variables. Finally, the non-convex terms in the objective function are approximated using piecewise linear functions, which leads to a convex QMIP. The methodology is applied to a real-world problem by considering the Gulf-Southwest region of the U.S. as a case study. We define five scenarios representing different decision-making structures and varying underlying assumptions to compare and contrast the results of those obtained by solving the bilevel problem. The results show that an LNG player's presence can put upward pressure on the local natural gas prices. The higher demand brought about by the LNG player raises the demand for natural gas locally and hence the prices. However, this effect is controlled to an extent by the NG producer's higher production in response to the higher demand. Another significant result that emphasizes the requirement for a bilevel framework under a non-cooperative setting is that if the LNG operator does not account for the higher-than-expected prices the

NG producer can charge after the facility location decisions are finalized, the LNG operator's profits can suffer substantially.

In Chapter 4, we developed a stochastic risk-based bilevel modeling framework to study the strategic interactions between two players in a leader-follower setting under demand uncertainty. We explore how the leader's risk behavior can impact the optimal decisions of both players and how the decisions change under different risk strategies. We employ the conditional-value-at-risk (CVaR) to quantify the risk associated with the leader's decisions under the risk-averse setting. An expected value maximization problem is solved for the risk-neutral setting. The follower is assumed to be risk-neutral in both cases. The resulting stochastic bilevel problem in both cases is not tractable with a large number of scenarios, limiting our ability to perform detailed analysis. Since stochastic bilevel problems are generally hard to solve, we focus on finding high-quality feasible solutions to the problems relatively fast. We proposed an algorithm that uses the problem's underlying network structure to find feasible solutions using an iterative approach. The computational experiments on randomly generated instances of different sizes show the algorithm's high computational efficiency. The analysis clearly shows that we attain high-quality solutions using the algorithm, with the feasible solutions found being very close to the optimal solutions.

The stochastic bilevel model is then used to study the strategic interaction between two players, an LNG operator and an NG producer, in the natural gas market. The LNG operator is considered to be the leader since his decisions are high-cost, high-impact, and have long-term effects. Hence, we also explore how both players' optimal strategies change depending on the LNG operator's risk behavior. The case study explores the Gulf-Southwest region of the U.S. with demand uncertainty in the LNG market, spot market, and the LNG operator's gas procurement market. We see that a risk-averse decision-maker ends up making more conservative decisions, resulting in a lower expected profit but does not incur a loss in any scenario. In contrast, following the risk-neutral solution results in a higher expected

profit but can result in an overall loss if faced with a specific, unfavorable scenario. When following a risk-neutral strategy, the decision to have multiple LNG facilities open provides the LNG operator with some control over the prices the NG producer charges for the gas. Meanwhile, employing the more conservative approach under the risk-averse strategy results in the LNG operator losing the ability to exert any control over the gas price, essentially acting as a price taker. Hence, we see that each risk-based strategy has several pros and cons, and the decisions can change drastically when the risk behavior of the decision-maker changes.

5.2 Limitations

As with any mathematical model, the modeling frameworks proposed in this dissertation also have their limitations. The multi-decadal timeframe and national scope of the problem considered in Chapter 2 required us to make several simplifying assumptions in order to address the questions we set out to explore. The model described in Chapter 2 considers temporal and spatial aggregation to a level that may fail to shed light on the detailed dispatch with high resolution in space or time. Since we use the model to identify possible long-term transition pathways of the U.S. electricity system under different policy settings as opposed to its exact path of evolution, the assumptions made do not significantly impact the results gleaned from the analysis. We assume five-year time steps to reduce the computational burden associated with solving the large-scale model. While using a more refined time step could help accommodate factors like incorporating precise construction lead times for different technologies, this would not affect the results significantly given the long analysis time frame.

Similarly, modeling the U.S. electricity system as being controlled by single optimizing agent that manages all investment and operational decisions to minimize cost is an abstrac-

tion of the much more complex decision-making structure in reality. In reality, the U.S. electricity system is managed by many different decision-makers, who may not always have a common goal in mind when making decisions. The assumption of perfect foresight in parameters does not hold as the parameters become more uncertain as time progresses. Although we attempt to explore the variations of the model outcomes across several important parameterizations using scenario and sensitivity analysis, several other parameter assumptions may not be precise representations of how they would evolve in reality. Some of the model parameters like upper bounds on technology growth rates are relatively subjective values adopted from the literature or approximated based on historical experience. As is the case in essentially any energy modeling study that develops long-term scenarios, the modeling framework is unable to predict the emergence of fundamentally new technologies that could be introduced before 2050.

In Chapter 3, the primary objective of the modeling and analysis is to understand the strategic interactions between an LNG operator and an NG producer operating under a non-cooperative setting. The main idea was to develop a tractable bilevel model capable of aiding in both players' decision-making while accounting for the effects of the LNG export industry's growth on the domestic gas markets. The model's computational tractability is preserved by considering both players in isolation and observing their interaction dynamics. However, this computational tractability comes with some limitations. One of the main limitations of this modeling approach is that we consider only one LNG operator in the upper-level who owns and operates the LNG infrastructure network and one NG producer in the lower-level who owns and operates all the production facilities and the pipeline network. This assumption effectively enforces each player's monopoly in their respective supply chain segments, which contrasts with reality. Natural gas markets are often quite competitive, with multiple LNG operators and NG producers operating concurrently in a given region. Besides, the natural gas supply chain consists of multiple moving parts or players operating in tandem, including

the other players like the pipeline operator, traders, and storage operators. However, we do not explicitly model these other players in our framework. Moreover, we assume that the pipeline network is owned and operated by the NG producer, although it is generally owned and operated by a separate entity in real-world markets.

The stochastic bilevel model we consider in Chapter 4 is designed to get an overarching idea of how uncertainty in the future demand and the decision-maker's risk preferences can impact the optimal strategies of both the players. Most of the limitations of the model described in Chapter 3 apply to this model as well since we create this model by extending the model in Chapter 3 to incorporate demand uncertainty in the markets. We capture the market uncertainty by considering different demand levels in the markets and using them to specify different demand scenarios. We consider that different markets can face different demand levels and the demand level in different markets are uncorrelated. We define discrete probability distributions across all possible combinations of scenarios we can achieve. The scenarios are constructed so that they represent the uncertainties in the market to study the interactions between the LNG operator and the NG producer. Although we can glean actionable insights from the discrete set of scenarios defined in the case study, we lose the ability to conduct a detailed analysis by not considering continuous probability distributions across the scenarios. Limiting the consideration to a discrete distribution and a limited number of scenarios also helps manage the model's computational burden that can significantly increase with the number of scenarios.

Furthermore, for comparing the risk-averse and risk-neutral decision-making approaches, we only consider the LNG operator to be risk-averse while assuming the NG producer to be risk-neutral in both cases. Due to the less capital-intensive decisions of the NG producer compared to the much lumpier and large-scale investment decisions of the LNG operator, the NG producer's risk behavior is not explicitly explored in the model described in Chapter 4. Although considering the LNG operator as a risk-averse decision-maker is more crucial

given his high-cost and capital-intensive long-term investments, it may also be possible that the NG producer chooses to be risk-averse as well. This specific instance of NG producer as a risk-averse decision-maker alongside the LNG operator is not covered in our modeling framework.

5.3 Future research directions

The electricity infrastructure modeling framework presented in Chapter 2 can be extended to address some of the limitations described in Section 5.2. The model provided can be modified to address a variety of problems. It can be employed as a short-term decision-making tool by reducing the time horizon considered for the analysis. Reducing the time horizon allows the user to add more spatial and temporal resolution to the model without significantly increasing its computational complexity. For instance, the 13 regions considered in the study can be further disaggregated to represent states or counties as required to attain more spatial resolution in the model. As mentioned in Section 5.2, the analysis assumes perfect foresight and does not explicitly model the uncertainties associated with some of the parameters. The model results indicate a shift to renewable generation as the time frame progresses, which are guided in part by different parameters like the demand forecasts, costs of renewables and how they would evolve in the future, their capacity factors, and other fuel prices. Although we conduct a series of sensitivity analyses to address the result's robustness to some of these parameters, a stochastic programming model can be employed to attain a more realistic representation of the system and its uncertainties. This stochastic framework can be especially critical if the model is employed as a short-term decision-making tool for investment and operational decisions at the utility level.

Another possible extension to the model with higher spatial resolution would be to consider the technology investment decisions to be integer variables to construct an MILP

in place of the LP, which can help provide more accurate and detailed investment decisions. Similarly, including binary variables to capture the addition of generation capacities only in pre-specified quantities can realistically capture the behavior for certain technologies for which capacities generally get added in set bulk values. Similarly, the analysis presented in Chapter 2 can also be further extended to include the transportation sector into the model, which can help study different policy implications related to the electrification of the transportation sector in the U.S. and the integration between electricity generation and electric vehicle loads.

In the current model, resource adequacy is modeled using a constraint that ensures that the net contribution to generation from each technology type balances the forecasted peak load along with a reserve margin buffer. This representation of different generation technologies' contribution using pre-specified capacity credits becomes an unrealistic representation, especially as the renewable fraction in generation increases. Since the results clearly show a transition to a generation fleet with over 40% renewable generation, as the capacity investments in renewable technologies increase, we are not accurately representing the contributions of these technologies towards satisfying peak demand. Hence, it will be a valuable contribution to the model if we can find a more realistic way to model the capacity credits for renewable generation technologies like wind and solar PV without adding to the model's computational complexity.

There could be many extensions to the bilevel model that is presented in Chapter 3. One of the main limitations of the model as discussed in Section 5.2 is the assumption of a single LNG operator and NG producer, which effectively grants each player a monopoly in its respective level of the market. Considering multiple players in the lower-level problem while retaining a single player in the upper level leads to a single-leader-multiple-follower bilevel structure, which has been implemented in the literature (Pozo et al., 2017). This model can effectively capture the natural gas market's competitive nature with multiple players, hence

avoiding the monopolistic behavior in the natural gas markets while still considering that LNG terminals are owned and operated by a single player.

Furthermore, both the players' monopolistic behavior can be further moderated by considering multiple decision-makers in the upper and lower-level problems. The resulting model considers multiple LNG operators and multiple NG producers operating in tandem in their respective markets, effectively competing against each other. The ensuing multiple-leader-multiple-follower structure ultimately leads to a more comprehensive formulation that can provide more realistic results regarding the prices and actual natural gas consumption in the markets. The general computational intractability of bilevel problems and the difficulties associated with solving them presents a serious computational challenge. Besides, the literature on multiple-leader-multiple-follower bilevel problems is minimal, providing for a novel and challenging problem.

The model presented in Chapter 3 considers the LNG operator and the NG producer and their interactions in isolation. We also assume that the pipeline network is owned and operated by the NG producer, which in reality is done by a separate pipeline operator. A natural extension of the model would be to consider a pipeline operator as a follower alongside the NG producer, resulting in a single-leader-multiple-follower bilevel model. The LNG operator would be the leader, and the NG producer and the pipeline operator will be followers, each of the players acting with the objective of maximizing their individual profits while anticipating the actions of the other players. Alternatively, this interaction can also be modeled using a tri-level model representing the actions of the LNG operator, the NG producer, and the pipeline operator.

The stochastic bilevel model considered in Chapter 4 extends the model presented in Chapter 3 to incorporate demand uncertainty in the markets. Hence, most of the proposed extensions for the bilevel model can be applied to the stochastic bilevel model as well, like considering multiple leaders and multiple followers in the upper-level and lower-level

problems. This model can lead to a much richer formulation that can more realistically represent the natural gas market. Another avenue worth exploring would be to study how the NG producer and LNG operator's decisions change when the LNG operator and the NG producer are both risk-averse decision-makers.

The model analyzed for the case study in Chapter 4 follows a discrete demand distribution, constructed based on deviation from the base demand curve estimated from the data. The model and solution methodology can be effectively extended to accommodate continuous demand distributions in conjunction with relevant scenario reduction techniques. The estimation of demand distribution can be challenging and would require access to detailed historical demand data. Suppose the underlying probability distribution remains unknown, or we are unable to estimate the distribution accurately due to lack of data. In that case, we can consider using a distributionally robust optimization (DRO) approach that considers that the actual distribution lies in an ambiguity set of probability distributions. Significant research has been done in the theory, modeling, and solution methodology development in the area of distributionally robust optimization in the past years. There are examples of models that present DRO in the context of risk-averse optimization as well in the literature. Hence, the extension of the risk-based stochastic bilevel model considered in Chapter 4 using the DRO approach could be another interesting problem to explore.

Appendices

Appendix A

U.S. electricity infrastructure of the future: Generation and transmission pathways through 2050

A.1 Sensitivity analysis results

Table A.1. Variation in non-renewable, renewable, and transmission capacity additions with the value of the discount rate parameter (δ). Its value in the main scenarios is 5%.

	Non-renewable capacity (GW)			Renewable capacity (GW)			Transmission capacity (GW-miles)		
Year	$\delta = 3\%$	$\delta = 5\%$	$\delta = 7\%$	$\delta = 3\%$	$\delta = 5\%$	$\delta = 7\%$	$\delta = 3\%$	$\delta = 5\%$	$\delta = 7\%$
2020	1224.1	1223.3	1222.7	275.4	275.4	275.4	1298.9	1298.9	1298.9
2025	1309.3	1308.6	1308.1	322.7	322.6	322.6	3403.4	3403.4	3403.4
2030	1422.7	1421.9	1421.0	408.4	408.3	408.2	5362.1	5362.1	5362.1
2035	1563.9	1563.0	1562.3	539.8	539.3	538.3	7371.5	7371.5	7371.5
2040	1791.1	1790.7	1786.7	723.8	723.8	723.4	7371.5	7371.5	7371.5
2045	2071.2	2070.8	2068.7	1032.0	1031.4	1031.1	7371.5	7371.5	7371.5
2050	2179.4	2178.4	2177.3	1111.8	1110.5	1109.4	7371.5	7371.5	7371.5

Table A.2. Variation in non-renewable, renewable, and transmission capacity additions with the value of ξ, the parameter that controls the fractional contribution of import transmission capacity toward satisfying the local reserve margin requirement. Its value in the main scenarios is 0.5.

	Non-renewable capacity (GW)			Renewable capacity (GW)			Transmission capacity (GW-miles)		
Year	$\xi = 0.1$	$\xi = 0.5$	$\xi = 0.9$	$\xi = 0.1$	$\xi = 0.5$	$\xi = 0.9$	$\xi = 0.1$	$\xi = 0.5$	$\xi = 0.9$
2020	1227.2	1223.3	1219.4	275.8	275.4	275.3	1298.9	1298.9	1298.9
2025	1313.2	1308.6	1304.1	323.0	322.6	322.4	3403.4	3403.4	3403.4
2030	1426.5	1421.9	1417.4	408.9	408.3	408.0	5362.1	5362.1	5362.1
2035	1567.6	1563.0	1558.3	539.7	539.3	538.6	7371.5	7371.5	7371.5
2040	1795.3	1790.7	1788.4	726.3	723.8	720.2	7371.5	7371.5	7371.5
2045	2075.4	2070.8	2068.5	1032.9	1031.4	1027.8	7371.5	7371.5	7371.5
2050	2183.0	2178.4	2176.1	1112.8	1110.5	1106.9	7371.5	7371.5	7371.5

Table A.3. Variation in annual CO_2 emissions and minimized objective value with the emissions reduction target mandated for 2050. The increase in cost is relative to the No Policy scenario with no emissions reduction target in place.

			Annual emissions (Million metric tons CO_2)							
Emissions reduction target (%)	Objective value ($B)	Increase in cost (%)	2016	2020	2025	2030	2035	2040	2045	2050
50	5051.6	0.0	1720.1	1388.2	1177.8	1072.7	894.3	890.5	722.5	814.8
60	5150.6	1.9	1720.1	1388.6	1177.6	1072.3	892.8	885.3	718.7	688.0
70	5328.9	5.5	1720.1	1388.6	1176.5	1070.2	887.4	870.2	693.1	516.0
80	5498.4	8.8	1720.1	1387.0	1174.1	1066.1	862.9	748.7	546.4	344.0
90	5763.6	14.1	1720.1	1377.4	1163.0	1051.1	827.3	627.3	399.7	172.0
92.5	5973.3	18.2	1720.1	1376.7	1163.4	1046.1	821.7	597.0	363.0	129.0
95	6278.0	24.3	1720.1	1373.6	1159.9	1036.0	806.9	566.6	326.3	86.0
97.5	6726.2	33.1	1720.1	1367.0	1153.7	1023.8	782.9	536.3	289.6	43.0
100	8554.3	69.3	1720.1	1369.0	1136.0	1000.1	758.9	505.9	252.9	0

A.2 Full model formulation

Sets

YEAR	Set of years; $y \in Y$
REGION	Set of regions; $r \in R$
TECHNOLOGY	Set of technologies; $t \in T$

TIMESLICE	Set of timeslices; $l \in L$
FUEL	Set of fuels; $f \in F$
EMISSION	Set of emissions; $e \in E$
MODEOFOPERATION	Mode of operations for technologies; $m \in M$
SEASON	Set of seasons; $se \in SE$
STORAGE	Set of storage technologies; $s \in S$

Subsets

NONRENEWABLE	Set of non-renewable technologies (subset of technologies); $t \in NRT$
RENEWABLE	Set of renewable technologies(subset of technologies); $t \in RT$

Parameters

Global

$\text{YearSplit}_{l,y}$	Fraction of year y in timeslice l
$\text{TimeSliceInSeason}_{l,s}$	Timeslice l in season s
$\text{DiscountRate}_{r,t}$	Discount rate for technology t in year y

StepSize	Time step considered for the model (5 years)
BaseYear	Start year of the study (2016)
EndYear	Final year included in the study (2050)

Demand

$\text{SpecifiedAnnualDemand}_{r,f,y}$	Demand for fuel f in region r in year y
$\text{SpecifiedDemandProfile}_{r,l,t,y}$	Fraction of annual demand for fuel f in timeslice l in region r in year y
$\text{AccumulatedAnnualDemand}_{r,f,y}$	Total exogenous demand of each fuel f in region r in year y

Performance

$\text{CapacityToActivityUnit}_{r,t}$	Potential quantity of electricity that could be produced by each available GW capacity of technology t in region r
$\text{TechWithCapacityToMeetPeakTS}_{r,t}$	Technology t that can contribute to meet the peak demand in region r
$\text{CapacityFactor}_{r,t,l,y}$	Fraction of the capacity of technology t available for generation in timeslice l in region r in year y

$\text{AvailabilityFactor}_{r,t}$	Fraction of the time technology t is available annually for generation in region r
$\text{OperationalLife}_{r,t}$	Operational lifetime of technology t in region r
$\text{ResidualCapacity}_{r,t,y}$	Existing capacity of technology t in region r at the beginning of year y
$\text{InputActivityRatio}_{r,t,f,m,y}$	Rate of use of fuel f as a ratio to the rate of activity of the technology t when in m mode of operation in region r in year y
$\text{OutputActivityRatio}_{r,t,f,m,y}$	Rate of production of fuel f as a ratio to the rate of activity of the technology t in operation mode m in region r in year y

Technology costs

$\text{CapitalCost}_{r,t,y}$	Capital cost of each technology t in a region r for year y
$\text{VariableCost}_{r,t,m,y}$	Variable cost of operating technology t in mode m in region r in year y
$\text{FixedCost}_{r,t,y}$	Fixed cost for maintaining technology t in region r in year y

Storage parameters

$\text{TechnologyToStorage}_{r,t,s,m}$	Indicates which technologies t can contribute (mode of operation $m = 1$, charging) to storage s in mode of operation m $(= 1)$ in region r
$\text{TechnologyFromStorage}_{r,t,s,m}$	Indicates which technologies t can use (mode of operation $m = 2$, discharging) stored energy from storage technology s in region r
$\text{MinStorageCharge}_{r,s,y}$	Minimum storage charge in storage s in region r in year y
$\text{ConversionLoss}_{s}$	Conversion loss in storage s when charging and discharging
$\text{C}_{\text{battery}}$	Conversion coefficient for battery capacity to charging limits

Capacity parameters

$\text{TotalAnnualMaxCapacity}_{r,t,y}$	Maximum allowable capacity for technology t in region r in year y
$\text{TotalAnnualMinCapacity}_{r,t,y}$	Minimum allowable capacity for technology t in region r in year y

Technology growth parameters

$\text{MaxCapacityGrowthRate}_{r,t}$	Maximum growth rate for technology t in region r in each time step of the model
StartUpValue_{t}	Capacity available to start investments in new technology t

Investment parameters

$\text{AnnualMaxCapInvestment}_{r,t,y}$	Maximum capacity investment possible in technology t in year y in region r
$\text{AnnualMinCapInvestment}_{r,t,y}$	Minimum capacity investment possible in technology t in year y in region r

Activity parameters

$\text{AnnualActivityUpperLimit}_{r,t,y}$	Maximum production from technology t in year y in region r
$\text{AnnualActivityLowerLimit}_{r,t,y}$	Minimum production from technology t in year y in region r
$\text{ModelPeriodActivityUpperLimit}_{r,t}$	Maximum production from from technology t in region r for the whole model time frame
$\text{ModelPeriodActivityLowerLimit}_{r,t}$	Minimum production from technology t in region r for the whole model time frame

Reserve margin parameters

$\text{ReserveMarginTagTechnology}_{r,t,y}$	Indicates if technology t can contribute towards reserve margin in region r in year y
$\text{ReserveMarginTagFuel}_{r,f,y}$	Indicates in a reserve margin should be maintained for fuel f in region r in year y
$\text{ReserveMargin}_{r,y}$	The reserve margin to be maintained in region r in year y

Emissions & emission penalties

$\text{EmissionActivityRatio}_{r,t,e,m,y}$	The the rate of pollutant e emitted as a ratio to the rate of a mode of activity m for a technology t in region r in year y
$\text{EmissionsPenalty}_{r,e,y}$	Cost per unit of pollutant e emitted in region r in year y
$\text{AnnualExogenousEmission}_{r,e,y}$	Exogenous emissions for pollutant e in region r in year y
$\text{AnnualEmissionLimit}_{e,y}$	Upper limit on the net emissions of pollutant e for year y

Transmission parameters

$\text{CostMatrix}_{r_1,r_2,f,y}$	The variable cost of transmission for fuel f from region r_1 to r_2 in year y
$\text{DistanceMatrix}_{r_1,r_2}$	Geographical distance between region r_1 and r_2 (centroidal distance)
$\text{ResidualTransmissionCapacity}_{r_1,r_2,f,y}$	Existing transmission capacity between region r_1 to r_2 for fuel f in year y
$\text{TransmissionCapitalCost}_{r_1,r_2,f,y}$	Capital cost of installing a transmission capacity between region r_1 to r_2 for fuel f in year y
$\text{CapacityPerTransmissionLane}_{y}$	Capacity of each transmission line installed in year y. Energy in GW per 345 kV line
$\text{MaxTransmissionGrowthRate}_{r_1,r_2,f}$	Maximum rate at which transmission capacity for fuel f can grow between regions r_1 and r_2
$\text{OperationalLifeTransmission}_{r}$	Operational lifetime of transmission in region r
$\text{DiscountRateTransmission}_{r,f}$	Discount rate for transmission system for fuel f in region r

Decision variables

Capacity variables

$\text{NewCapacity}_{(r,t,y)}$	New investment in capacity for technology t in year y in region r
$\text{AccumulatedNewCapacity}_{(r,t,y)}$	Total new capacity investments in technology t till year y in region r
$\text{TotalCapacityAnnual}_{(r,t,y)}$	Total capacity (residual + new) available for technology t in year y in region r

Activity variables

$\text{Activity}_{(r,l,t,m,y)}$	This variable indicates if a technology t is operating under any mode m (producing or using a fuel) in a given timeslice l in year y in region r
$\text{RateOfActivity}_{(r,l,t,m,y)}$	The rate of activity for technology t operating under mode m in timeslice l in year y in region r
$\text{RateOfTotalActivity}_{(r,l,t,y)}$	Total rate of activity for technology t in timeslice l in year y in region r
$\text{TotalTechnologyAnnualActivity}_{(r,t,y)}$	Total activity for technology t in year y in region r

$\text{TotalAnnualTechnologyActivityByMode}_{(r,t,m,y)}$	Total activity for technology t in mode m for year y in region r
$\text{RateOfProductionByTechnologyByMode}_{(r,l,t,m,f,y)}$	Total production of fuel f from technology t when in operation mode m in timeslice l in year y in region r
$\text{RateOfProductionByTechnology}_{(r,l,t,f,y)}$	Rate of production of fuel f from technology t in timeslice l in year y in region r
$\text{ProductionByTechnology}_{(r,l,t,f,y)}$	Production of fuel f from technology t in timeslice l in year y in region r
$\text{ProductionByTechnologyAnnual}_{(r,f,t,y)}$	Total production of fuel f from technology t in year y in region r
$\text{RateOfProduction}_{(r,l,f,y)}$	Total rate of production of fuel f from all technologies in timeslice l in year y in region r
$\text{Production}_{(r,l,f,y)}$	Total production of fuel f from all technologies in timeslice l in year y in region r

$\text{RateOfUseByTechnologyByMode}_{(r,l,t,m,f,y)}$	Rate of use of fuel f by technology t when in operation mode m in timeslice l in year y in region r
$\text{RateOfUseByTechnology}_{(r,l,t,f,y)}$	Rate of use of fuel f by technology t in timeslice l in year y in region r
$\text{UseByTechnology}_{(r,l,t,f,y)}$	Use of fuel f by technology t in timeslice l in year y in region r
$\text{UseByTechnologyAnnual}_{(r,t,f,y)}$	Total use of fuel f by technology t in year y in region r
$\text{RateOfUse}_{(r,l,f,y)}$	Rate of use of fuel f by technology t in year y in region r
$\text{Use}_{(r,l,f,y)}$	Total use of fuel f by all technologies in timeslice l in year y in region r

Demand variables

$\text{RateOfDemand}_{(r,l,f,y)}$	Rate of demand for fuel f in timeslice l in year y in region r
$\text{Demand}_{(r,l,f,y)}$	Demand for fuel f in timeslice l in year y in region r

$\text{ProductionAnnual}_{(r,f,y)}$	Total production of fuel f in year y in region r
$\text{UseAnnual}_{(r,f,y)}$	Total use of fuel f in year y in region r

Cost variables

$\text{CapitalInvestment}_{(r,t,y)}$	Capital investment costs for technology t in year y in region r
$\text{DiscountedCapitalInvestment}_{(r,t,y)}$	Discounted capital investment costs for technology t in year y in region r
$\text{SalvageValue}_{(r,t,y)}$	Salvage value for technology t in year y in region r
$\text{DiscountedSalvageValue}_{(r,t,y)}$	Discounted salvage value for technology t in year y in region r
$\text{OperatingCost}_{(r,t,y)}$	Operational costs for technology t in year y in region r
$\text{OperatingCostBaseYear}_{(r,t,y)}$	Operational costs discounted to the beginning of the 5 year period (StepSize)

$\text{DiscountedOperatingCost}_{(r,t,y)}$	Discounted operational costs for technology t in year y in region r
$\text{AnnualVariableOperatingCost}_{(r,t,y)}$	Variable costs associated with technology t in year y in region r
$\text{AnnualFixedOperatingCost}_{(r,t,y)}$	Fixed costs associated with technology t in year y in region r
$\text{VariableOperatingCost}_{(r,t,l,y)}$	Operational costs for technology t in timeslice l in year y in region r
$\text{TotalDiscountedCost}_{(r,t,y)}$	Total discounted costs for technology t in year y in region r
$\text{ModelPeriodCostByRegion}_{r}$	Total cost for full model timeframe for region r

Storage variables

$\text{NetStorageCharge}_{(s,r,l,y)}$	Net storage charge in storage s in timeslice l in year y in region r
$\text{StorageLevel}_{(s,r,l,y)}$	Storage level in storage s in timeslice l in year y in region r

$\text{StorageCharge}_{(s,r,l,y)}$	Net storage charge going into storage s in timeslice l in year y in region r
$\text{StorageDischarge}_{(s,r,l,y)}$	Net discharge from storage s in timeslice l in year y in region r
$\text{StorageUpperLimit}_{(s,r,y)}$	Maximum charge storage s can hold in year y in region r
$\text{StorageLowerLimit}_{(s,r,y)}$	Minimum charge storage s can hold in year y in region r

Reserve margin variables

$\text{TotalCapacityInReserveMargin}_{(r,y)}$	Total reserve margin capacity required in region r in year y
$\text{DemandNeedingReserveMargin}_{(r,l,y)}$	Demand needing reserve margin in timeslice l in region r in year y
$\text{NetRenewableFraction}_{(r,y)}$	The fraction of reserve margin met by renewable technologies in region r in year y

Emission variables

$\text{AnnualTechnologyEmissionByMode}_{(r,t,e,m,y)}$	Emissions of pollutant s from technology t operating in mode m in year y in region r
$\text{AnnualTechnologyEmission}_{(r,t,e,y)}$	Emissions of pollutant s from technology t in year y in region r
$\text{AnnualTechEmissionPenaltyByEmission}_{(r,t,e,y)}$	Emissions penalty for pollutant s emitted by technology t in year y in region r
$\text{AnnualTechnologyEmissionsPenalty}_{(r,t,y)}$	Total emissions penalty in year y in region r
$\text{DiscountedTechnologyEmissionsPenalty}_{(r,t,y)}$	Discounted total emissions penalty in year y in region r

Transmission variables

$\text{RateofImports}_{(r_1,r_2,f,l,y)}$	Rate of imports for fuel f from region r_1 and r_2 for timeslice l in year y
$\text{Imports}_{(r_1,r_2,f,l,y)}$	Imports for fuel f from region r_1 and r_2 for timeslice l in year y
$\text{AnnualImportCost}_{(r,y)}$	Cost of imports to a region r in year y

$\text{DiscountedAnnualImportCost}_{(r,y)}$	Discounted cost of imports to a region r in year y
$\text{DiscountedAnnualTransmissionCost}_{(r,y)}$	Discounted cost of transmission in a region r in year y
$\text{TransmissionCapitalInvestment}_{(r_1,r_2,f,y)}$	Capital cost of investing in transmission between region r_1 and r_2 in year y
$\text{DiscTransmissionCapitalInvestment}_{(r_1,r_2,f,y)}$	Discounted capital cost of investing in transmission between region r_1 and r_2 in year y
$\text{SalvageValueTransmission}_{(r_1,r_2,f,y)}$	Salvage value of transmission investments between region r_1 and r_2 in year y
$\text{DiscSalvageValueTransmission}_{(r_1,r_2,f,y)}$	Discounted salvage value of transmission investments between region r_1 and r_2 in year y
$\text{NewTransmissionCapacity}_{(r_1,r_2,f,y)}$	New transmission investment capacity between region r_1 and r_2 in year y

$\text{AccumulatedNewTransmissionCapacity}_{(r_1,r_2,f,y)}$	Net new transmission investment capacity between region r_1 and r_2 until year y
$\text{TotalTransmissionCapacityAnnual}_{(r_1,r_2,f,y)}$	Total transmission investment capacity between region r_1 and r_2 until year y

A.2.1 Optimization Problem

$$\min \sum_{r\in R}\sum_{t\in T}\sum_{y\in Y} \text{TotalDiscountedCost}_{(r,t,y)} + \sum_{r\in R}\sum_{y\in Y} \text{DiscountedAnnualTransmissionCost}_{(r,y)}$$

subject to

$$\text{RateOfDemand}_{(r,l,f,y)} * \text{YearSplit}_{(l,y)} = \text{SpecifiedAnnualDemand}_{(r,f,y)} * \text{SpecifiedDemandProfile}_{(r,f,l,y)} \quad \forall \quad r \in R, f \in F, l \in L, y \in Y$$

Storage

$$\text{NetStorageCharge}_{(s,r,l,y)} = \sum_{t,m} \text{RateOfActivity}_{(r,l,t,m,y)} * \text{YearSplit}_{(l,y)} * (\text{TechnologyToStorage}_{(r,t,s,m)} - \text{TechnologyFromStorage}_{(r,t,s,m)}) \quad \forall \quad r \in R, s \in S, l \in L, y \in Y$$

$$\text{NetStorageCharge}_{(s,r,l,y)} = \text{StorageLevel}_{(s,r,l,y)} - \text{StorageLevel}_{(s,r,l-1,y)} \quad \forall \quad r \in R, s \in S, l \in L, y \in Y$$

$$\text{StorageLevel}_{(s,r,l,y)} \geq \text{StorageLowerLimit}_{(s,r,y)} * \text{DaysInSeason}_{l} \quad \forall \quad r \in R, s \in S, l \in L, y \in Y$$

$$\text{StorageLevel}_{(s,r,l,y)} \leq \text{StorageUpperLimit}_{(s,r,y)} * \text{DaysInSeason}_{l} \quad \forall \quad r \in R, s \in S, l \in L, y \in Y$$

$$\text{StorageLowerLimit}_{(s,r,y)} = \text{MinStorageCharge}_{(s,r,y)} * \text{StorageUpperLimit}_{(s,r,y)} \quad \forall \quad r \in R, s \in S, y \in Y$$

$$\text{StorageUpperLimit}_{(s,r,y)} = \text{C}_{\text{battery}} * \text{TotalCapacityAnnual}_{(r,\text{BATTERY},y)} \quad \forall \quad r \in R, s \in S, y \in Y$$

Capacity Adequacy

$$\text{AccumulatedNewCapacity}_{(r,t,y)} = \sum_{\substack{yy:y-yy\geq 0 \\ y-yy<\text{OperationalLife}_{(r,t)}}} \text{NewCapacity}_{(r,f,y)} \quad \forall\, r \in R, t \in T, y \in Y$$

$$\text{TotalCapacityAnnual}_{(r,t,y)} = \text{AccumulatedNewCapacity}_{(r,t,y)} + \text{ResidualCapacity}_{(r,t,y)} \quad \forall \quad r \in R, t \in T, y \in Y$$

$$\text{RateOfTotalActivity}_{(r,l,t,y)} = \sum_{m \in M} \text{RateOfActivity}_{(r,l,t,m,y)} \quad \forall \quad r \in R, t \in T, l \in L, y \in Y$$

$$\text{RateOfTotalActivity}_{(r,l,t,y)} \leq \text{TotalCapacityAnnual}_{(r,t,y)} * \text{CapacityFactor}_{(r,t,l,y)} * \text{CapacityToActivityUnit}_{(r,t)} \quad \forall \quad r \in R, t \in T, l \in L, y \in Y$$

$$\sum_{l \in L} \text{RateOfTotalActivity}_{(r,l,t,y)} * \text{YearSplit}_{(l,y)} \leq \sum_{l \in L} \text{TotalCapacityAnnual}_{(r,t,y)} * \text{CapacityFactor}_{(r,t,l,y)} * \text{AvailabilityFactor}_{(r,t,y)} * \text{CapacityToActivityUnit}_{(r,t)} \, \forall \, r \in R, t \in T, y \in Y$$

Energy Balance

$$\text{RateOfProductionByTechnologyByMode}_{(r,l,t,m,f,y)} = \text{RateOfActivity}_{(r,l,t,m,y)} * \text{OutputActivityRatio}_{(r,t,f,m,y)} \quad \forall \quad r \in R, l \in L, t \in T, f \in F, m \in M, y \in Y$$

$$\sum_{m \in M} \text{RateOfProductionByTechnologyByMode}_{(r,l,t,m,f,y)} = \text{RateOfProductionByTechnology}_{(r,l,t,f,y)} \quad \forall \quad r \in R, l \in L, t \in T, f \in F, y \in Y$$

$$\sum_{t \in T} \text{RateOfProductionByTechnology}_{(r,l,t,f,y)} =$$

$$\text{RateOfProduction}_{(r,l,f,y)} \quad \forall \quad r \in R, f \in F, l \in L, y \in Y$$

$$\text{Production}_{(r,l,f,y)} = \text{RateOfProduction}_{(r,l,f,y)} * \text{YearSplit}_{(l,y)} \quad \forall \quad r \in R, f \in F, l \in L, y \in Y$$

$$\text{RateOfUseByTechnologyByMode}_{(r,l,t,m,f,y)} = \text{RateOfActivity}_{(r,l,t,m,y)}$$
$$* \text{InputActivityRatio}_{(r,t,f,m,y)} \quad \forall \quad r \in R, l \in L, t \in T, f \in F, m \in M, y \in Y$$

$$\sum_{m \in M} \text{RateOfUseByTechnologyByMode}_{(r,l,t,m,f,y)} =$$
$$\text{RateOfUseByTechnology}_{(r,l,t,f,y)} \quad \forall \quad r \in R, l \in L, t \in T, f \in F, y \in Y$$

$$\sum_{t \in T} \text{RateOfUseByTechnology}_{(r,l,t,f,y)} = \text{RateOfUse}_{(r,l,f,y)} \quad \forall \quad r \in R, f \in F, l \in L, y \in Y$$

$$\text{Use}_{(r,l,f,y)} = \text{RateOfUse}_{(r,l,f,y)} * \text{YearSplit}_{(l,y)} \quad \forall \quad r \in R, f \in F, l \in L, y \in Y$$

$$\text{Demand}_{(r,l,f,y)} = \text{RateOfDemand}_{(r,l,f,y)} * \text{YearSplit}_{(l,y)} \quad \forall \quad r \in R, f \in F, l \in L, y \in Y$$

$$\text{Production}_{(r,l,f,y)} \geq \text{Demand}_{(r,l,f,y)} + Use_{(r,l,f,y)} \quad \forall \quad r \in R, f \in F, l \in L, y \in Y$$

Capital Cost

$$\text{CapitalInvestment}_{(r,t,y)} = \text{CapitalCost}_{(r,t,y)} * \text{NewCapacity}_{(r,t,y)} \quad \forall \quad r \in R, t \in T, y \in Y$$

$$\text{DiscountedCapitalInvestment}_{(r,t,y)} = \frac{CapitalInvestment_{(r,t,y)}}{(1 + \text{DiscountRate}_{(r,t)})^{(y - \text{BaseYear})}} \quad \forall \quad r \in R, t \in T, y \in Y$$

Operational Cost

$$\sum_{m \in M} \text{TotalAnnualTechnologyActivityByMode}_{(r,t,m,y)} * \text{VariableCost}_{(r,t,m,y)} =$$
$$\text{AnnualVariableOperatingCost}_{(r,t,y)} \quad \forall \quad r \in R, t \in T, y \in Y$$

$$\text{AnnualFixedOperatingCost}_{(r,t,y)} = \text{FixedCost}_{(r,t,y)} *$$
$$\text{TotalCapacityAnnual}_{(r,t,y)} \quad \forall \quad r \in R, t \in T, y \in Y$$

$$\text{OperatingCost}_{(r,t,y)} = \sum_{m \in M} \text{AnnualFixedOperatingCost}_{(r,t,y)} +$$

$$\text{AnnualVariableOperatingCost}_{(r,t,y)} \quad \forall \quad r \in R, t \in T, y \in Y$$

$$\text{OperatingCostBaseYear}_{(r,t,y)} = \sum_{i=y}^{y+\text{StepSize}} \frac{\text{OperatingCost}_{(r,t,y)}}{(1+\text{DiscountRate}_{(r,t)})^{(y-i)}} \quad \forall \quad r \in R, t \in T, y \in Y$$

$$\text{DiscountedOperatingCost}_{(r,t,y)} = \frac{\text{OperatingCostBaseYear}_{(r,t,y)}}{(1+\text{DiscountRate}_{(r,t)})^{(y-\text{BaseYear}+0.5)}} \quad \forall \quad r \in R, t \in T, y \in Y$$

Salvage Value

$$\text{SalvageValue}_{(r,t,y)} = 0 \quad \forall \quad r \in R, t \in T, y \in \{y : y + \text{OperationalLife}_{(r,t)} < \text{EndYear}\}$$

$$\text{SalvageValue}_{(r,t,y)} = \frac{1-(1+\text{DiscountRate}_{(r,t)})^{\text{EndYear}-y+1}-1}{(1+\text{DiscountRate}_{(r,t)})^{\text{OperationalLife}_{(r,t)}-1}} * \text{NewCapacity}_{(r,t,y)} *$$

$$\text{CapitalCost}_{(r,t,y)} \quad \forall \quad r \in R, t \in T, y \in \{y : y + \text{OperationalLife}_{(r,t)} \geq \text{EndYear}\}$$

$$\text{DiscountedSalvageValue}_{(r,t,y)} =$$

$$\frac{\text{SalvageValue}_{(r,t,y)}}{(1+\text{DiscountRate}_{(r,t)})^{(1+\text{EndYear}-\text{StartYear})}} \quad \forall \quad r \in R, t \in T, y \in Y$$

Total Costs

$$\text{TotalDiscountedCost}_{(r,t,y)} = \text{DiscountedCapitalInvestment}_{(r,t,y)} +$$

$$\text{DiscountedOperatingCost}_{(r,t,y)} + \text{DiscountedTechnologyEmissionsPenalty}_{(r,t,y)} -$$

$$\text{DiscountedSalvageValue}_{(r,t,y)} \quad \forall \quad r \in R, t \in T, y \in Y$$

Capacity Growth Rate

$$\text{NewCapacity}_{(r,t,y)} \leq \text{TotalCapacityAnnual}_{(r,t-\text{StepSize},y)} *$$

$$\text{MaxCapacityGrowthRate}_{(r,t)} \quad \forall \quad r \in R, t \in T, y \in Y$$

Capacity Constraints

$$\text{NewCapacity}_{(r,t,y)} \leq \text{AnnualMaxCapInvestment}_{(r,t,y)} \quad \forall \quad r \in R, t \in T, y \in Y$$

$$\text{NewCapacity}_{(r,t,y)} \geq \text{AnnualMinCapInvestment}_{(r,t,y)} \quad \forall \quad r \in R, t \in T, y \in Y$$

$$\text{AccumulatedNewCapacity}_{(r,t,y)} \leq \text{TotalAnnualMaxCapacity}_{(r,t,y)} \quad \forall \quad r \in R, t \in T, y \in Y$$

$$\text{AccumulatedNewCapacity}_{(r,t,y)} \geq \text{TotalAnnualMinCapacity}_{(r,t,y)} \quad \forall \quad r \in R, t \in T, y \in Y$$

Activity Constraints

$$\sum_{m \in M} \sum_{l \in L} \text{RateOfActivity}_{(r,l,t,m,y)} * \text{YearSplit}_{(l,y)} \leq$$

$$\text{AnnualActivityUpperLimit}_{(r,t)} \quad \forall \quad r \in R, t \in T, y \in Y$$

$$\sum_{m \in M} \sum_{l \in L} \text{RateOfActivity}_{(r,l,t,m,y)} * \text{YearSplit}_{(l,y)} \geq$$

$$\text{AnnualActivityLowerLimit}_{(r,t)} \quad \forall \quad r \in R, t \in T, y \in Y$$

$$\sum_{m \in M} \sum_{l \in L} \sum_{y \in Y} \text{RateOfActivity}_{(r,l,t,m,y)} * \text{YearSplit}_{(l,y)} \leq$$

$$\text{ModelPeriodActivityUpperLimit}_{(r,t)} \quad \forall \quad r \in R, t \in T$$

$$\sum_{m,l,y} \text{RateOfActivity}_{(r,l,t,m,y)} * \text{YearSplit}_{(l,y)} \geq$$

$$\text{ModelPeriodActivityLowerLimit}_{(r,t)} \quad \forall \quad r \in R, t \in T$$

Reserve Margins Constraints

$$\sum_{t \in NRT} \text{TotalCapacityAnnual}_{(r,t,y)} * \text{ReserveMarginTagTechnology}_{(r,t,y)} * \text{CapacityFactor}_{(r,t,l,y)} *$$

$$\text{CapacityToActivityUnit}_{(r,t)} + \text{NetRenewableFraction}_{(r,y)} +$$

$$\eta \sum_{i \in R} \text{TotalTransmissionCapacityAnnual}_{(i,r,f,y)} \geq$$

$$\text{TotalCapacityInReserveMargin}_{(r,y)} \quad \forall \quad r \in R, f \in \{ELC\}, y \in Y$$

$$\text{NetRenewableFraction}_{(r,y)} \leq \sum_{t \in RT} \text{TotalCapacityAnnual}_{(r,t,y)} * \text{CapacityFactor}_{(r,t,l,y)} *$$

$$\text{CapacityToActivityUnit}_{(r,t)} * \text{ReserveMarginTagTechnology}_{(r,t,y)} \quad \forall \quad r \in R, y \in Y$$

$$\text{DemandNeedingReserveMargin}_{(r,l,y)} = \sum_{f \in F} \text{RateOfProduction}_{(r,l,f,y)} *$$

$$\text{ReserveMarginTagFuel}_{(r,f,y)} \quad \forall \quad r \in R, l \in L, y \in Y$$

$$\text{TotalCapacityInReserveMargin}_{(r,y)} = \text{DemandNeedingReserveMargin}_{(r,l,y)} *$$

$$\text{ReserveMargin}_{(r,y)} \quad \forall \quad r \in R, l \in L, y \in Y$$

Emission Accounting

$$\sum_{m \in M} \sum_{l \in L} \text{EmissionActivityRatio}_{(r,t,e,m,y)} * \text{YearSplit}_{(l,y)} =$$

$$\text{AnnualTechnologyEmission}_{(r,t,e,y)} \quad \forall \quad r \in R, t \in T, e \in E, y \in Y$$

Flow Balance

$$\text{Imports}_{(i,r,f,l,y)} = \text{RateofImports}_{(i,r,f,l,y)} * \text{YearSplit}_{(l,y)} \qquad \forall \quad i \in R, r \in R, f \in F, l \in L, y \in Y$$

$$\text{Production}_{(r,l,f,y)} + \sum_{i \in R} \text{Import}_{(i,r,l,f,y)} \geq \text{Demand}_{(r,l,f,y)} + \text{Use}_{(r,l,f,y)} +$$

$$\sum_{i \in R} Import((r,i,l,f,y)) \quad \forall \quad r \in R, l \in L, y \in Y$$

$$\sum_{l \in L} \text{Production}_{(r,l,f,y)} + \sum_{l \in L} \sum_{i \in R} \text{Import}_{(i,r,l,f,y)} - \text{Import}_{(r,i,l,f,y)} \geq \sum_{l \in L} \text{Use}_{(r,l,f,y)} +$$

$$\text{AccumulatedAnnualDemand}_{(r,f,y)} \quad \forall \quad r \in R, l \in L, y \in Y$$

New Transmission

$$\text{AccumulatedNewTransmissionCapacity}_{(i,r,f,y)} = \sum_{yy} \text{CapacityPerTransmissionLane}_{y} *$$

$$\text{NewTransmissionCapacity}_{(i,r,f,yy)} \quad \forall \quad i \in R, r \in R, f \in F, y \in Y,$$

$$yy \in \{yy : y - yy \geq 0, y - yy < \text{OperationalLifeTransmission}_r\}$$

$$\text{TotalTransmissionCapacityAnnual}_{(i,r,f,y)} = \text{AccumulatedNewTransmissionCapacity}_{(i,r,f,y)} +$$
$$\text{ResidualTransmissionCapacity}_{(i,r,f,y)} \quad \forall \quad i \in R, r \in R, f \in F, y \in Y$$

$$\text{RateofImports}_{(i,r,f,l,y)} \leq \text{TotalTransmissionCapacityAnnual}_{(i,r,f,y)} *$$
$$\text{CapacityToActivityRatioTransmission}_{(r,f)} \quad \forall \quad i \in R, r \in R, f \in F, l \in L, y \in Y$$

$$\sum_{l \in L} \text{Imports}_{(i,r,f,l,y)} \leq \text{ConversionCoeff} *$$
$$\text{TotalTransmissionCapacityAnnual}_{(i,r,f,y)} \quad \forall \quad i \in R, r \in R, f \in F, l \in L, y \in Y$$

Import Costs

$$\sum_{i \in R} \sum_{l \in L} \text{CostMatrix}_{(i,r,f,y)} * \text{Imports}_{(i,r,f,l,y)} = \text{AnnualImportCost}_{(r,y)} \quad \forall \quad r \in R, y \in Y$$

$$\text{AnnualImportCostBaseYear}_{(r,y)} = \sum_{i=y}^{y+\text{StepSize}} \frac{\text{AnnualImportCost}_{(r,y)}}{(1 + \text{DiscountRate}_r)^{(y-i)}} \quad \forall \quad r \in R, y \in Y$$

$$\text{DiscountedAnnualImportCost}_{(r,y)} = \frac{\text{AnnualImportCostBaseYear}_{(r,y)}}{(1 + \text{DiscountRate}_r)^{(y - \text{BaseYear} + 0.5)}} \quad \forall \quad r \in R, y \in Y$$

Salvage Value Transmission

$$\text{SalvageValueTransmission}_{(i,r,f,y)} = 0$$
$$\forall \quad i \in R, r \in R, f \in F, y \in \{y : y + \text{OperationalLifeTransmission}_r < \text{EndYear}\}$$

$$\text{SalvageValueTransmission}_{(i,r,t,y)} = \text{TransmissionCapitalInvestment}_{(i,r,f,y)} *$$
$$\frac{1 - (1 + \text{DiscountRateTransmission}_{(r,f)})^{\text{EndYear} - y + 1} - 1}{(1 + \text{DiscountRateTransmission}_{(r,f)})^{\text{OperationalLifeTransmission}_r - 1}}$$
$$\forall \quad i \in R, r \in R, f \in F, y \in \{y : y + \text{OperationalLifeTransmission}_r \geq \text{EndYear}\}$$

$$\text{DiscSalvageValueTransmission}_{(r,t,y)} =$$
$$\frac{\text{SalvageValueTransmission}_{(r,t,y)}}{(1+\text{DiscountRateTransmission}_{(r,t)})^{(1+\text{EndYear}-\text{StartYear})}} \forall \quad i \in R, r \in R, f \in F, y \in Y$$

Transmission Costs

$$\text{DiscountedAnnualTransmissionCost}_{(r,y)} = \sum_{i \in R} \text{DiscTransmissionCapitalInvestment}_{(i,r,f,y)} +$$
$$\text{DiscountedAnnualImportCost}_{(r,y)} - \sum_{i \in R} \text{DiscSalvageValueTransmission}_{(i,r,f,y)} \quad \forall r \in R, y \in Y$$

Appendix B

Strategic interactions between liquefied natural gas and domestic gas markets: A bilevel model

B.1 Sensitivity analysis: pipeline investment cost

The following table presents the sensitivity of pipeline capacity investments to the unit capacity cost of pipeline investments. Although the current costs assumed in the model do not result in any pipeline capacity investments, lowering the costs associated with building the pipelines in effect increases the pipeline capacity investments. The sensitivity analysis is conducted by varying the pipeline investment costs to fractions of the currently assumed pipeline investment costs C^{pipe}. The results of the sensitivity analysis are summarized in Table. B.1.

Table B.1. Sensitivity of pipeline investments to costs.

Pipeline costs (as fraction of C^{pipe})	**Total pipeline capacity investment (Bcf)**
$C^{\text{pipe}}/5$	0
$C^{\text{pipe}}/10$	357.7
$C^{\text{pipe}}/20$	563.82
$C^{\text{pipe}}/30$	1156.48
$C^{\text{pipe}}/40$	2043.36
$C^{\text{pipe}}/50$	3691.03

Appendix C

Risk-averse stochastic bilevel programming: An application to natural gas markets

C.1 27 scenario solution

In this section, we present the results for the problem discussed in the case study with nine nodes for 27 scenarios. We generate the scenarios employing a similar strategy described in Section 4.7.1., where each market could face demand scenarios of high (H), medium (M), and low (L) demand with a given probability ($\psi^{\text{market}}_{\text{demand}}$). We assume that the uncertainties in each market are uncorrelated with the other markets. Thus, the demand uncertainties in the LNG market, gas procurement market for the LNG operator, and the spot market are independent of each other. This set of demand uncertainties considered for all three of the markets, namely the LNG market, LNG operator's gas procurement market, and the NG spot market, leads to a total of 27 scenarios.

The investment results for the risk-averse LNG operator and risk-neutral NG producer are summarized in Table C.1. The results, including production, gas procured by the LNG operator, spot sales, and average gas prices for both the spot market and LNG operator's gas procurement market for the 27 scenario problem, are provided in Table C.2. The LNG market results, including sales and LNG market prices, are reported in Table C.3. We see similar overall results as those under the 9 scenario case regarding the overall investment capacities and locations. The scenario-specific results are different as the 27 scenario case

Table C.1. Investment decisions for risk averse decision maker for 9 scenario and 27 scenario.

Variable	**9 scenario**	**27 scenario**
Number of LNG facilities open	1	1
Total LNG capacity open	1000.0	1000.0
Total production capacity	6894.977	6872.518
LNG operator's (Leader) expected profit	4.3953	4.3561
NG producer's (Follower) expected profit	46.9584	46.5082

can account for more demand setting the markets would face and how each interacts with the other's dynamics. The LNG operator's lowest gas price achieved is lower in this case compared to the 9 scenario case. The regional spot prices are similar in both the 27 scenarios and the 9 scenario case. We see similar trends in the LNG market dynamics as well, with the total LNG sales and the average LNG market prices.

Table C.2. Result summary for 27 scenario for risk averse decision maker (CVaR).

Scenario	Demand	Production (Bcf)	Gas procured by LNG operator (Bcf)	Spot market sales (Bcf)	Average spot market price ($)	Average gas price faced by LNG operator ($)
1	(H, H, H)	6872.518	1000.000	5872.518	10.046625	10.763
2	(H, H, M)	6163.233	1000.000	5163.234	8.747375	10.763
3	(H, H, L)	4442.278	1000.000	3442.279	8.747125	10.763
4	(H, M, H)	6872.518	1000.000	5872.518	10.046625	7.565
5	(H, M, M)	6163.232	1000.000	5163.233	8.747375	7.565
6	(H, M, L)	4442.278	1000.000	3442.279	8.747125	7.565
7	(H, L, H)	6872.518	1000.000	5872.518	10.046625	1.170
8	(H, L, M)	6163.232	1000.000	5163.233	8.747375	1.170
9	(H, L, L)	4442.279	1000.000	3442.279	8.747125	1.170
10	(M, H, H)	6872.518	1000.000	5872.518	10.046625	10.763
11	(M, H, M)	6163.232	1000.000	5163.233	8.747375	10.763
12	(M, H, L)	4442.278	1000.000	3442.279	8.747125	10.763
13	(M, M, H)	6872.518	1000.000	5872.518	10.046625	7.565
14	(M, M, M)	6163.233	1000.000	5163.234	8.747375	7.565
15	(M, M, L)	4442.278	1000.000	3442.279	8.747125	7.565
16	(M, L, H)	6872.518	931.051	5941.469	9.976375	2.493
17	(M, L, M)	6163.232	1000.000	5163.233	8.747375	1.170
18	(M, L, L)	4149.595	707.300	3442.295	8.747125	6.786
19	(L, H, H)	6872.518	1000.000	5872.518	10.046625	10.763
20	(L, H, M)	6163.232	1000.000	5163.233	8.747375	10.763
21	(L, H, L)	4442.278	1000.000	3442.279	8.747125	10.763
22	(L, M, H)	6872.518	931.051	5941.469	9.976375	8.447
23	(L, M, M)	6163.232	1000.000	5163.233	8.747375	7.565
24	(L, M, L)	4442.278	1000.000	3442.279	8.747125	7.565
25	(L, L, H)	6872.518	935.697	5936.822	9.981000	2.404
26	(L, L, M)	5949.504	786.236	5163.268	8.747375	5.271
27	(L, L, L)	4442.279	1000.000	3442.279	8.747125	1.170

Table C.3. LNG market result summary for 27 scenario for risk averse decision maker (CVaR).

Scenario	Demand	LNG market sales (Bcf)	Average LNG market price ($)
1	(H, H, H)	900.000	18.2000
2	(H, H, M)	900.000	18.2000
3	(H, H, L)	900.000	18.2000
4	(H, M, H)	900.000	18.2000
5	(H, M, M)	900.000	16.4995
6	(H, M, L)	900.000	18.2000
7	(H, L, H)	900.000	16.0335
8	(H, L, M)	900.000	16.4995
9	(H, L, L)	706.362	16.9635
10	(M, H, H)	900.000	17.4810
11	(M, H, M)	900.000	17.4810
12	(M, H, L)	900.000	17.4810
13	(M, M, H)	900.000	15.7805
14	(M, M, M)	900.000	15.7805
15	(M, M, L)	900.000	17.4810
16	(M, L, H)	837.946	17.6795
17	(M, L, M)	900.000	17.4810
18	(M, L, L)	636.570	18.3225
19	(L, H, H)	900.000	15.1170
20	(L, H, M)	900.000	15.1160
21	(L, H, L)	900.000	14.3430
22	(L, M, H)	722.999	16.8170
23	(L, M, M)	900.000	13.4920
24	(L, M, L)	900.000	15.9695
25	(L, L, H)	842.127	15.6725
26	(L, L, M)	707.612	16.9650
27	(L, L, L)	805.295	12.6190

Bibliography

Gemayqzel Bouza Allende and Georg Still. Solving bilevel programs with the KKT-approach. *Mathematical Programming*, 138(1-2):309–332, 2013.

Karla Arredondo-Ramírez, José María Ponce-Ortega, and Mahmoud M El-Halwagi. Optimal planning and infrastructure development for shale gas production. *Energy Conversion and Management*, 119:91–100, 2016.

Richard Audoly, Adrien Vogt-Schilb, Céline Guivarch, and Alexander Pfeiffer. Pathways toward zero-carbon electricity required for climate stabilization. *Applied Energy*, 225: 884–901, 2018.

Andrew Baker. *Mexico Natural Gas Prices a Mixed Bag for August*, 2018. URL https://www.naturalgasintel.com/articles/115929-mexico-natural-gas-prices-a-mixed-bag-for-august.

Galen Barbose, Ryan Wiser, Jenny Heeter, Trieu Mai, Lori Bird, Mark Bolinger, Alberta Carpenter, Garvin Heath, David Keyser, Jordan Macknick, Andrew Mills, and Dev Millstein. A retrospective analysis of benefits and impacts of U.S. renewable portfolio standards. *Energy Policy*, 96:645–660, 2016.

Jonathan F Bard, John Plummer, and Jean Claude Sourie. A bilevel programming approach to determining tax credits for biofuel production. *European Journal of Operational Research*, 120(1):30–46, 2000.

Luis Baringo and Antonio J Conejo. Transmission and wind power investment. *IEEE Transactions on Power Systems*, 27(2):885–893, 2012.

Omar Ben-Ayed and Charles E Blair. Computational difficulties of bilevel linear programming. *Operations Research*, 38(3):556–560, 1990.

Wayne F Bialas and Mark H Karwan. Two-level linear programming. *Management Science*, 30(8):1004–1020, 1984.

John E. Bistline. Economic and technical challenges of flexible operations under large-scale variable renewable deployment. *Energy Economics*, 64:363–372, 2017.

Geoffrey J. Blanford, James H. Merrick, and David Young. A clean energy standard analysis with the US-REGEN model. *Energy Journal*, 35:137–164, 2014.

David P. Brown. Capacity payment mechanisms and investment incentives in restructured electricity markets. *Energy Economics*, 74:131–142, 2018.

Max T Brozynski and Benjamin D Leibowicz. Decarbonizing power and transportation at the urban scale: An analysis of the Austin, Texas Community Climate Plan. *Sustainable Cities and Society*, 43:41–54, 2018.

Lauren K. Busch. *Review of natural gas models - EIA*, 2014. URL https://www.eia.gov/outlooks/documentation/workshops/pdf/Review%20of%20Natural%20Gas%20Models.pdf.

Diego C Cafaro and Ignacio E Grossmann. Strategic planning, design, and development of the shale gas supply chain network. *AIChE Journal*, 60(6):2122–2142, 2014.

Eduardo Camponogara, Luiz F Nazari, and Claudio N Meneses. A revised model for compressor design and scheduling in gas-lifted oil fields. *IIE Transactions*, 44(5):342–351, 2012.

CGA Canadian Gas Association. *Gas Stats*, 2018. URL https://www.cga.ca/gas-stats/.

Miguel Carrión, José M Arroyo, and Antonio J Conejo. A bilevel stochastic programming approach for retailer futures market trading. *IEEE Transactions on Power Systems*, 24 (3):1446–1456, 2009.

R Cervigni, R Liden, J.E. Neumann, and K.M. Strzepek. *Enhancing the Climate Resilience of Africa's Infrastructure*. The World Bank, Washington, D.C., 2015.

Nathan W. Chan and John W. Morrow. Unintended consequences of cap-and-trade? Evidence from the Regional Greenhouse Gas Initiative. *Energy Economics*, 80:411–422, 2019.

Snorre Christiansen, Michael Patriksson, and Laura Wynter. Stochastic bilevel programming in structural optimization. *Structural and multidisciplinary optimization*, 21(5):361–371, 2001.

Christopher T.M. Clack, Staffan A. Qvist, Jay Apt, Morgan Bazilian, Adam R. Brandt, Ken Caldeira, Steven J. Davis, Victor Diakov, Mark A. Handschy, Paul D.H. Dines, Paulina Jaramillo, Daniel M. Kammen, Jane C.S. Long, M. Granger Morgan, Adam Reed, Varun Sivaram, James Sweeney, George R. Tynan, David G. Victor, John P. Weyant, and Jay F. Whitacre. Evaluation of a proposal for reliable low-cost grid power with 100% wind, water, and solar. *Proceedings of the National Academy of Sciences*, 114(26):6722–6727, 2017.

Wesley Cole and A. Will Frazier. Impacts of increasing penetration of renewable energy on the operation of the power sector. *Electricity Journal*, 31(10):24–31, 2018.

Wesley J Cole, Kenneth B Medlock III, and Aditya Jani. A view to the future of natural gas and electricity: An integrated modeling approach. *Energy Economics*, 60:486–496, 2016.

Benoît Colson, Patrice Marcotte, and Gilles Savard. An overview of bilevel optimization. *Annals of operations research*, 153(1):235–256, 2007.

John J Conti, Paul D Holtberg, JA Beamon, A Michael Schaal, JC Ayoub, and James T Turnure. Annual energy outlook 2018. *US Energy Information Administration*, 2, 2018.

Jared R. Creason, John E. Bistline, Elke L. Hodson, Brian C. Murray, and Charles G. Rossmann. Effects of technology assumptions on US power sector capacity, generation and emissions projections: Results from the EMF 32 Model Intercomparison Project. *Energy Economics*, 73:290–306, 2018.

Felipe da Silva Alves, Jame Neiva Miranda de Souza, and André Luiz Hemerly Costa. Multi-objective design optimization of natural gas transmission networks. *Computers & Chemical Engineering*, 93:212–220, 2016.

Gustavo Nikolaus Pinto de Moura, Luiz Fernando Loureiro Legey, and Mark Howells. A Brazilian perspective of power systems integration using OSeMOSYS SAMBA – South America Model Base – and the bargaining power of neighbouring countries: A cooperative games approach. *Energy Policy*, 115:470–485, 2018.

Fernando J. de Sisternes, Jesse D. Jenkins, and Audun Botterud. The value of energy storage in decarbonizing the electricity sector. *Applied Energy*, 175:368–379, 2016.

Joseph F. DeCarolis, Kevin Hunter, and Sarat Sreepathi. The case for repeatable analysis with energy economy optimization models. *Energy Economics*, 34(6):1845–1853, 2012.

Stephan Dempe. *Foundations of Bilevel Programming*. Springer Science & Business Media, 2002.

Stephan Dempe, Vyacheslav Kalashnikov, and Roger Z Rıos-Mercado. Discrete bilevel programming: Application to a natural gas cash-out problem. *European Journal of Operational Research*, 166(2):469–488, 2005.

Stephan Dempe, Vyacheslav V Kalashnikov, Gerardo A Pérez-Valdés, and Nataliya I Kalashnykova. Natural gas bilevel cash-out problem: convergence of a penalty function method. *European Journal of Operational Research*, 215(3):532–538, 2011.

Thomas Arthur Edmunds and Jonathan F Bard. Algorithms for nonlinear bilevel mathematical programs. *IEEE Transactions on Systems, Man, and Cybernetics*, 21(1):83–89, 1991.

EERE. *Geothermal Resource of the United States*, 2014. URL https://www.energy.gov/eere/geothermal/geothermal-maps.

Ruud Egging. Benders Decomposition for multi-stage stochastic mixed complementarity problems – Applied to a global natural gas market model. *European Journal of Operational Research*, 226(2):341–353, 2013.

Ruud Egging, Steven A Gabriel, Franziska Holz, and Jifang Zhuang. A complementarity model for the european natural gas market. *Energy Policy*, 36(7):2385–2414, 2008.

Ruud Egging, Franziska Holz, and Steven A Gabriel. The world gas model: A multi-period mixed complementarity model for the global natural gas market. *Energy*, 35(10):4016–4029, 2010.

EIA. *Annual Energy Outlook 2017 Assumption Table 8.2*, 2017a.

EIA. *Annual Energy Outlook 2017*, 2017b.

EIA. *Electric System Operating Data 2017*, 2017c.

EIA. *EIA Form 860: Annual Electric Generator Report*, 2017d.

EIA. *Oil and gas production*, 2018a. URL https://www.eia.gov/finance/performanceprofiles/oil_gas.php.

EIA. *Annual Energy Outlook 2018*, 2018b. URL https://www.eia.gov/outlooks/aeo/pdf/AEO2020%20Electricity.pdf.

EIA. *Natural gas consumption by end use*, 2018. URL https://www.eia.gov/dnav/ng/ng_cons_sum_a_EPG0_VC0_mmcf_a.htm.

EIA. U.s. liquefied natural gas exports have declined by more than half so far in 2020. https://www.eia.gov/todayinenergy/detail.php?id=44196, 06 2020.

EIA. Monthly crude oil and natural gas production. https://www.eia.gov/petroleum/production, 02 2021.

Erik Ela, Michael Milligan, Aaron Bloom, Jaquelin Cochran, Audun Botterud, Aaron Townsend, and Tood Levin. Overview of Wholesale Electricity Markets. In Fernando Lopes and Helder Coelho, editors, *Electricity Markets with Increasing Levels of Renewable Generation: Structure, Operation, Agent-based Simulation, and Emerging Designs*, chapter 1, pages 3–22. Springer, Cham, Switzerland, 2015.

ERCOT. *Monthly Forecast of Peak Demand and Energy, 2017*, 2017a.

ERCOT. *ERCOT Hourly Load Data, 2017*, 2017b.

Kelly Eurek, Wesley Cole, David Bielen, Nate Blair, Stuart Cohen, Bethany Frew, Jonathan Ho, Venkat Krishnan, Trieu Mai, Benjamin Sigrin, and Daniel Steinberg. Regional Energy Deployment System (ReEDS) Model Documentation: Version 2016. *National Renewable Energy Laboratory Technical Report*, 6A20-67067, 2016.

Felipe Feijoo, Gokul C. Iyer, Charalampos Avraam, Sauleh A. Siddiqui, Leon E. Clarke, Sriram Sankaranarayanan, Matthew T. Binsted, Pralit L. Patel, Nathalia C. Prates, Evelyn Torres-Alfaro, and Marshall A. Wise. The future of natural gas infrastructure development in the United states. *Applied Energy*, 228:149–166, 2018.

FERC. *FERC Form 714: Annual Electric Balancing Authority Area and Planning Area Report*, 2017.

Mark Finley. Bp statistical review of world energy. *bp. com/statisticalreview*, 2013.

Roger Fouquet. The slow search for solutions: Lessons from historical energy transitions by sector and service. *Energy Policy*, 38(11):6586–6596, 2010.

Steven A. Gabriel, Supat Kiet, and Jifang Zhuang. A Mixed Complementarity-Based Equilibrium Model of Natural Gas Markets. *Operations Research*, 53(5):799–818, 2005.

Steven A. Gabriel, Jifang Zhuang, and Ruud Egging. Solving stochastic complementarity problems in energy market modeling using scenario reduction. *European Journal of Operational Research*, 197(3):1028–1040, 2009.

Francesco Gardumi, Abhishek Shivakumar, Robbie Morrison, Constantinos Taliotis, Oliver Broad, Agnese Beltramo, Vignesh Sridharan, Mark Howells, Jonas Hörsch, Taco Niet, Youssef Almulla, Eunice Ramos, Thorsten Burandt, Gabriela Peña Balderrama, Gustavo Nikolaus Pinto de Moura, Eduardo Zepeda, and Thomas Alfstad. From the development of an open-source energy modelling tool to its application and the creation of communities of practice: The example of OSeMOSYS. *Energy Strategy Reviews*, 20: 209–228, 2018.

Farhad Samadi Gazijahani and Javad Salehi. Optimal bilevel model for stochastic risk-based planning of microgrids under uncertainty. *IEEE Transactions on Industrial Informatics*, 14(7):3054–3064, 2017.

Vikas Goel, M Slusky, W-J van Hoeve, Kevin C Furman, and Yufen Shao. Constraint programming for LNG ship scheduling and inventory management. *European Journal of Operational Research*, 241(3):662–673, 2015.

Government of Canada. *Natural Gas Facts*, 2018. URL https://www.nrcan.gc.ca/science-data/data-analysis/energy-data-analysis/energy-facts/natural-gas-facts/20067#L6%20(canada%20provincial%20percentages).

Markus Groissböck and Matthias J. Pickl. An analysis of the power market in Saudi Arabia: Retrospective cost and environmental optimization. *Applied Energy*, 165:548–558, 2016.

Roar Grønhaug, Marielle Christiansen, Guy Desaulniers, and Jacques Desrosiers. A branch-and-price method for a liquefied natural gas inventory routing problem. *Transportation Science*, 44(3):400–415, 2010.

Arnulf Grubler. Energy transitions research: Insights and cautionary tales. *Energy Policy*, 50:8–16, nov 2012.

Arnulf Grubler, Nebojsa Nakicenovic, and David G Victor. Dynamics of energy technologies and global change. *Energy Policy*, 27(5):247–280, 1999.

Vijay Gupta and Ignacio E Grossmann. An efficient multiperiod MINLP model for optimal planning of offshore oil and gas field infrastructure. *Industrial & Engineering Chemistry Research*, 51(19):6823–6840, 2012.

Shelly Hagerman, Paulina Jaramillo, and M. Granger Morgan. Is rooftop solar PV at socket parity without subsidies? *Energy Policy*, 89:84–94, 2016.

Elin E Halvorsen-Weare and Kjetil Fagerholt. Routing and scheduling in a liquefied natural gas shipping problem with inventory and berth constraints. *Annals of Operations Research*, 203(1):167–186, 2013.

Jingkuan Han, Yingjun Xu, Dingzhi Liu, Yanfang Zhao, Zhongde Zhao, Shuhui Zhou, Tianhu Deng, Mengying Xue, Junchi Ye, and Zuo-Jun Max Shen. Operations research enables

better planning of natural gas pipelines. *INFORMS Journal on Applied Analytics*, 49(1): 23–39, 2019.

Benjamin F. Hobbs and Shmuel S. Oren. Three Waves of U.S. Reforms: Following the Path of Wholesale Electricity Market Restructuring. *IEEE Power and Energy Magazine*, 17(1): 73–81, 2019.

Mark Howells, Holger Rogner, Neil Strachan, Charles Heaps, Hillard Huntington, Socrates Kypreos, Alison Hughes, Semida Silveira, Joe DeCarolis, Morgan Bazillian, and Alexander Roehrl. OSeMOSYS: The Open Source Energy Modeling System. An introduction to its ethos, structure and development. *Energy Policy*, 39(10):5850–5870, 2011.

Yuping Huang, Qipeng P Zheng, and Jianhui Wang. Two-stage stochastic unit commitment model including non-generation resources with conditional value-at-risk constraints. *Electric Power Systems Research*, 116:427–438, 2014.

Daniel Huppmann. Endogenous production capacity investment in natural gas market equilibrium models. *European Journal of Operational Research*, 231(2):503–506, 2013.

IEA. *World Energy Outlook 2017*. OECD Publishing, 2017. URL https://www.oecd-ilibrary.org/content/publication/weo-2017-en.

IEA. *Gas demand by region and scenario, 2018-2040 - IEA*, 2019. URL https://www.iea.org/data-and-statistics/charts/gas-demand-by-region-and-scenario-2018-2040.

IGU. *2020 World LNG Report*, 2020. URL https://www.igu.org/publications-page.

IPCC. *IPCC AR5 WG3 Annex III*, 2017.

ISO-NE. *Forecast Report of Energy and Loads, 2017*, 2017.

ISO-NE. *NE Region Hourly Load Forecast, 2017*, 2017.

Rabih A Jabr. Robust self-scheduling under price uncertainty using conditional value-at-risk. *IEEE Transactions on Power Systems*, 20(4):1852–1858, 2005.

Mark Z. Jacobson, Mark A. Delucchi, Mary A. Cameron, and Bethany A. Frew. Low-cost solution to the grid reliability problem with 100% penetration of intermittent wind, water, and solar for all purposes. *Proceedings of the National Academy of Sciences*, 112 (49):15060–15065, 2015.

Gordon Jaremko. *NGIs daily gas price index*, 2019. URL https://www.naturalgasintel.com/articles/117000-proposed-18-bcfd-quebec-pipeline-a-conduit-for-lng-\exports-say-sponsors.

Gopika Jayadev. *Github: EIoF Data*, 2019. URL https://github.com/users/GopikaJayadev/projects/1.

Shan Jin and Sarah M Ryan. A tri-level model of centralized transmission and decentralized generation expansion planning for an electricity market—Part I. *IEEE Transactions on Power Systems*, 29(1):132–141, 2013.

Alireza Kabirian and Mohammad Reza Hemmati. A strategic planning model for natural gas transmission networks. *Energy Policy*, 35(11):5656–5670, 2007.

Vyacheslav V Kalashnikov, Gerardo A Pérez, and Nataliya I Kalashnykova. A linearization approach to solve the natural gas cash-out bilevel problem. *Annals of Operations Research*, 181(1):423–442, 2010a.

Vyacheslav V Kalashnikov, Gerardo A Pérez-Valdés, Asgeir Tomasgard, and Nataliya I Kalashnykova. Natural gas cash-out problem: bilevel stochastic optimization approach. *European Journal of Operational Research*, 206(1):18–33, 2010b.

Evaggelos G Kardakos, Christos K Simoglou, and Anastasios G Bakirtzis. Optimal offering strategy of a virtual power plant: A stochastic bi-level approach. *IEEE Transactions on Smart Grid*, 7(2):794–806, 2015.

Venkat Krishnan, Jonathan Ho, Benjamin F. Hobbs, Andrew L. Liu, James D. McCalley, Mohammad Shahidehpour, and Qipeng P. Zheng. Co-optimization of electricity transmission and generation resources for planning and policy analysis: review of concepts and modeling approaches. *Energy Systems*, 7(2):297–332, 2016.

Pavlo Krokhmal, Jonas Palmquist, and Stanislav Uryasev. Portfolio optimization with conditional value-at-risk objective and constraints. *Journal of risk*, 4:43–68, 2002.

Guoming Lai, Mulan X Wang, Sunder Kekre, Alan Scheller-Wolf, and Nicola Secomandi. Valuation of storage at a liquefied natural gas terminal. *Operations Research*, 59(3):602–616, 2011.

Benjamin D Leibowicz. The cost of policy uncertainty in electric sector capacity planning: Implications for instrument choice. *The Electricity Journal*, 31:33–41, 2018.

Benjamin D. Leibowicz, Volker Krey, and Arnulf Grubler. Representing spatial technology diffusion in an energy system optimization model. *Technological Forecasting and Social Change*, 103:350–363, 2016.

Richard Loulou and Maryse Labriet. ETSAP-TIAM: the TIMES integrated assessment model Part I: Model structure. *Computational Management Science*, 5(1-2):7–40, 2007.

Richard Loulou, Gary Goldstein, and Ken Noble. *Documentation for the MARKAL Family of Models*, 2004.

Amory B Lovins. Reliably integrating variable renewables : Moving grid fl exibility resources from models to results. *The Electricity Journal*, 30(10):58–63, 2017.

Alexander E. MacDonald, Christopher T.M. Clack, Anneliese Alexander, Adam Dunbar, James Wilczak, and Yuanfu Xie. Future cost-competitive electricity systems and their impact on US CO2 emissions. *Nature Climate Change*, 6:526–531, 2016.

Trieu Mai, John Bistline, Yinong Sun, Wesley Cole, Cara Marcy, Chris Namovicz, and David Young. The role of input assumptions and model structures in projections of variable renewable energy: A multi-model perspective of the U.S. electricity system. *Energy Economics*, 76:313–324, 2018.

Lajos Maurovich-Horvat, Trine K Boomsma, and Afzal S Siddiqui. Transmission and wind investment in a deregulated electricity industry. *IEEE Transactions on Power Systems*, 30(3):1633–1643, 2014.

McKinsey & Company. *Global gas and LNG outlook to 2035*, 2019. URL https://www.mckinsey.com/industries/oil-and-gas/our-insights/global-gas-and-lng-outlook-to-2035.

Sabine Messner and Leo Schrattenholzer. MESSAGE-MACRO: Linking an energy supply model with a macroeconomic module and solving it iteratively. *Energy*, 25(3):267–282, 2000.

Richard S. Middleton and Jeffrey M. Bielicki. A scalable infrastructure model for carbon capture and storage: SimCCS. *Energy Policy*, 37(3):1052–1060, 2009.

Bryan K Mignone, Sharon Showalter, Frances Wood, Haewon McJeon, and Daniel Steinberg. Sensitivity of natural gas deployment in the us power sector to future carbon policy expectations. *Energy Policy*, 110:518–524, 2017.

MISO. *MISO Independent Load Forecast, 2017*, 2017a.

MISO. *MISO Hourly Load, 2017*, 2017b.

Seksun Moryadee and Steven A Gabriel. Panama Canal expansion: Will Panama Canal be a game-changer for liquefied natural gas exports to Asia? *Journal of Energy Engineering*, 143(1):04016024, 2017.

Brian C. Murray, John Bistline, Jared Creason, Evelyn Wright, Amit Kanudia, and Francisco de la Chesnaye. The EMF 32 study on technology and climate policy strategies for greenhouse gas reductions in the U.S. electric power sector: An overview. *Energy Economics*, 73:286–289, 2018.

Fatih Mutlu, Mohamed K Msakni, Hakan Yildiz, Erkut Sönmez, and Shaligram Pokharel. A comprehensive annual delivery program for upstream liquefied natural gas supply chain. *European Journal of Operational Research*, 250(1):120–130, 2016.

Reza Naghash. An overview of global lng plant development costs. https://www.linkedin.com/pulse/overview-global-lng-plant-develepment-costs-reza-naghash-cpm-p-e-/, 11 2017.

James Nelson, Josiah Johnston, Ana Mileva, Matthias Fripp, Ian Hoffman, Autumn Petros-Good, Christian Blanco, and Daniel M. Kammen. High-resolution modeling of the western North American power system demonstrates low-cost and low-carbon futures. *Energy Policy*, 43:436–447, 2012.

NERC. *Monthly Electricity Energy & Demand, 2017*, 2017.

David Newbery. Missing money and missing markets: Reliability, capacity auctions and interconnectors. *Energy Policy*, 94:401–410, 2016.

Tatsushi Nishi and Okihiro Yoshida. Optimization of multi-period bilevel supply chains under demand uncertainty. *Procedia CIRP*, 41:508–513, 2016.

William D. Nordhaus. Revisiting the social cost of carbon. *Proceedings of the National Academy of Sciences*, 114(7):1518–1523, 2017.

NREL. *Annual Technology Baseline*, 2017a.

NREL. *System Advisor Model*, 2017b.

NYISO. *Load and Capacity Data, 2017*, 2017a.

NYISO. *NYISO Hourly Loads, 2017*, 2017b.

Stefan Pfenninger, Adam Hawkes, and James Keirstead. Energy systems modeling for twenty-first century energy challenges. *Renewable and Sustainable Energy Reviews*, 33: 74–86, 2014.

Benjamin R. Phillips and Richard S. Middleton. SimWIND: A geospatial infrastructure model for optimizing wind power generation and transmission. *Energy Policy*, 43:291–302, 2012.

PJM. *Load Forecast Report, 2017*, 2017a.

PJM. *Hourly Load Data, 2017*, 2017b.

W. B. Powell and S. Meisel. Tutorial on stochastic optimization in energy—part i: Modeling and policies. *IEEE Transactions on Power Systems*, 31(2):1459–1467, 2016a. doi: 10.1109/TPWRS.2015.2424974.

W. B. Powell and S. Meisel. Tutorial on stochastic optimization in energy—part ii: An energy storage illustration. *IEEE Transactions on Power Systems*, 31(2):1468–1475, 2016b. doi: 10.1109/TPWRS.2015.2424980.

David Pozo and Javier Contreras. A chance-constrained unit commitment with an nk security criterion and significant wind generation. *IEEE Transactions on Power systems*, 28(3): 2842–2851, 2012.

David Pozo, Enzo Sauma, and Javier Contreras. Basic theoretical foundations and insights on bilevel models and their applications to power systems. *Annals of Operations Research*, 254(1-2):303–334, 2017.

RRC Railroad Commission of Texas. *Oil and gas division district boundaries*, 2020. URL https://www.rrc.texas.gov/media/21430/districts_color_8x11.pdf?fbclid=IwAR0XnyVmabHZNAxTQuv6nPLmVmM9hKjlCC13VWmcK4I3Zn4oSIJVck0kkmk.

Andrew Reimers, Wesley Cole, and Bethany Frew. The impact of planning reserve margins in long-term planning models of the electricity sector. *Energy Policy*, 125:1–8, 2019.

Joshua D. Rhodes. The State of the US Energy Sector. *ONE J: Oil and Gas, Natural Resources, and Energy Journal*, 4(4):547–560, 2018.

Werner Römisch. Scenario reduction techniques in stochastic programming. In *International Symposium on Stochastic Algorithms*, pages 1–14. Springer, 2009.

Frode Rømo, Asgeir Tomasgard, Lars Hellemo, Marte Fodstad, Bjørgulf Haukelidsæter Eidesen, and Birger Pedersen. Optimizing the Norwegian natural gas production and transport. *Interfaces*, 39(1):46–56, 2009.

B Rothfarb, H Frank, DM Rosenbaum, Kenneth Steiglitz, and Daniel J Kleitman. Optimal design of offshore natural-gas pipeline systems. *Operations Research*, 18(6):992–1020, 1970.

Mahmoud Roustai, Mohammad Rayati, Aras Sheikhi, and AliMohammad Ranjbar. A scenario-based optimization of smart energy hub operation in a stochastic environment using conditional-value-at-risk. *Sustainable cities and society*, 39:309–316, 2018.

Walter Short, Patrick Sullivan, Trieu Mai, Matthew Mowers, Caroline Uriarte, Nate Blair, Donna Heimiller, Andrew Martinez, Walter Short, Patrick Sullivan, Trieu Mai, Matthew Mowers, Caroline Uriarte, Nate Blair, Donna Heimiller, and Andrew Martinez. Regional Energy Deployment System (ReEDS). *National Renewable Energy Laboratory Technical Report*, 6A20-46534, 2011.

Ramteen Sioshansi. Using Storage-Capacity Rights to Overcome the Cost-Recovery Hurdle for Energy Storage. *IEEE Transactions on Power Systems*, 32(3):2028–2040, 2017.

Varun Sivaram, John O. Dabiri, and David M. Hart. The Need for Continued Innovation in Solar, Wind, and Energy Storage. *Joule*, 2(9):1639–1642, 2018.

Vaclav Smil. Examining energy transitions: A dozen insights based on performance. *Energy Research and Social Science*, 22:194–197, 2016.

Brian Songhurst. LNG plant cost reduction 2014–18. *Oxford Institute for Energy Studies*, 2018.

Erkut Sönmez, Sunder Kekre, Alan Scheller-Wolf, and Nicola Secomandi. Strategic analysis of technology and capacity investments in the liquefied natural gas industry. *European Journal of Operational Research*, 226(1):100–114, 2013.

Statistics Canada. *Supply and disposition of natural gas*, 2018. URL https://www150.statcan.gc.ca/t1/tbl1/en/cv.action?pid=2510005501.

Man-Wen Tian, Abdol Ghaffar Ebadi, Kittisak Jermsittiparsert, Marsel Kadyrov, Andrei Ponomarev, Nima Javanshir, and Sayyad Nojavan. Risk-based stochastic scheduling of energy hub system in the presence of heating network and thermal energy management. *Applied Thermal Engineering*, 159:113825, 2019.

Hoang Tuy, Athanasios Migdalas, and Peter Värbrand. A global optimization approach for the linear two-level program. *Journal of Global Optimization*, 3(1):1–23, 1993.

Nina Linn Ulstein, Bjørn Nygreen, and Jan Richard Sagli. Tactical planning of offshore petroleum production. *European Journal of Operational Research*, 176(1):550–564, 2007.

U.S. Department of Energy. Global lng fundamentals. https://www.energy.gov/sites/prod/files/2018/03/f49/Global%20LNG%20Fundamentals%2C%20Updated%203.15.18.pdf, 03 2018.

US DOE. *NEW STREAM-REACH DEVELOPMENT RESOURCE ASSESSMENT*, 2014. URL https://hydrosource.ornl.gov/hydropower-potential/new-stream-reach-development-resource-assessment.

Halit Üster and Şebnem Dilaveroğlu. Optimization for design and operation of natural gas transmission networks. *Applied Energy*, 133:56–69, 2014.

Shalini P. Vajjhala and Paul S. Fischbeck. Quantifying siting difficulty: A case study of US transmission line siting. *Energy Policy*, 35(1):650–671, 2007.

Jaber Valinejad and Taghi Barforoushi. Generation expansion planning in electricity markets: A novel framework based on dynamic stochastic mpec. *International Journal of Electrical Power & Energy Systems*, 70:108–117, 2015.

Manuel Welsch, Paul Deane, Mark Howells, Brian O Gallachóir, Fionn Rogan, Morgan Bazilian, and Hans Holger Rogner. Incorporating flexibility requirements into long-term energy system models - A case study on high levels of renewable electricity penetration in Ireland. *Applied Energy*, 135:600–615, 2014.

Jordan T. Wilkerson, Benjamin D. Leibowicz, Delavane D. Turner, and John P. Weyant. Comparison of integrated assessment models: Carbon price impacts on U.S. energy. *Energy Policy*, 76:18–31, 2015.

Sonja Wogrin, Efraim Centeno, and Julián Barquín. Generation capacity expansion in liberalized electricity markets: A stochastic mpec approach. *IEEE Transactions on Power Systems*, 26(4):2526–2532, 2011.

Kevin Yeh, Craig Whittaker, Matthew J Realff, and Jay H Lee. Two stage stochastic bilevel programming model of a pre-established timberlands supply chain with biorefinery investment interests. *Computers & Chemical Engineering*, 73:141–153, 2015.

D. Young, G. Blanford, J. Bistline, S. Rose, F. de la Chesnaye, R. Bedilion, and Wilson T. US-REGEN Model Documentation. *Electric Power Research Institute Technical Report*, 3002010956, 2017.

Yiduo Zhan and Qipeng P Zheng. A multistage decision-dependent stochastic bilevel programming approach for power generation investment expansion planning. *IISE Transactions*, 50(8):720–734, 2018.

Jianzhong Zhang and Detong Zhu. A bilevel programming method for pipe network optimization. *SIAM Journal on Optimization*, 6(3):838–857, 1996.

Ella Zhou, Wesley Cole, and Bethany Frew. Valuing variable renewable energy for peak demand requirements. *Energy*, 165:499–511, 2018.

Carl Zichella and Johnathan Hladik. Siting: Finding a home for renewable energy and transmission. *Electricity Journal*, 26(8):125–138, 2013.